

Mechanisms of potential novel antimalarials and proteomics of *Plasmodium falciparum* resistance

Denise Steyn

Submitted in partial fulfilment of the degree *Magister Scientiae* Pharmacology
In the Faculty of Health Sciences
University of Pretoria
Pretoria

30 September 2015

Supervised by: Prof AD Cromarty (Department of Pharmacology, UP)
Co-supervised by: Prof L-M Birkholtz (Department of Biochemistry, UP)

UNIVERSITY OF PRETORIA
FACULTY OF HEALTH SCIENCES
DEPARTMENT OF PHARMACOLOGY

Declaration of Originality

Full names of student:

Denise Steyn

Student number:

27074472

Topic of work:

Mechanisms of potential novel antimalarials and proteomics of *Plasmodium falciparum* resistance

Declaration

1. I understand what plagiarism is and am aware of the University's policy in this regard.
2. I declare that this dissertation is my own original work. Where other people's work has been used (either from a printed source, Internet or any other source), this has been properly acknowledged and referenced in accordance with departmental requirements.
3. I have not used work previously produced by another student or any other person to hand in as my own.
4. I have not allowed, and will not allow, anyone to copy my work with the intention of passing it off as his or her own work.

SIGNATURE



Funding and Acknowledgements

Acknowledgement is due to the Department of Biochemistry at the University of Pretoria who provided training and generously granted access to the necessary culturing facilities, parasite strains, reagents and equipment to facilitate the completion of this research project.

Financial aid has been received from the National Research Foundation-German Academic Exchange Service (NRF-DAAD) (Grant holder number 82790, reference no. SFD1208055823). Further funding was provided by the Departments of Pharmacology and Biochemistry of the University of Pretoria.

Special thanks are due to Prof. Lyn-Marie Birkholtz, Prof. A. Duncan Cromarty, Dr. Japie van Tonder, Mrs. Janette Reader, Ms. Tracey Hurrell and Dr. Jandelie Niemand for their immense insight and guidance in respective areas of the project. Further acknowledgement is extended to the Council of Scientific and Industrial Research (CSIR) Biosciences division, specifically Dr. Stoyan Stoychev, for his expertise and assistance with proteomics analyses. A thanks is also due to the Proteomics Department of the University of the Western Cape for the mass spectrometric analysis of peptide extracts.

Thank you to Dr. CJ Henley-Smith who graciously offered to proof-read this manuscript in exchange for a week's worth of transport to work. Thank you to my family for their patience and consistent willingness to support me. Thank you to my understanding husband, who admires everything I have achieved and pushes me to go further. Everyone's contributions and words of encouragement have culminated in the completion of this work.

Ethics

Ethical approval, reference no. 259/2013, was obtained from the University of Pretoria's Research Ethics Committee for the *in vitro* use of *Plasmodium falciparum* strains and the mammalian cell line HepG2, as well as for the drawing of blood from healthy volunteers.

The Department of Biochemistry renews their ethical approval status yearly for the use of healthy donor blood in *P. falciparum* parasite culture and testing by students, as issued by the Ethics Committee of the Faculty of Natural and Agricultural Sciences of the University of Pretoria, reference no. EC120821-077.

Table of Contents

Declaration of Originality	i
Funding and Acknowledgements	ii
Ethics	iii
Table of Contents	iv
Abstract	vi
Glossary of abbreviations	viii
List of Figures	xi
List of Tables	xii
Chapter 1: Literature Review	1
1.1 The clinical manifestation of malaria and acquired immunity	1
1.2 Prevalence and distribution of malaria	2
1.3 Current eradication and treatment strategies and their shortcomings	3
1.4 <i>Plasmodium falciparum</i> survival strategies and antimalarial resistance	14
1.5 Research question	16
1.6 Study design	17
Chapter 2: Antiplasmodial efficacy and selective toxicity	18
2.1 Introduction	18
2.2 Materials and Methods	19
2.3 Results	28
2.4 Discussion	35
2.5 Conclusion	38
Chapter 3: Stage specificity (parasite life-cycle progression) analysis of drugs	39
3.1 Introduction	39
3.2 Materials and methods	40
3.3 Results	42
3.4 Discussion	47
3.5 Conclusion	48
Chapter 4: Chloroquine sensitisation of resistant <i>Plasmodium falciparum</i>	49
4.1 Introduction	49
4.2 Materials and methods	50
4.3 Results	51
4.4 Discussion	53
4.5 Conclusion	54
Chapter 5: Harvesting trophozoite food vacuole membrane proteins	55
5.1 Introduction	55
5.2 Materials and methods	56
5.3 Results	58
5.4 Discussion	60

5.5 Conclusion	60
Chapter 6: Proteomic analysis	61
6.1 Introduction	61
6.2 Materials and methods	63
6.3 Results	70
6.4 Discussion	80
6.5 Conclusion	84
Concluding discussion	85
References	90
Appendix A: Glossary of terms	101

Abstract

Keywords: *Plasmodium falciparum*, drug resistance, food vacuole, SYBR green, selectivity index, clofazimine, proteomics

Introduction: *Plasmodium falciparum* is the dominant cause of severe malaria in humans, with the highest number of global deaths occurring in Africa, India and Southeast Asia. Even though artemisinin-derivative combination therapies are readily available in Africa there are numerous reports of poor quality products which may lead to the development of drug resistance in *Plasmodium* parasites. Other aspects such as counterfeit medicines with sub-therapeutic levels of active ingredients may also be a contributing factor. The exact mechanism of *P. falciparum* drug resistance is still poorly understood, but numerous proteins linked to multi-drug resistance have been identified. The aim of this study was to ascertain whether clofazimine can act as a chemotherapeutic sensitizer as reported, and to determine its ability to alter the expression of chloroquine resistance gene products *in vitro*.

Materials and Methods: In this study the 50% inhibitory concentrations of (IC₅₀) humic and fulvic acid, the 3-hydroxy-3-methyl-glutaryl-Coenzyme A (HMG-CoA) reductase inhibitor mevastatin (lovastatin) and a riminophenazine antibiotic clofazimine were established using SYBR® green dye and fluorometric assays using chloroquine sensitive (3D7), chloroquine sensitive-pyrimethamine resistant (HB3) and chloroquine resistant (W2) parasites which demonstrate mefloquine, antifolate and chloroquine resistance respectively. Eflornithine (DFMO) is a polyamine synthesis inhibitor that was used in sensitivity assays for comparison. The selective toxicity of each of these agents was determined by Sulforhodamine B (SRB) colorimetric assays in hepatocarcinoma cells (HepG2). Flow cytometry techniques were employed to establish any alterations in life-cycle progression. Comparative proteomics of possible resistance proteins expressed on the membrane of the parasite food vacuole was conducted on W2, 3D7 and clofazimine-treated W2 strains of *P. falciparum*. Food vacuoles isolated by MidiMACS magnetic purification were separated using one dimensional gel electrophoresis, followed by in-gel

trypsinisation, sample clean-up, fractionation by nano-liquid chromatography and mass spectrometric analysis by Matrix-Assisted Laser Desorption/Ionisation (MALDI) and Time of Flight (TOF) assays. Proteins were further identified *in silico* through the use of proteomic databases and homology comparison software.

Results: Mevinolin showed poor antiplasmodial efficacy (IC_{50} of $1.19 \times 10^5 \pm 1.02$ nM), in comparison to artemisinin and chloroquine (32.61 ± 1.03 nM and 8.36 ± 1.03 nM, respectively) in 3D7 strains. Clofazimine showed greater antiplasmodial efficacy than DFMO in W2 strains (IC_{50} of 272.00 ± 1.04 and $3.39 \times 10^5 \pm 1.06$ nM, respectively). W2 strains were confirmed to be less susceptible to chloroquine ($p < 0.001$). All test compounds showed decreased toxicity for model mammalian cells ($p < 0.001$), except for mevinolin. Clofazimine (constant dose 375 nM) sensitised W2 strains to the actions of chloroquine ($p < 0.05$), decreasing the IC_{50} of chloroquine by 40 nM. Food vacuoles were successfully harvested (confirmed by light microscopy), but quantities were below optimum value for reliable proteomic analysis and samples appeared to be contaminated with other cellular debris. Consequently proteins previously reported to be linked to drug resistance were not positively identified, while proteins involved in trafficking, motility and invasion of parasites were abundant and identified.

Conclusion: The identification of novel antimalarials and the establishment of compounds that can be used in combination therapies to reverse resistance in *P. falciparum* parasites could greatly benefit communities suffering from the deadly malaria pandemic. Further research is required to establish the feasibility of clofazimine, or its derivatives, as adjunct therapy for the potential to decrease parasites' active efflux of antimalarials.

Glossary of abbreviations

1D	One-dimensional
1DE	One-dimensional electrophoresis
1N	One nucleus
2N	Two nuclei
3D7	Chloroquine sensitive <i>P. falciparum</i> strain of African origin
7C12	Chloroquine resistant <i>P. falciparum</i> strain progeny of Dd2 and HB3 cross
7G8	Chloroquine resistant <i>P. falciparum</i> strain of Brazilian origin
ACN	Acetonitrile
ACTs	Artemisinin combination therapies
ANOVA	Analysis of variance
BCA	Bicinchoninic acid
BSA	Bovine serum albumin
CQ	Chloroquine
CSIR	Council for Scientific and Industrial Research of South Africa
Da	Dalton
Dd2	Chloroquine resistant <i>P. falciparum</i> strain collected from Indochina/Laos
DDT	Dichlorodiphenyltrichloroethane
DFMO	α -Difluoromethylornithine or eflornithine
DNA	Deoxyribonucleic acid
DSMO	Dimethyl sulfoxide
EDTA	Ethylenediaminetetraacetic acid
EMEM	Eagle's minimum essential medium
EmPAI	Exponentially modified protein abundance index
ETRAMP5	Early transcribed membrane protein 5
FCS	Foetal calf serum
FITC	Fluorescein isothiocyanate
FV	Food vacuole
H ⁺	Proton or Hydrogen ions

HB3	Chloroquine sensitive <i>P. falciparum</i> strain collected in Honduras
HCCA	α -Cyano-4-hydroxy-cinnamic acid matrix
HCD	High-energy collisional dissociation
HCH	Hexachlorocyclohexane
hct	Haematocrit
HEPES	4-(2-Hydroxyethyl)-1-piperazineethanesulfonic acid
HepG2	Human hepatocellular carcinoma (ATCC® HB-8065™)
HIV	Human Immunodeficiency Virus
HMG-CoA	3-hydroxy-3-methyl-glutaryl-Coenzyme A
HSP	Heat shock protein
IC ₅₀	Drug concentration at which 50% growth is inhibited
IE	Intra-erythrocytic
IEC	Intra-erythrocytic life-cycle
IPTp	Intermittent preventive treatments in pregnancy
IRS	In-door residual spraying
ITNs	Insecticide treated bed-nets
KCl	Potassium chloride
LOWESS	Locally weighted scatterplot smoothing
m/z	Mass-to-charge ratio
MACS	Magnetism-assisted cell sorting
MALDI	Matrix-assisted laser desorption ionisation
MDR	Multi-drug resistance
MMV	Medicines for Malaria Venture
MOWSE	Molecular weight search score
MPI	Max Planck Institute of Biochemistry Martinsried
MS	Mass spectrometry
MSF	Malaria SYBR Green-1® based fluorescence assay
nLC	Nano Liquid Chromatography
nm	Nanometer
nM	NanoMolar
No.	Number
PAGE	Polyacrylamide Gel Electrophoresis

PBS	Phosphate buffered saline
PCR	Polymerase chain reaction
PCV	Packed cell volume (erythrocytes)
<i>Pf</i> ATP6	<i>P. falciparum</i> Sarco-endoplasmic reticulum Ca ²⁺ -ATPase or SERCA
<i>Pf</i> CRT	<i>P. falciparum</i> chloroquine resistance transporter
<i>Pf</i> EMP1	<i>Plasmodium falciparum</i> erythrocyte membrane protein 1
<i>Pf</i> MDR1	<i>P. falciparum</i> multi-drug resistance protein 1
<i>Pfmdr1</i>	<i>Plasmodium falciparum</i> multi-drug resistance gene 1
<i>Pf</i> NHE	<i>P. falciparum</i> Na ⁺ -H ⁺ exchanger
Pgh1	P-glycoprotein homolog 1
PgP	P-glycoprotein
PMSF	Phenylmethanesulphonyl fluoride
R ²	Coefficient of determination
RAP2	Rhoptry-associated protein 2
RBC	Erythrocyte
RIPA	Radioimmunoprecipitation assay detergent mixture
RNA	Ribonucleic acid
RPMI-1640	Roswell Park Memorial Institute-1640 culture medium
SANBS	South African National Blood Services
SDS	Sodium dodecyl sulphate
SEM	Standard error of the mean
SI	Selectivity index
SRB	Sulforhodamine B
T9-94	Pyrimethamine resistant <i>P. falciparum</i> strain collected from Thailand
TB	Tuberculosis
TCA	Trichloroacetic acid
TFA	Trifluoroacetic acid
TMP	Tetramethylpiperidine-linked
TOF	Time of flight
Tris	Tris(hydroxymethyl)aminomethane
UWC	University of Western Cape
W2	Mefloquine sensitive, chloroquine resistant <i>P. falciparum</i> strain derived from Indochina III/CDC

List of Figures

Chapter 1

Figure 1.1 The <i>Plasmodium falciparum</i> life-cycle	7
Figure 1.2 The intra-erythrocytic (IE) stages of <i>Plasmodium</i> parasites	8
Figure 1.3 Transmission electron microscope image of a late stage trophozoite	9

Chapter 2

Figure 2.1 The mean growth inhibition of mammalian and <i>Plasmodium falciparum</i> cells exposed to artemisinin, chloroquine and mevinolin	30
Figure 2.2 The mean growth inhibition by clofazimine and DFMO of mammalian and <i>Plasmodium falciparum</i> cells	33
Figure 2.3 The mean growth inhibition of <i>Plasmodium falciparum</i> strains exposed to humic compounds	35

Chapter 3

Figure 3.1 The change in parasitaemia of <i>Plasmodium</i> 3D7 and W2 strains	42
Figure 3.2 Overlay histogram of fluorescent DNA content in parasites over time	44
Figure 3.3 Overlay histogram of fluorescent DNA content of “events” as detected by flow cytometry	45
Figure 3.4 Microcopy images of schizonts and their fluorescent DNA	46

Chapter 4

Figure 4.1 Dose-response curves of W2 parasites exposed to chloroquine alone or with clofazimine	52
--	----

Chapter 5

Figure 5.1 Light microscope images of Giemsa stained clofazimine (un)treated W2 strains	58
Figure 5.2 Light microscope images of food vacuole isolation steps	59

Chapter 6

Figure 6.1 <i>Plasmodium falciparum</i> Chloroquine Resistance Transporter (<i>PfCRT</i>) topology of the transmembrane domains	61
Figure 6.2 <i>Plasmodium falciparum</i> Multi-drug resistance transporter (<i>PfMDR1</i> or <i>Pgh-1</i>) topology of transmembrane domains	62
Figure 6.3 SDS-PAGE of <i>Plasmodium falciparum</i> food vacuole protein samples	72
Figure 6.4 Mass spectrum of untreated <i>Plasmodium falciparum</i> W2 endocytic vesicles and cell debris (wash step)	73
Figure 6.5 Mass spectrum of untreated <i>Plasmodium falciparum</i> 3D7 food vacuoles	74

List of Tables

Chapter 2

Table 2.1 Drug concentrations (in nM) screened during Plasmodium viability testing	24
Table 2.2 Calculated gravimetric yields of fulvic acid and humic acid samples	25
Table 2.3 Test compound concentrations screened in mammalian toxicity testing.....	26
Table 2.4 IC ₅₀ values of drugs after 96 h for Plasmodium falciparum compared to HepG2 cells	31
Table 2.5 Selectivity index (SI) values for drugs	32
Table 2.6 The IC ₅₀ values (g/100mL) of humic compounds on <i>Plasmodium falciparum</i> strains	34

Chapter 3

Table 3.1 Test compound concentrations (in nM) for life-cycle progression study.....	40
--	----

Chapter 6

Table 6.1 Gradient Run for nLC on a Thermo Scientific EASY-nLC II	68
Table 6.2 Protein sample concentrations and quantities loaded to SDS-PAGE wells	70
Table 6.3 Description of sample treatment and location on SDS-PAGE gel	71
Table 6.4 ProteinScape (3.0) and Swissprot database identification of proteins	76
Table 6.5 PeptideShaker (0.36.1) and UniProt database identification of proteins	77

Chapter 1: Literature Review

Numerous important discoveries have led to our current level of understanding of human malaria. Among these were the reprinted observations by Charles Louis Alphonse Laveran, originally made in the early 1880s of mobile “amoeboid bodies” living within the blood cells of malaria-infected patients (Laveran, 1982). Today it is common knowledge that these bodies are parasitic protozoa classified under the genus *Plasmodium* (Yaeger, 1996). These parasites are transmitted into the blood of human hosts by mosquitoes as carrier vectors. Even though there are 450 known *Anopheles* mosquitoes, only 60 species are considered to be malaria vectors, with the female *Anopheles gambiae* mosquitoes as the the most important (Cohuet *et al.*, 2010).

To date five major species of *Plasmodium* parasites have been identified and are known to cause malaria symptoms in humans. Previously *Plasmodium knowlesi* has been categorised as a “zoonotic invader” but reports have emerged since 2004 of this species causing human infections in Southeast Asia (Singh & Daneshvar, 2013). The remaining species include *Plasmodium ovale*, *Plasmodium vivax*, *Plasmodium malariae* and *Plasmodium falciparum*; the latter of which causes severe malaria (Mita & Tanabe, 2012) and is prevalent in southern Africa. Due to the impact of *P. falciparum* in severe malaria, this parasite has been the main focus of this research project.

1.1 The clinical manifestation of malaria and acquired immunity

Another discovery made by the early clinical pathologist, Camillo Golgi, identified the link between parasite life-cycles and the clinical manifestations of fevers in patients with malaria infections (Macchi, 1999). Haemolysis and anaemia are inherent features of most *Plasmodium* parasites infections (Tuteja, 2007). *P. falciparum* intracellular stages alter the morphology of erythrocytes and restrict the blood flow through the host’s fine vasculature causing potentially fatal cerebral, respiratory, renal or placental malaria (Bartoloni & Zammarchi, 2012; Frevert &

Nacer, 2014; Moya-Alvarez *et al.*, 2014). Placental malaria has been found to negatively affect foetal development and increase the odds of post-natal malaria infection in infants (Moya-Alvarez *et al.*, 2014). Severe malaria is of major concern due to high mortality rates, particularly in African children under the age of five (González *et al.*, 2012; Manning *et al.*, 2014). However, it has been documented that adults surviving exposure to malaria in their youth develop partial immunity to further malaria infections and this is commonly referred to as non-severe or uncomplicated malaria (Bartoloni & Zammarchi, 2012; Omosun *et al.*, 2009). An acquired immunity reduces the risk of developing malaria, and increases the probability of survival. Researchers have confirmed that antibodies against the *P. falciparum* erythrocyte membrane protein 1 (PfEMP1), expressed on the surface of *Plasmodium* infected erythrocytes, contributed to the development of acquired immunity in these individuals (Gatton & Cheng, 2004).

1.2 Prevalence and distribution of malaria

The current global distribution of malaria is in tropical regions, but is estimated to shift due to climate change and other population changes (Caminade *et al.*, 2014; Noor *et al.*, 2014; Tuteja, 2007). Global efforts have prevented a number of malaria-related deaths between 2001 and 2012, yet it is estimated that 207 million malaria cases and 630 000 malaria deaths have been reported globally in 2012 (World Health Organization, 2013). In 2010 Africa was estimated to contribute 99% to the area of malaria infected land and 95% of the malaria infected population from global estimates (Gething *et al.*, 2011). The majority of malaria episodes are reported by countries in sub-Saharan Africa followed by Brazil, and southern Asia, whereas the United States of America and Europe mostly report occasional traveller's malaria and malaria due to exposure to infected blood products (Bhatia *et al.*, 2013; Cullen & Arguin, 2014; Singh & Sehgal, 2010; Tuteja, 2007). Bhatia, *et al.* have concluded that the incidence of malaria has dropped in Asia due to community involvement in the establishment of programmes funded by global collaborations (Bhatia *et al.*, 2013).

An increased availability of funds alone is insufficient in eradicating malaria, Amazigo *et al.* emphasise that other solutions could include approaches such as mass drug administration, enhancement of healthcare facilities and infrastructure, sustained training and deployment of health care professionals and establishment of community driven interventions (Amazigo *et al.*, 2012). The incidence of malaria in countries such as Bangladesh and Malaysia is estimated to have dropped by 75% between 2013 and 2015, and it has been found that the populations residing in highly endemic regions of Africa have decreased by approximately 12% between the years 2000 and 2010 (Bhatia *et al.*, 2013; Noor *et al.*, 2014).

1.3 Current eradication and treatment strategies and their shortcomings

1.3.1 Primary vector control

Many entomologists believe that malaria can be eradicated by eliminating the *Anopheles* vector through insecticide treated bed-nets (ITNs), indoor residual spraying (Spengler *et al.*) (Spengler *et al.*) and by larval management (Killeen *et al.*, 2013). *Anopheles gambiae* species tend to feed on human hosts indoors, consequently insecticide treated bed nets have been of immense value in decreasing the population of *An. gambiae* in central and southern Africa (Mutuku *et al.*, 2011). However, due to the fact that different species have variations in their feeding habits, alternative methods to suppress *An. arabiensis* and *An. funestus* populations are required (Mutuku *et al.*, 2011; Raman *et al.*, 2011). IRS has been shown to be effective in the Maputo province of Mozambique where malaria infections amongst teenagers has dropped by approximately 50% within a seven year period (Raman *et al.*, 2011).

Concerns over the pollutant and carcinogenic potential of pesticides such as dichlorodiphenyltrichloroethane (DDT) and hexachlorocyclohexane (HCH), used in ITNs and

IRS, have led to the banning of these substances in countries such as India (Yadav *et al.*, 2015). The feasibility of ITNs and IRS as vector control initiatives is questionable given that a number of malaria vectors do not feed indoors thereby avoiding pesticide exposure (Reddy *et al.*, 2011). The inaccessibility of a number of *Anopheles* larval development sources poses another challenge to this form of vector control (Killeen *et al.*, 2013).

1.3.2 Vaccine development

The emergence of resistance to previous primary drug regimens has motivated the global research community to prioritise the development of robust drug therapies or antimalaria vaccines. It is estimated that 80 trials are currently underway to test novel entities' efficacy as potential malaria vaccines (World Health Organisation, 2015). The majority of successful vaccines used to induce active immunity against non-malaria diseases have been designed from live-attenuated or inactivated whole micro-organisms (mostly bacteria) or viruses.

One anti-malarial vaccine is the RTS,S/AS01 candidate (Trade Name Mosquirix) which has undergone phase III clinical testing in 11 African countries, and has initially been found to reduce the acquisition of severe malaria in approximately half the population of infants treated (Agnandji *et al.*, 2012; Mwangoka *et al.*, 2013). AS01 functions as an adjuvant to enhance the immunogenicity of the parasitic circumsporozoite (Butykai *et al.*) protein, the major surface antigen of pre-erythrocytic sporozoites for which a modified version is present in the RTS,S vaccine (Butykai *et al.*; Casares *et al.*, 2010; Dame *et al.*, 1984; Wilby *et al.*, 2012).

The decisions on the roll-out of this vaccine are dependent on its proposed impact on public health, but it is estimated by Penny *et al.* that the “initial efficacy [of this vaccine] will probably be high, but [it will] decay rapidly” (Penny *et al.*, 2015). Various limitations for Mosquirix have been identified. There was a noted decrease in efficacy against severe malaria in infants (under

the age of five), especially in those who did not receive a follow-up booster shot, and there was no confirmation that vaccinated children were able to acquire immunological memory (Partnership Clinical Trials R.T.S./S., 2015). A small number of children exposed to the vaccine developed meningitis or generalised convulsive seizures, but there is no evidence that this was a causal effect (Partnership Clinical Trials R.T.S./S., 2015). Therefore Mosquirix cannot be considered a cure for malaria but rather as a contributor to the eradication efforts in malaria in endemic areas.

Another promising vaccine is undergoing small scale proof-of-concept, clinical testing and has been designed from non-replicating sporozoite stages of the *P. falciparum* malaria parasite, the intravenously administered PfSPZ vaccine (Seder *et al.*, 2013). Further research has not yet been publicised on this prototype vaccine. A different approach by researchers in Germany and the Netherlands has been the combination of numerous antigens from diverse stages of the *P. falciparum* life-cycle in a “multi-stage-specific cocktail” vaccine. Optimisation of chosen antigens and quantities thereof is required before *in vivo* testing can commence (Boes *et al.*, 2015).

Obstacles to the creation of a successful vaccine include the rapid life-cycle progression of the parasite associated with different therapeutic targets, the heterogeneity of strains, and the multiple mechanisms employed by the parasite to evade host immune responses (Aditya *et al.*, 2013). There are also a number of other logistical issues that will aggravate vaccine roll-out, such as the delivery of enough vaccines to remote and temperate endemic areas whilst ensuring product stability with proper transport, handling and storage. Furthermore, trained staff are required for vaccine administration, follow up monitoring and patient education. These issues also pertain to our current drug regimen.

1.3.3 Therapeutics in the pipeline

Since the sequencing of the *P. falciparum* 3D7 genome in 2002 numerous potential targets for novel therapies have been identified, including polyamine synthesis inhibitors and multi-stage active spiroindolones (Niemand *et al.*, 2013; Smith *et al.*, 2014). The Medicines for Malaria Venture (MMV) aims to research and develop affordable and efficacious alternatives to current drug treatments (Wells *et al.*, 2015).

1.3.4 Antimalarial therapeutics and their sites of action

Both severe malaria and non-severe malaria, also known as uncomplicated malaria, are treatable (Bartoloni & Zammarchi, 2012). Artemisinin-based combination therapies (ACTs), such as artesunate or artemether and either lumefantrine, amodiaquine, mefloquine, piperaquine or sulfadoxine-pyrimethamine are currently the first-line treatments in 84 countries globally (Veiga *et al.*, 2011; Visser *et al.*, 2014). Chloroquine is still used as a monotherapy for non-*Falciparum* infections as well as in regions of the Americas where resistance has not yet become a significant problem (Visser *et al.*, 2014). An introduction to the life-cycle progression of *P. falciparum*, the sites and the probable mechanisms of antimalarial action of these drugs are outlined below.

The *Plasmodium* parasite follows a complex, two host, multistage life-cycle during which the various stages can be identified by the morphological and functional changes in the parasite. The sexual and asexual parasite replication occurs in the different hosts which completes the full life-cycle. Figure 1.1 offers a brief outline of the *Plasmodium falciparum* life-cycle in the human and the major targets of drug treatment and vaccine development.

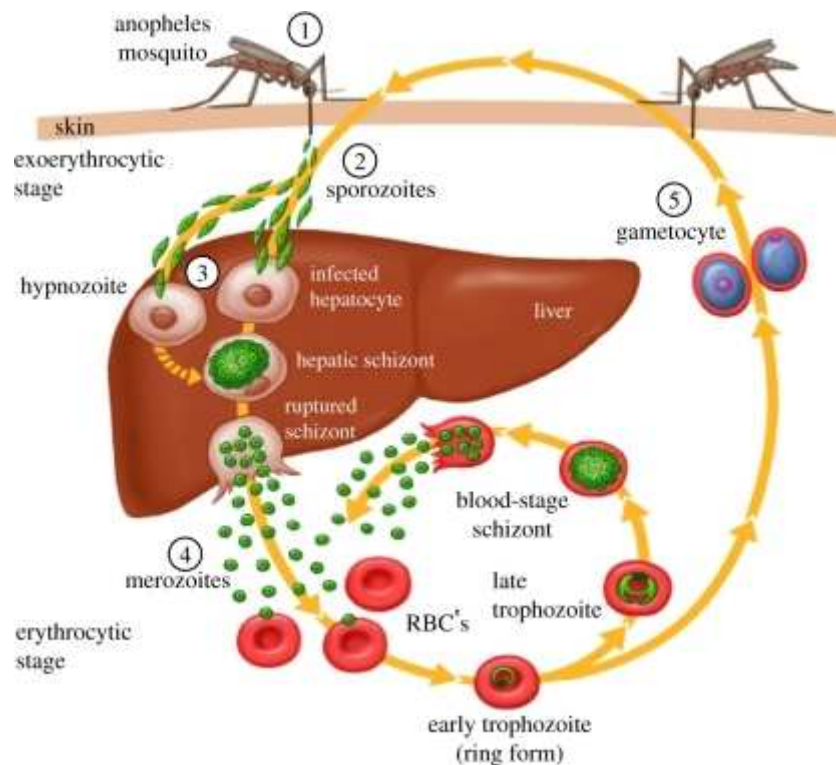


Figure 1.1 The *Plasmodium falciparum* life-cycle

(1) The female *Anopheles* mosquito ejects (2) sporozoites into the host circulation that migrate to the (3) liver where proliferation results in rupturing of hepatocytes and (4) release of merozoites into the host blood stream initiating the intra-erythrocytic life-cycle of the parasite, from which (5) gametocytes mature and are ingested by a new vector. Image taken from (Life-cycle of the malaria parasite, 2011).

A healthy human individual becomes infected with malaria when a *Plasmodium*-infected female *Anopheles* mosquito injects saliva containing *Plasmodium* sporozoites into the blood stream while taking a blood meal from the human host to nourish her eggs (Cohuet *et al.*, 2010). These sporozoites migrate via the circulating blood to the liver of the human host, where it invades hepatic cells then matures over about 10 days, dividing to form hepatic schizonts, which rupture the hepatocytes and release invasive merozoites (Hanssen *et al.*, 2010). Merozoites mark the beginning of the cyclical asexual replication stages of these parasites, characterised by intra-erythrocytic (IE) and brief extra-erythrocytic stages (Bannister *et al.*, 2000; Dixon *et al.*, 2012). The mechanism by which merozoites invade erythrocytes have been described previously and involves an intricate sequential interaction between proteins on the merozoites and surface proteins of the host erythrocyte to enable attachment, re-orientation and controlled entry of the parasite into the cytoplasm of the erythrocyte within a protective parasitophorous vacuole (Boyle

et al., 2010a; Cowman & Crabb, 2006). This invasion process does not compromise the newly invaded cell, which acts as host and food for the development of the next proliferative cycle of the parasite. Doubly infected erythrocytes have a decreased probability of successfully harbouring parasites.

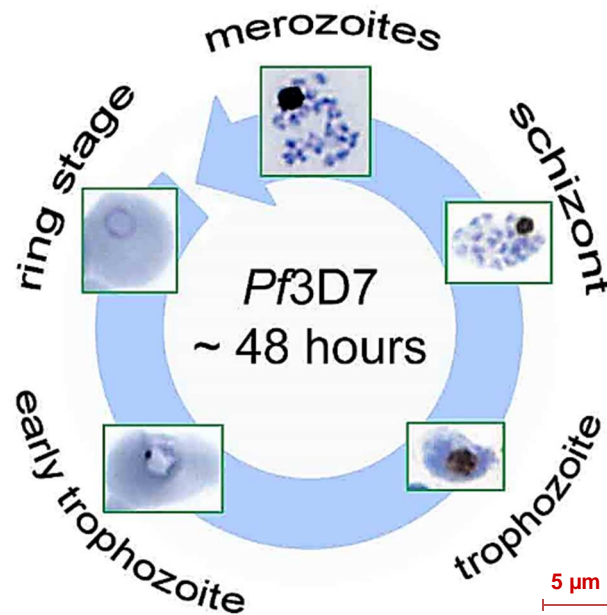


Figure 1.2 The intra-erythrocytic (IE) stages of *Plasmodium* parasites

Egressed merozoites invade healthy erythrocytes to initiate the IE cycle which consecutively develops into a ring stage, a trophozoite, a schizont and then more merozoites are released from the ruptured erythrocyte within a 48 h cycle.

P. falciparum progresses through its IE cycle (IEC) within 48 h during which the intracellular merozoite develops into the ring stage, followed by the trophozoite stage (Figure 1.2). During the next schizont stage, nuclear replication takes place through schizogony to form 16 to 30 new complete invasive merozoites that are released into the bloodstream upon rupture of the erythrocyte membrane. This results in an increase in the parasitaemia or parasite load (Bannister *et al.*, 2000). As the parasite progresses through its IEC the DNA content increases gradually, and can be annotated as having one nucleus (1N) during the ring and early trophozoite stages, 2N during the trophozoite stage, and >2N during the schizont stage (Izumiyama *et al.*, 2009; Niemand *et al.*, 2013).

Research findings suggest that endoplasmic reticulum stress upregulates the expression of proteins involved in gametocytogenesis, by enhancing the activation of Activating Protein (AP-2) transcription factors (Chaubey *et al.*, 2014). The *var* gene products work hand-in-hand with this process, and the expression thereof is enhanced when *P. falciparum* histone deacetylase 2 (PfHda-2), a virulence controlling gene, is suppressed in the asexual parasite (Coleman *et al.*, 2014). When an adequate parasitaemia is reached, maturing parasites are triggered to develop into gametocytes. This sexual stage of the parasite resembles sickle cells that are taken up into a healthy mosquito to continue the *Plasmodium* life-cycle (Dixon *et al.*, 2012).

The IEC of the *Plasmodium* parasite has been the focus of this study, specifically the trophozoite stage of parasitic development. In this stage parasites consume the content of the erythrocyte, breaking down large quantities of the most abundant erythrocyte protein, haemoglobin into nutrients and amino acids to make space for parasite growth, to regulate osmotic pressure and for metabolic processes, whilst producing haematin as a toxic by-product (Goldberg *et al.*, 1991; Mauritz *et al.*, 2009). The haeme is converted into inert, inherently magnetic haemozoin crystals which are stored in the parasite's digestive or food vacuole (FV), visible in the top right of the trophozoite in Figure 1.3 (Ribaut *et al.*, 2008).

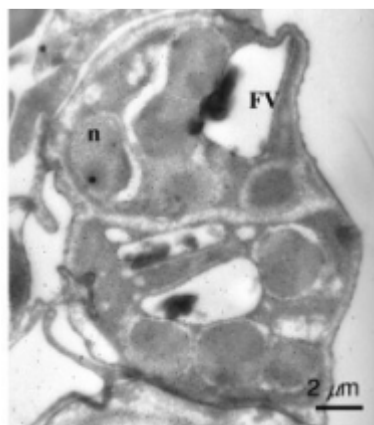


Figure 1.3 Transmission electron microscope image of a late stage trophozoite

The nucleus (n) and food vacuole (FV) are visible on the left and right-hand side of the image, respectively. Image taken from (Bhowmick *et al.*, 2009), magnification not provided.

Many common antimalarial substances act within the trophozoite food vacuole (Maeno *et al.*, 1993; Sullivan Jr *et al.*, 1996). The food vacuole membrane is a bilayer of approximately 4 -16 nm thickness across which chloroquine readily diffuses, and becomes trapped in the internal, acidic environment (Ehlgen *et al.*, 2012; Kapishnikov *et al.*, 2013).

1.3.4.1 Artemisinin and derivatives

Artemisinin is painstakingly extracted from the plant *Artemisia annua*, then derivatised to form artesunate which is systemically bioavailable for the treatment of severe malaria (D'Hulst *et al.*, 1996; ElSohly *et al.*, 1990). Artemisinin is a prodrug which is converted into dihydroartemisinin within target cells where free radicals are induced resulting in intracellular parasite death, artemisinin also targets gametocytes decreasing malaria transmission (Cui & Su, 2009; Garner, 2004). These substances and their analogues are used preferentially in combination with others due to their short half-life, distinct schizonticidal activity, and patient tolerability (Maeno *et al.*, 1993; Visser *et al.*, 2014). Reduced neutrophil and reticulocyte counts as well as elevated liver enzymes are the most commonly reported adverse clinical events for artemisinin and its derivatives (Olliaro, 1998).

1.3.4.2 Dihydrofolate reductase inhibitors and sulphonamides

Pyrimethamine and sulfadoxine are used in combination as a chemoprophylactic regimen in pregnancy (Le Port *et al.*, 2011; Visser *et al.*, 2014), with a favourable safety profile after organogenesis in the second and third trimester (Peters *et al.*, 2007). Treatment with this preventative therapy earlier in pregnancy is reported to cause neural tube developmental disorders in the foetus (Peters *et al.*, 2007).

Due to the occurrence of resistance in *P. falciparum* strains to the sulphonamide drug class, there is limited use for these drugs clinically (Mutuku *et al.*, 2011). Pyrimethamine specifically inhibits dihydrofolate reductase, and sulfadoxine (a sulphonamide) prevents the activity dihydropteroate synthase both of which are essential for parasite folate synthesis pathways and consequent cell replication (Wang *et al.*, 1997; Yaro, 2009; Zimmerman *et al.*, 1987). Point mutations in genes reduce the affinity of pyrimethamine and sulfaxine to their target enzymes and confers drug resistance in *Plasmodium* parasites (Basco *et al.*, 1996; Basco & Ringwald, 1998).

1.3.4.3 Protein synthesis inhibitors

Doxycycline and clindamycin are both classified as protein synthesis inhibitors which prevent parasitic ribosomal mRNA translation (Wilson *et al.*, 2013). These drugs are commonly prescribed in combination with chloroquine for malaria prevention in travellers (Aditya *et al.*, 2013). Atovaquone/proguanil is a common remedy for non-*Falciparum* malaria in Europe, and is prescribed as malaria prophylaxis for travellers, this drug combination acts by suppression of cellular respiration through inhibition of the electron transport chain (Smith *et al.*, 2014; Visser *et al.*, 2014; Wilson *et al.*, 2013).

Eflornithine (also known as difluoromethylornithine or DFMO) is classified as an ornithine decarboxylase inhibitor, which reduces the formation of the polyamines; spermidine, spermine and putrescine required for successful polyamine synthesis (Assaraf *et al.*, 1988). Interestingly DFMO is used in the treatment of the parasitic infection trypanosomiasis and female hirsutism as a topical ointment but its use was limited as an anticancer agent due to the cost per treatment (Amazigo *et al.*, 2012); (Croft, 1999). DFMO has only recently been adopted for its antiplasmodial effect in late-stage cerebral malaria (Birkholtz *et al.*, 2011). This study assessed the efficacy of DFMO as an antimalarial in comparison to other agents.

1.3.4.4 HMG-CoA reductase inhibitors

Statins are used for the treatment of hypercholesterolemia in humans, and act as a competitive inhibitor of the 3-hydroxy-3-methyl-glutaryl-Coenzyme A (HMG-CoA) reductase enzyme preventing the hepatic formation of mevalonate; an important precursor of cholesterol in humans (Pradines *et al.*, 2007). Lovastatin, also known as mevinolin, has been found to hinder growth of certain *Salmonella*, *Trypanosoma* and *Leishmania* species, possibly due to the expression of HMG-CoA reductase enzymes in these organisms (Catron *et al.*, 2004; Coppens *et al.*, 1995; Montalvetti *et al.*, 2000). The expression of this enzyme has not been confirmed in *P. falciparum* species, yet an IC₅₀ value between 0.25-0.5 µM has previously been obtained for *in vitro* exposure of *P. falciparum* strains to active mevinolin (in its beta-hydroxy acid form) (Grellier *et al.*, 1994; Pradines *et al.*, 2007). Statins have been found to prevent cytoadherence of infected erythrocytes to micro-vasculature, suppressing events such as cerebral malaria and endothelial damage, therefore *in vitro* and clinical data may still confirm statins to be efficient preventative therapies (Taoufiq *et al.*, 2011). The antimalarial activity of mevinolin was assessed in this study.

1.3.4.5 Organic constituents

Humic substances, consisting of humic acid, the related lower molecular weight substance fulvic acid and humin, are formed through the decomposition of organic matter resulting in alkali soluble polymeric compounds with relatively high molecular weights (Beckett *et al.*, 1987). The traditional uses for humic substances is vast, and include applications such as topical treatment of burns, skin infections and even treatment of poisonings or bone fractures. Findings support humic substances as antimicrobial and anti-inflammatory agents and anecdotal claims suggest decreased incidence of malaria in individuals taking these substances, further investigation into the antiplasmodial properties of humic and fulvic acids is necessary (Gandy *et al.*, 2012; Sherry *et al.*, 2012). This study aimed to assess the antiplasmodial activity of humic and fulvic acids.

1.3.4.6 Anti-mycobacterials

Clofazimine is an outdated riminophenazine antibiotic forming part of the primary leprosy treatment regimen (Cholo *et al.*, 2012; Makgatho *et al.*, 2000). The clinical efficacy of this compound is associated with its anti-inflammatory properties, however due to its extreme lipophilicity and consequent extended half-life numerous unwanted side-effects occur. The most prevalent of these side effects is the dose-related discoloration of the skin and conjunctiva of patients (Cholo *et al.*, 2012). Studies have found that tetramethylpiperidine-linked (TMP) riminophenazines have potent anti-mycobacterial properties and also inhibit P-glycoprotein (P-gP) activity in multiple drug resistant (MDR) cancer cell lines, sensitising the cells to the action of chemotherapeutic agents without altering the expression of the target protein (Makgatho *et al.*, 2000; Van Rensburg *et al.*, 1998). Clofazimine has been found to inhibit the Wnt-signalling pathway in mammalian breast cancer cells, associated with inhibition of cell growth and metastasis (Koval *et al.*, 2014). In this study the antiplasmodial capability of clofazimine was assessed and an aim was to determine whether treatment with clofazimine could aid in the reversal of chloroquine resistance by altering the action and/or expression of the P-glycoprotein homologue 1 (Pgh1) transport protein, the *Plasmodium* parasite's homologue of the mammalian MDR transporter (Saliba *et al.*, 2008).

1.3.4.7 4-Aminoquinolones and derivatives

Quinine was originally derived from the cinchona tree, and is associated with the serious condition of cinchonism linked to cardiac abnormalities, consequently more tolerable analogues were invented (Visser *et al.*, 2014). Primaquine is the only clinically used quinine that targets gametocyte stages of the parasite, and has applications in preventing relapse associated with *P. vivax* and prevention of malaria transmission. Quinine toxicity is prevalent and presents as cardiac and neurologic anomalies in patients receiving high doses, and reported complications include renal failure and aborted pregnancies (Smith *et al.*, 2014; Wilson *et al.*, 2013).

Chloroquine is the prototype drug in this class, with amodiaquine, piperaquine and naphthoquine as structural analogues, however decreased parasite sensitivity has been reported for all of these quinine derivatives (Veiga *et al.*, 2011). Chloroquine exerts its toxicity on *Plasmodium* parasites through inhibition of the sequestration of haem by-products in the food vacuole during the trophozoite stage (Wilson *et al.*, 2013). Chloroquine resistance by malaria parasites has led to the global use of artemisinin-based combination therapies to control and treat malaria infections (Visser *et al.*, 2014). It is postulated that the mechanism by which *P. falciparum* protozoa evade chloroquine's ability to prevent the conversion of toxic haem by-products into haemozoin crystals is through the active removal of chloroquine from the parasite food vacuole and the parasitophorous membrane (Veiga *et al.*, 2011).

1.4 *Plasmodium falciparum* survival strategies and antimalarial resistance

There are various strains of *P. falciparum* each with a distinct susceptibility profile to current and past antimalarial regimens. The Dd2 and HB3 strains have been found to be resistant to antifolate drugs and these strains are then referred to as an antifolate resistant phenotype with Dd2 being resistant to sulfadoxine, and HB3 and 7G8 strains to pyrimethamine (Cowman *et al.*, 1988; Wang *et al.*, 2004; Wang *et al.*, 1997). The last two mentioned drugs form the basis of intermittent preventive treatments in pregnancy in many African countries, and the prevalence of resistant strains of plasmodia is of concern (Moya-Alvarez *et al.*, 2014). It has been found that W2 and Dd2, T9-94, 7C12 and 7G8 strains are chloroquine resistant whereas HB3, D6 and 3D7 are chloroquine sensitive (Castellini *et al.*, 2011). Artemisinin combination therapies have been the treatment of choice for the last 10 years, however reports of resistance are now widespread across Southeast Asia (Ashley *et al.*, 2014). Amodiaquine (a chloroquine analogue), for which resistance was first reported in 2004 in Tanzania, is currently experiencing efficacy problems in Angola due to the presence of the *PfCRT* haplotype (*P. falciparum* chloroquine resistance

transporter) (Sa & Twu, 2010). Similar reports have arisen for mefloquine, an analogue of quinine (Visser *et al.*, 2014). Chloroquine resistance has been the focus of this research project.

1.4.1 Chloroquine resistance

The primary proteins involved in chloroquine resistance of *P. falciparum* have been identified as *PfCRT* and *PfMDR1* (*P. falciparum* multiple drug resistance protein 1) also known as Pgh1 (P-glycoprotein homologue 1), which are 45 kDa and 162 kDa proteins respectively (Raj *et al.*, 2009; Valderramos & Fidock, 2006). Both proteins are located within the membrane of the trophozoite food vacuole (FV) (Duraisingh & Cowman, 2005). The presence of point mutations, other alterations in the genes encoding these proteins or increases in expression of the proteins have been found to produce some *P. falciparum* strains demonstrating resistant phenotypes (Raj *et al.*, 2009; Reed *et al.*, 2000; Valderramos & Fidock, 2006). The location and inherent function of *PfCRT* and *PfMDR1* lead researchers to believe that they are intrinsically involved in processes that allow the expulsion of drug compounds from either the parasite itself or its food vacuole, rendering the drug based treatments obsolete (Valderramos & Fidock, 2006). These evasive mechanisms are believed to occur due to accumulative effects of a number of genes instead of single point mutations, and may be the underlying basis for multi-drug resistance (Duraisingh & Cowman, 2005; Reed *et al.*, 2000; Saliba *et al.*, 2008; Valderramos & Fidock, 2006).

The genetic plasticity of *P. falciparum* associated with increased drug resistance phenotypes necessitates the continued investigations of new potential antimalarial agents. The efflux of chloroquine has been linked to the presence of P-glycoprotein (PgP) homologue entities, encoded by the *Pfmdr1* gene, present on the food vacuole membrane (Cowman *et al.*, 1991; Saliba *et al.*, 2008; Veiga *et al.*, 2011). This parasite PgP homologue is similar in structure to the mammalian multi-drug resistance (MDR) pump, responsible for the drug resistance of many

human cancers. The mammalian MDR pump may be inhibited, without altering the expression of the protein, by various chemotherapeutic sensitisers including clofazimine and its analogue B669 (Van Rensburg *et al.*, 1998). This research project aimed to determine whether chloroquine-resistant strains of *P. falciparum* could be sensitised to the action of chloroquine by co-exposure to a chemotherapeutic agent, clofazimine. If sensitisation was induced, the study furthermore aimed to establish whether sensitised strains of *P. falciparum* then expressed altered quantities of food vacuole membrane proteins in comparison to expression levels of chloroquine susceptible and resistant phenotypes of the parasite. This research project was novel in the attempt to sensitise resistant malaria parasites to chloroquine by the use of the Pgp inhibiting, antimycobacterial clofazimine. An additional aspect was to assess the antiplasmodial ability of the ubiquitous organic compounds; humic and fulvic acid, due to anecdotal claims that these compounds prevent malaria. In this project, proteomic analysis was performed to attempt to detect and interpret changes in resistance on the protein level.

1.5 Research question

The following research question was posed:

Does clofazimine induce re-sensitisation of chloroquine resistant *Plasmodium* strains and is the expression of multi-drug resistance proteins on the food vacuolar surface of the resistant *Plasmodium falciparum* trophozoite stage parasites altered thereby?

1.5.1 Aims of the study

The aims of this research project were to screen compounds approved for other indications to ascertain their antiplasmodial activity and life-cycle specificity on chloroquine-sensitive and – resistant *P. falciparum* strains and to assess the changes in expression of resistance proteins on the surface of trophozoite food vacuoles between these.

1.5.2 Objectives

The objectives formulated for this research project were:

- To determine the antiplasmodial activity, mammalian cytotoxic effects, and parasite stage-specificity of humic and fulvic acids, mevinolin (lovastatin), and clofazimine
- To compare the efficacy and potency of the above compounds to the standard antimalarials; chloroquine, artemisinin and α -difluoromethylornithine (DFMO)
- To assess if resistant strains of *P. falciparum* (W2) can be sensitised to chloroquine through clofazimine treatment
- To conduct comparative proteomics on resistance proteins harvested from food vacuole membranes of clofazimine treated (possibly chloroquine sensitised) W2 parasites, wild type W2 and untreated 3D7 strains by spectral counting.

1.6 Study design

This research project was an *in vitro* analytical, experimental study with components that comprised parasite culturing, drug or compound sensitivity assessment, the assessment of mammalian hepatocyte drug susceptibility and isolation and purification of trophozoite protein samples. *In vitro* assessment of altered parasite life-cycle progression after drug exposure was performed. Proteomics results were analysed to attempt the identification of proteins and detection of possible changes in protein abundances, specifically membrane transport proteins previously linked to *Plasmodium* parasite drug resistance.

Chapter 2: Antiplasmodial efficacy and selective toxicity

2.1 Introduction

Since the 1970's, when *Plasmodium* parasites were first successfully cultured *in vitro* in glass jars with tea-lights, a number of enhancements and adaptations on *Plasmodium falciparum* culturing techniques have been made. It is now possible to culture all the stages of the entire *Plasmodium* life-cycle *in vitro* under host model-conditions (Miao *et al.*, 2013; Schuster, 2002; Trager & Jensen, 1976).

In order to answer a number of research questions on the efficacy of drug compounds on specific *Plasmodium* species, it is essential to know which population-stage of parasites is being investigated. *Plasmodium* parasites express different proteins and receptors depending on their IE stage and do not progress through their life-cycle in unison in *in vitro* cultures (Florens *et al.*, 2002; Lemieux *et al.*, 2009). There are numerous methods by which parasite populations can be synchronised. The most accepted methods are those that use Percoll or sorbitol treatment. The Percoll method entails the centrifugation of parasite samples through a Percoll gradient trapping schizont stages, however, this method is not recommended for parasite isolates for which sensitivity to the treatment is unknown (Childs *et al.*, 2013; Dwek *et al.*, 1980). Another less cumbersome method achieves synchronisation by exposing parasite mixed stage cultures to 5% (w/v) D-sorbitol, with an osmolality of 287 mOs/kg, which lyses the erythrocyte membranes of the susceptible trophozoite and schizont populations (Lambros & Vanderberg, 1979). This treatment method results in a selected population of approximately 95% ring stage parasites with uninfected erythrocytes. Sorbitol and Percoll toxicity is however a concern which can be overcome with routine alteration of the synchronisation method employed or incorporation of a few rest days for cultures to recover prior to re-treatment.

Mature uninfected erythrocytes are anucleate whereas infected erythrocytes contain *P. falciparum* parasites that may express various concentrations of DNA depending on their level of maturation (Gerald *et al.*, 2011). This phenomenon can be exploited as a method to determine parasite viability by the use of a fluorescent SYBR Green-1® dye which binds double-stranded DNA (Dragan *et al.*, 2012). SYBR Green-1® is a membrane permeant dye and penetrates live and dead cells (Zipper *et al.*, 2004).

The antimalarial ability of humic and fulvic acid, mevinolin, clofazimine were assessed in comparison to artemisinin, chloroquine and DFMO using the Malaria SYBR Green-1® Fluorescence assay (MSF Assay). These drugs were tested against the following strains; *P.falciparim* 3D7, W2 (chloroquine resistant, originating from Indochina), and HB3. The susceptibility of mammalian hepatic cells to the action of these drugs was assessed in order to determine their selective toxicity as reported by selectivity indices (SI).

2.2 Materials and Methods

2.2.1 Routine culture of *Plasmodium falciparum*

Parasites and blood were handled according to aseptic, sterile techniques in Class 2 laminar-flow safety cabinets with appropriate personal protective equipment. All non-sterile solutions and reagents were filter-sterilised (0.22 µm filter) or autoclaved prior to use. All reagents that are not heat sensitive were heated in a waterbath (Scientific 34 L 132 Model) to 37°C for at least 15 min before use. Roswell Park Memorial Institute (RPMI)-1640 medium (Sigma), containing 25 mM 4-(2-hydroxyethyl)-1-piperazineethanesulfonic acid (HEPES), 0.2% (w/v) glucose, 0.2 mM hypoxanthine, 23.81 mM sodium bicarbonate, and 5 g/L Albumax II was stored at 4°C until use within two weeks. Complete medium was used in all experiments unless where stated that incomplete culture medium (RPMI-1640 without addition of Albumax II) was used. All parasite waste was treated with a sodium hypochlorite bleach solution before disposal. Methods were

adapted from previous publications (Allen & Kirk, 2010; Scheibel *et al.*, 1979; Trager & Jensen, 1976). Briefly, *P. falciparum* 3D7 (chloroquine sensitive), W2 (chloroquine resistant), and HB3 (antifolate resistant) strains were maintained in human erythrocytes at approximately 5% haematocrit (hct) in complete RPMI-1640 culture medium. The blood groups of donors were recorded. The parasites were incubated in an orbital shaker incubator (MRC, TOU-50) at 60 rpm, in a 37°C atmosphere of 5% O₂, 5% CO₂ and 90% N₂ (Afrox Scientific).

2.2.1.1 Thawing cryofrozen parasites to start-up culture

P. falciparum parasite strains were removed from liquid nitrogen storage (1 mL, 5% hct, 10% parasitaemia in cryotubes) and thawed at 37°C as required. Once thawed, membranes of infected erythrocytes were conditioned with 0.2 mL of 12% (w/v) NaCl followed by 1.8 mL of 1.6% (w/v) NaCl solutions for five min each. The NaCl and parasite solutions were transferred to 15 mL tubes and centrifuged at 2500 g (BOECO, C-28A) for five min, after which the supernatant was removed. Culture medium and blood were added to obtain a 10% erythrocyte suspension at a final hct of 5%. The suspension was transferred to a 75 cm² culture flask, gassed for 30 seconds (5% O₂, 5% CO₂ and 90% N₂; Afrox Scientific) and incubated at 37°C in an orbital shaker incubator (MRC, TOU-50) set at 60 rpm.

2.2.1.2 Human blood for *Plasmodium falciparum* culture

Whole blood (O⁺ or A⁺) was drawn by staff of the South African National Blood Services (SANBS) from healthy human volunteers as required and stored at 4°C in sterile, non-pyrogenic SO Fenwal[®] AFRO193 blood bags containing citrate phosphate, glucose, and adenine anticoagulant solution (Adcock Ingram, South Africa). The following method has been explained previously, by Jensen *et al.* (Trager & Jensen, 1976). Whole blood was decanted into 50 mL tubes and stored for at least 24 h at 4°C to allow for separation of the serum and buffy coat. The separated serum and buffy coat were removed by Pasteur pipettes connected to a flask

evacuated with a vacuum pump (Integra Vacusafe). The remaining packed erythrocytes (PCV) were washed by addition of 1x phosphate buffered saline (PBS) (137 mM NaCl, 2.7 mM KCl, 10 mM phosphate, pH 7.4) before being diluted (1:1) with incomplete culture medium. This 50% working solution of blood was stored at 4°C until use within two weeks. This erythrocyte enriched suspension was used in all experiments unless stated that packed erythrocytes were required.

2.2.1.3 Estimation of percentage parasitaemia from thin smears

Approximately 100 µl of the parasite infected erythrocyte suspension was removed from the culture flask with a Pasteur pipette and transferred to an Eppendorf tube, centrifuged (1 min) and a few microliters of medium removed to obtain a 50% infected erythrocyte suspension. A drop of the suspension was placed on a microscope slide and spread using a second microscope slide held at a 45° angle to form a monolayer of erythrocytes. The prepared slide was air-dried, fixed in pure methanol (1-2 seconds), tapped dry, stained for 5 min in a 14% (v/v) Giemsa solution (Sigma), and rinsed gently under flowing tap water. After air-drying the slide was viewed under a compact light microscope (Nikon Labophot) with the oil immersion lens (1000x magnification, equipped with a grid on the ocular). The percentage parasitaemia was determined by counting the number of infected erythrocytes out of a total of 500 erythrocytes with a hand-held tally counter (Lasec). The parasitaemia was generally maintained between 3-8% prior to experiment preparation by diluting cultures and/or splitting flasks.

2.2.1.4 Routine feeding of parasites

Culture medium had to be replaced daily in order to remove by-products and replace essential nutrients. After parasitaemia estimation the remaining culture was transferred to a 50 mL tube, and centrifuged (Boeco, C-28A) for 5 min at 2500 g. The supernatant was aspirated with a plastic Pasteur pipette and a Pipette bouy (Hirschmann Laborgerate). The infected erythrocyte pellet was resuspended in 30 mL fresh, culture medium and transferred to a 75 cm² culture flask.

Before sealing and returning to the orbital shaker incubator (MRC, TOU-50) flasks were exposed to gas (5% O₂, 5% CO₂ and 90% N₂; Afrox Scientific) for 30 seconds using an unplugged glass Pasteur pipette and a 0.22 µm filter.

2.2.1.5 Diluting and splitting cultures

Flask content was diluted or split if the parasitaemia was estimated to be above 8%. This practise prevented parasite death resulting from lack of necessary nutrients as occurs at trophozoite parasitemias >10%. Splitting flasks also enabled parasite yields to be increased for experiment purposes. Parasite suspensions were decanted into 50 mL tubes from culturing flasks and centrifuged (BOECO, C-28A) at 2500 *g* for 5 min. Then the pellet was adjusted by addition of 50% erythrocyte suspension, if necessary, and the correct volume of new complete culture medium was added to retain an hct of 5%. The relevant number of 75 cm² culture flasks was then filled with 30 mL parasite suspension (5% hct), gassed and placed in the orbital shaker incubator (MRC, TOU-50). For example, to split a 30 mL culture (5% hct) at 10% parasitaemia into two 30 ml cultures with equal parasitaemia; 3 mL of 50% erythrocyte suspension was added to the infected erythrocyte pellet. The pellet was further resuspended in 27 mL of culture medium and two separate culture flasks were each filled with 15 mL of the suspension. A further 15 mL of fresh complete culture medium was added to each separate flask before being gassed, sealed and placed back in the orbital shaker incubator (MRC, TOU-50).

2.2.1.6 Cryopreservation of infected erythrocytes

Excess cultures consisting of early ring stages of parasites, 10-16 h post invasion, at 10% parasitaemia were frozen. Cultures were centrifuged (BOECO, C-28A) at 2500 *g* for 5 min, followed by addition of glycerolyte (5 parts) to the pellet (3 parts). Aliquots were placed in screw-cap cryotubes and stored in poly-styrofoam boxes for 24 h at -80°C before long term storage in liquid nitrogen. These methods were adapted from literature (Diggs *et al.*, 1975).

2.2.2 Synchronisation of *Plasmodium falciparum* cultures to ring stage

The unsynchronised cultures, visible as mixed trophozoites and ring stages, were transferred to sterile 50 ml centrifuge tubes and centrifuged (BOECO, C-28A) at 2500 *g* for 5 min. The supernatant was removed and 15 mL of 5% (w/v) D-sorbitol (in triple distilled H₂O, pre-heated to 37°C in a water bath) added to the packed infected erythrocytes. Fresh erythrocytes (50%) were added to compensate for the erythrocyte loss (approximately 1 mL), culture medium was added (to achieve a 5% hct) and cultures were gassed before returning to flask to the incubator. This process was repeated once, maximum twice, per week or prior to commencement of experimentation to obtain cultures that were synchronised to >95% in the early ring stage as trophozoite and later stage infected erythrocytes would lyse.

2.2.3 Test compound preparation and storage

Chemically pure commercial preparations of artemisinin, chloroquine, α -difluoromethylornithine hydrochloride (DFMO, also known as eflornithine) were provided by the Department of Biochemistry, University of Pretoria (Sigma, St Louis, USA). Stock concentrations of artemisinin were prepared in 100% (v/v) dimethyl sulphoxide (DMSO) and those of chloroquine and DFMO in distilled water. Fulvic Acid (Fulhold (Pty) Ltd) samples and humic acid (Sherston, Pretoria. pH 6.98) were in a liquid state and stock concentrations were determined as percent dry mass by a gravimetric yield method.

Stock concentrations of mevinolin (Sigma, St Louis, USA) were prepared in a ratio of 20:5:5 of 100% (v/v) DMSO, ethanol and distilled water respectively. Where appropriate, aliquots were stored between -20°C and 4°C for the duration of the study. Fulvic acid and humic acid samples were stored at room temperature in opaque containers.

2.2.4 *Plasmodium falciparum* viability testing

The antimalarial activities of the drug compounds were tested on three strains of *P. falciparum*, i.e. 3D7 (chloroquine sensitive), W2 (chloroquine resistant) and HB3 (antifolate resistant), on 96 well plates using the Malaria SYBR Green-1® based fluorescence (MSF) assay, as described previously (Bennett *et al.*, 2004; Smilkstein *et al.*, 2004; Verlinden *et al.*, 2011). Distilled water (200 µL) was pipetted into all the wells along the edge of the plate to avoid evaporation of sample-wells' content (edge effects) distorting data readings. A parasite suspension was pipetted (2% parasitaemia, 2% hct) at 100 µL/well in all the remaining wells. The positive growth control wells received 100 µL of complete culture medium. The negative growth control served as a blank for background fluorescence and these wells received 100 µL chloroquine (1 µM) per well (final concentration of 0.5 µM chloroquine/well). The remainder of the wells were dosed with 200 µL of two high concentrations, which were 2-fold serial diluted (100 µL test compound in 100 µL complete culture medium) into eight consecutive wells per concentration. This process was repeated for each of the test compound. Table 2.1 and Table 2.2 outline the test concentrations used for testing.

Table 2.1 Drug concentrations (in nM) screened during *Plasmodium* viability testing

	Artemisinin	Chloroquine	DFMO	Clofazimine	Mevinolin
3D7	200 and 250	60 and 80	3.14 x 10 ⁶ and 4.1x 10 ⁶	2.25 x 10 ³ and 3.44 x 10 ³	6.19 x 10 ⁵ and 5 x 10 ⁵
W2	200 and 250	160 and 240	2.05 x 10 ⁶ and 3.14 x 10 ⁶	2.250 x 10 ³ and 3.438 x 10 ³	3,1x 10 ⁵ and 5 x 10 ⁵
HB3		40 and 60	2.05 x 10 ⁶ and 3.14 x 10 ⁶		3,1x 10 ⁵ and 5 x 10 ⁵

As screened by the MSF assay, data are reported in nM. Two concentrations were placed in two separate wells of the microplates and consequently serial diluted (2-fold).

Humic and fulvic acid sample concentration were determined by gravimetric yield methods (Table 2.2), and stock solutions of these substances were used as maximum concentrations for *Plasmodium* viability testing and dose-response curve generations.

Table 2.2 Calculated gravimetric yields of fulvic acid and humic acid samples

Description used	Fulhold (Pty) Ltd description	Gravimetric yield (%)
Fulvic acid 1	#390	4.09 ± 0.1
Fulvic acid 2	#377/11	4.05 ± 0.8
Fulvic acid 3	#391/11	4.11 ± 0.2
Humic acid	Humic acid	26.27 ± 8

Data are reported as mean ± SEM (n=3)

Plates were placed in a modular gas chamber, and gassed for 1-2 min before incubation in a stationary incubator at 37°C for 96 hs. Thereafter, plates were frozen at -20°C overnight to aid erythrocyte lysis, thawed and resuspended. After resuspension of the well content, 100 µL of each well was transferred to matching wells in a clear plate containing 100 µL SYBR Green® dye solution (0.2 µL SYBR Green® dye from Life Technologies per milliliter lysis buffer consisting of 20 mM Tris, 5 mM EDTA, 0.008% w/v saponin, 0.08% v/v Triton X-100, pH 7.5). Clear plates were assessed for their fluorescence prior to filling and showed negligible interference, comparable to solid-white plates. Fluorescence was measured immediately (Fluoroskan Ascent FL Fluorometer, Thermo Labsystems) at an excitation wavelength of 485 nm and emission of 538 nm.

2.2.5. Mammalian toxicity screenings

As a predictive model of human hepatotoxicity the human liver cancer cell line HepG2 (ATCC® HB-8065™) was exposed to all test compounds and cell death was screened by the Sulforhodamine B (SRB) colorimetric assay, as described previously by Rubinstein *et al.* (Rubinstein *et al.*, 1990). These cells were maintained in Eagle's minimum essential medium (EMEM) supplemented with 2% (v/v) foetal calf serum (FCS) and incubated at 37°C in a 5% CO₂ atmosphere. Cells were seeded at 2.5 x 10⁵ cells/mL in a 96 well microplate and incubated

overnight to allow formation of a monolayer. Then a range of concentrations of the individual test compounds were pipetted into individual wells or serial diluted (two-fold) as outlines in Table 2.3 below.

Table 2.3 Test compound concentrations screened in mammalian toxicity testing

	Artemisinin	Chloroquine	DFMO	Clofazimine	Mevinolin
					1x 10 ⁶ , 5 x 10 ⁵ , 3.75 x 10 ⁵ ,
HepG2	6.68 x 10 ⁵	2 x 10 ⁵	1.27 x 10 ⁸	2 x 10 ⁴	2.5 x 10 ⁵ , 1.25 x 10 ⁵ , 5 x 10 ⁴ , 2 x10 ⁴ , 1x10 ⁴

As screened by the SRB assay, data are reported in nM. Where a concentration range is not indicated concentrations were serial diluted (2-fold) within wells for IC₅₀ determination.

Two-fold serial dilutions of artemisinin, chloroquine, DFMO and clofazimine were made in well in order to obtain concentration points on the final dose-response curves' slope between the limit of detection and the limit of quantitation. It has been noted previously that a number of antimalarials have steep dose-response curves, including chloroquine. Concentrations for mevinolin were however pipetted into well, at the concentrations indicated in Table 2.3.

A 0.25% (w/v) saponin solution (in well concentration) was included as a negative control for growth and served as a blank for background absorbance. For a positive control of 100% growth a number of wells received an equivalent volume of EMEM medium without addition of test compound. HepG2s were exposed to the drug treatments for 72 h, thereafter each well was exposed to 10% (w/v) trichloroacetic acid (TCA) for at least 48 h to allow for protein fixation and enhanced precipitation for SRB adhesion. The wells in the plates were gently rinsed with running tap water, allowed to dry, stained with 0.057% (w/v) SRB dye for 30 min at room temperature,

and the remaining unbound dye washed off with 1% (v/v) acetic acid. Dye that had interacted with proteins from the cells were dissolved in 10 mM Tris base solution and plates were read with a microplate reader (ELX 800, BioTek, with BioTek's Gen5™ software to calculate calibrations and extrapolations using best fit formulae) at an absorbance wavelength of 540 nm and a reference wavelength of 630 nm was set to account for the effect of extraneous precipitated protein and other debris.

2.2.6 Interpretation of SRB and MSF Assay results

All microplate experiments were performed in triplicate with three replicate wells for each test compound concentration assayed. The percentage inhibition of the test compounds at various test compound concentrations was expressed as a percentage inhibition relative to growth in untreated sample wells (i.e. the average of positive control wells) and was calculated in Excel, Microsoft Office 2010 using the following equation:

% Inhibition of cell OR parasite growth

$$= \left(\frac{\text{Mean sample readings} - \text{Mean blank (0.25\% } \left(\frac{w}{v}\right) \text{ saponin OR 0.5 } \mu\text{M CQ)}}{\text{Mean positive control readings (untreated HepG2 cells OR parasites) - Mean blank}} \right) \times 100$$

Data were plotted as drug response curves using percentage inhibition relative to untreated parasite wells or cells using GraphPad Prism version 5.0 software (GraphPad Software, San Diego California USA, www.graphpad.com). Non-linear LOWESS spline fit method was used to determine the concentration at which test compounds inhibited cell growth by 50% (IC₅₀). The standard error of the mean was also calculated for each concentration and for the IC₅₀ values calculated, and reported sample sizes (n) are from technical and biological repeats. To determine the statistical significance of IC₅₀ concentrations of compounds tested on *P. falciparum* strains and HepG2 cells, the one-way ANOVA and Bonferroni's *post-hoc* test were

performed (GraphPad Prism version 5.0). Results were considered to be significant if a *p*-value of less than 0.05 was indicated. All the concentrations on the axes of the dose-response curves are plotted on a logarithmic scale in order to visualise a wider range of concentrations and to provide a classical sigmoidal dose-response curve. The goodness of fit of all data points from the graphs was quantified by their corresponding coefficients of determination.

The selective toxicity of the test compounds for the *P. falciparum* parasite in comparison to mammalian HepG2 cells was visualised through a selectivity index (SI) value calculated by the following formula:

$$SI = IC_{50} \text{ of HepG2 cells} / IC_{50} \text{ of parasites}$$

A selectivity index value greater than 10, indicating greater toxicity to parasites versus toxicity to mammalian host cells, is considered adequate for an antimalarial therapy (Avery *et al.*, 2014). However a ratio greater than 1000 is ideal according to the Medicines for Malaria Venture (MMV).

2.3 Results

2.3.1 Routine culture of *P. falciparum*

Plasmodium strains were synchronised with sorbitol twice weekly to narrow down time lapse between life-cycle stages and to obtain a population of 95% early ring stages. This was done to improve accuracy of assays and food vacuole isolation for proteomic analysis. For the majority of experiments, a high yield of parasites was required. However, it was established that trophozoite cultures should not be allowed to exceed an 8% parasitaemia due to build-up of toxic lactic acid that reduces viability of parasites (Hikosaka *et al.*, 2015), unless medium was

replaced at 12 h intervals instead of 24 h intervals. Ring stages of *Plasmodium* parasites were found to be more tolerant to higher parasitaemia due to decreased metabolic activity as described previously (Mok *et al.*, 2011).

2.3.2 Antiplasmodial activity and selective toxicity of drug compounds

2.3.2.1 Artemisinin, chloroquine, DFMO, mevinolin and clofazimine

During this study, the IC₅₀ values of the standard drugs used in successful treatment of malaria, namely artemisinin, chloroquine and DFMO were determined afresh as a reference to interpret results obtained from the antiplasmodial screening of humic and fulvic acid, mevinolin and clofazimine.

A number of experimental repeats were required before dose-response curves and IC₅₀ values with acceptable variances were obtained. These variances are common among field isolates of *P. falciparum* due to various genetic differences, and have only sparsely been reported but are not uncommon for laboratory adapted strains, possibly due to the presence of Albumax® in culture medium (Kreidenweiss *et al.*, 2008; Matthews *et al.*, 2013). The most likely cause for this variability is in the inability to perfectly replicate *in vitro* culturing conditions to obtain identical parasite health, serial passages, and developmental stages. This is the reason that the exact IC₅₀ of compounds such as artemisinin, chloroquine and DFMO have not been reported but IC₅₀ are estimated to fall within drug concentration ranges.

Dose-response curves depicting the antiplasmodial efficacy of artemisinin, chloroquine and mevinolin are graphed in Figure 2.1 below. From these graphs it is visually striking how artemisinin (Figure 2.1, A) and chloroquine (Figure 2.1, B) have increased selectivity for *Plasmodium* species (blue, purple and green) in comparison to mammalian cells (orange), as expected from literature.

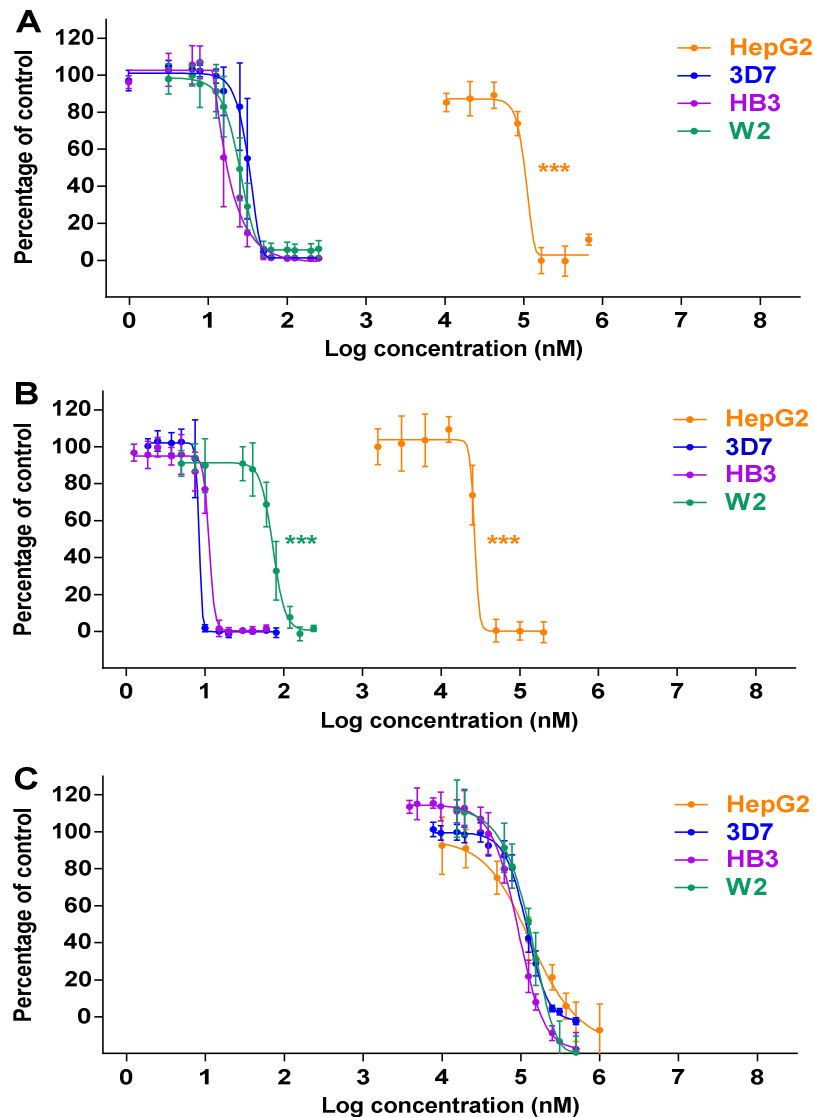


Figure 2.1 The mean growth inhibition of mammalian and *Plasmodium falciparum* cells exposed to artemisinin, chloroquine and mevinolin

HepG2 cells (orange) and *P. falciparum* strains 3D7 (blue), HB3 (purple) and W2 (green) when exposed to (A) artemisinin, (B) chloroquine and (C) mevinolin as indicated by the Sulforhodamine B (SRB) assay and MSF assay, respectively. All graphs are standardized to 120% of control and show up to log = 8. Significant differences in IC₅₀ values between cell types are depicted by *** are at $p < 0.001$.

It is also evident from Figure 2.1, C that the mechanism by which mevinolin elicits its toxicity is similar in *Plasmodium* species and mammalian cells. Table 2.4 shows that the W2 strain has a significantly decreased chloroquine susceptibility compared to 3D7 and HB3 strains ($p < 0.001$, $n = 9$, $R^2 > 0.9$ on regression curves), with an IC₅₀ value of 72.5 ± 1.03 in comparison to 8.4 ± 1.03 and 11.2 ± 1.03 nM, respectively.

Table 2.4 IC₅₀ values of drugs after 96 h for *Plasmodium falciparum* compared to HepG2 cells

Test Compound	3D7	HB3	W2	HepG2
Artemisinin	32.6 ± 1.03	17.1 ± 1.03	24.4 ± 1.03	1.1 x10 ⁵ ± 1.78***
Chloroquine	8.4 ± 1.03	11.2 ± 1.03	72.5 ± 1.03***	2.7 x10 ⁴ ± 40.83***
DFMO	5 x10 ⁵ ± 1.02	4.3 x10 ⁵ ± 1.04	3.4 x10 ⁵ ± 1.06	2.4 x10 ⁷ ± 1.06***
Clofazimine	349.1 ± 1.03	294.8 ± 1.03	272 ± 1.04	3.1 x10 ³ ± 1.18***
Mevinolin	1.2 x10 ⁵ ± 1.02	9.1 x10 ⁴ ± 1.03	1.3 x10 ⁵ ± 1.05	1.4 x10 ⁵ ± 1.26

Data are reported in nM ± SEM, n=9. Statistical significant differences in IC₅₀ as compared between the the different strains for each specific test compound are shown as *** $p < 0.001$; as tested by the One-way ANOVA.

From these results it is apparent that chloroquine had enhanced potency in comparison artemisinin on 3D7 and HB3 parasites. DFMO showed IC₅₀ values for 3D7, HB3 and W2 strains at concentrations approximately 15 000-, 25 000-, and 14 000 fold greater than artemisinin, for each respective strain. These effective concentrations are more than 100-fold greater than the IC₅₀ of 2 x 10³ nM previously determined against the FCD-3 (Indian isolate) strain for DFMO (Das *et al.*, 1995).

The greatest difference in toxicity is visible when comparing inhibitory concentrations obtained from HB3 parasites and HepG2 cells exposed to artemisinin, chloroquine and DFMO ($p < 0.001$, n=9). Clofazimine shows a greater antimalarial potency than DFMO, inhibiting the growth of 3D7, HB3 and W2 strains by 50% at concentrations 1400-, 1500-, and 1200- times lower than DFMO for these strains respectively (Table 2.4). Inhibitory concentrations determined in this study for DFMO are approximately 14000 times greater for 3D7 and W2 strains, and 25000 times greater for the HB3 strain in comparison to artemisinin. Mevinolin was shown to elicit its

toxic effects on 3D7, HB3 and W2 parasites at concentrations approximately 4-, 5- and 3 fold lower than DFMO (Table 2.4).

The selective toxicity of drug compounds was established by comparing IC₅₀ values for HepG2 cells versus *P. falciparum* parasites and tabulated here as selectivity index (SI) values (Table 2.5). Drugs with SI values above 10 have acceptable selective toxicity.

Table 2.5 Selectivity index (SI) values for drugs

Test Compound	3D7	HB3	W2
Artemisinin	>3000	>6000	>4000
Chloroquine	>2000	>2000	365
DFMO	28	32	42
Clofazimine	9	11	12
Mevinolin	1	1.3	0.9

SI values are calculated by the formula IC₅₀ of HepG2 cells/ IC₅₀ of *P. falciparum* parasites

The mevinolin concentration required to elicit toxicity in HepG2 cells was found to be significantly lower than those required for *P. falciparum* parasites ($p < 0.001$) for artemisinin, chloroquine, DFMO and clofazimine.

There was a 5.5 fold decrease in the selective toxicity of chloroquine to W2 strains relative to HepG2 cells (SI value of 365) as compared to the SI of chloroquine on HB3 strains (Table 2.5). Disappointingly, clofazimine only achieved SI values of 9, 11 and 12 on 3D7, HB3 and W2 parasite strains, respectively. Thus clofazimine does not exhibit selective toxicity comparable to the common antimalarials, chloroquine and artemisinin.

Mevinolin showed poor selective toxicity for all strains of parasites tested with SI values of 1, 1.3 and 0.9, respectively. SI testing for mevinolin on *Plasmodium* species has not been conducted before, therefore these results are the first depicting the selectivity of mevinolin. This indicates that mevinolin elicits its toxic effect through a non-species specific mechanism in both mammalian cells and *P. falciparum* parasites.

Dose-response curves for DFMO and clofazimine against *P. falciparum* strains and HepG2 cells are depicted in Figure 2.2.

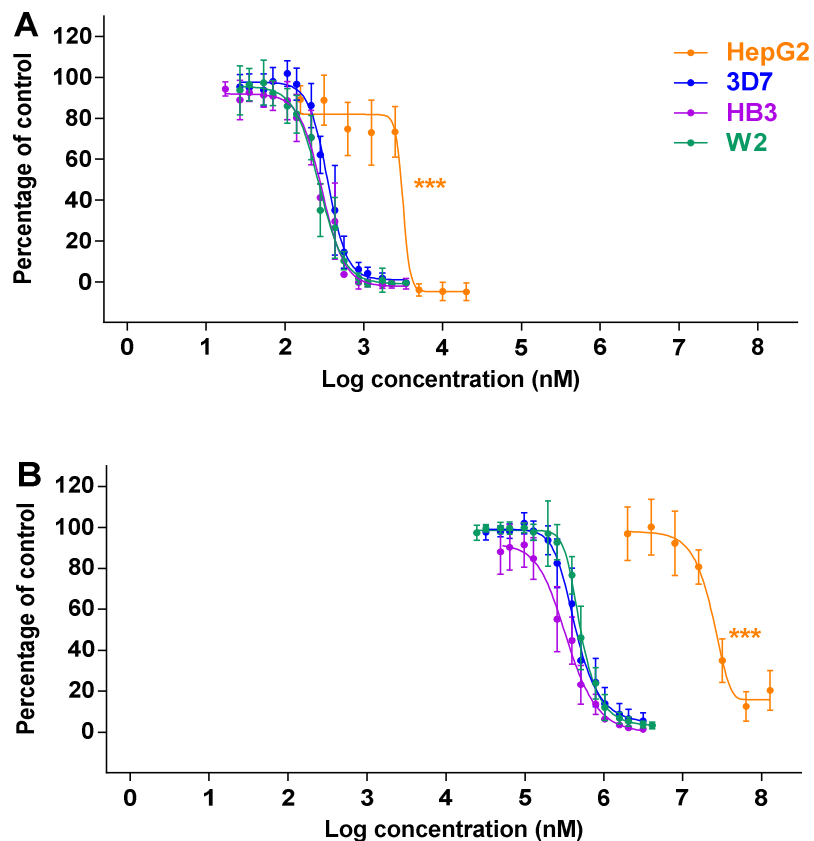


Figure 2.2 The mean growth inhibition by clofazimine and DFMO of mammalian and *Plasmodium falciparum* cells

HepG2 cells (orange) and *P. falciparum* strains 3D7 (blue), HB3 (purple) and W2 (green) when exposed to **(A)** clofazimine and **(B)** DFMO as indicated by the SRB assay and MSF assay, respectively. All graphs are standardized to 120% of control and show up to log = 8. Significant differences as depicted by *** are at $p < 0.001$.

DFMO showed the poor selective toxicity, being 32 times less toxic to mammalian HepG2 cells than to HB3 parasites *in vitro*, in comparison to >2000 and >6000 for chloroquine and artemisinin, respectively (Table 2.5). These findings confirm that DFMO is a poorer antimalarial than the current artemisinin-based treatments, supporting its limited use clinically.

2.3.1.2 Humic acid and fulvic acids

Table 2.6 groups the inhibitory concentrations of humic acid and fulvic acid samples tested for their antimalarial efficacy. Significantly lower IC₅₀ values were obtained for W2 parasites exposed to humic acid ($p < 0.001$, $n = 9$) and fulvic acid #377/11 ($p < 0.05$, $n = 9$) than on 3D7 and HB3 parasites, with values of 0.04 ± 1.06 and 0.08 ± 1.03 g/100mL, respectively (Table 2.6). The latter two concentrations compare to those IC₅₀ values obtained across all three *P. falciparum* strains exposed to either fulvic acid #390 or fulvic acid #391/11 (Table 2.6).

Table 2.6 The IC₅₀ values (g/100mL) of humic compounds on *Plasmodium falciparum* strains

Significant differences in IC₅₀ values between strains for each drug was calculated, One-way ANOVA, * at $p < 0.05$, and *** at $p < 0.001$. Data are reported in g/100mL \pm SEM, $n = 9$.

Test Compound	3D7	HB3	W2
Humic acid	0.11 \pm 1.08	0.12 \pm 1.06	0.04 \pm 1.06***
Fulvic acid #390	0.05 \pm 1.03	0.04 \pm 1.05	0.04 \pm 1.05
Fulvic acid #377/11	0.13 \pm 1.03	0.11 \pm 1.03	0.08 \pm 1.03*
Fulvic acid #391/11	0.05 \pm 1.04	0.07 \pm 1.04	0.05 \pm 1.04

The humic acid sample and fulvic acid #377/11 can not be considered as active antimalarials due to the high concentrations required to elicit any cytotoxic effect *in vitro*. These concentration would not be achievable in a physiological setting due to the doses that would be required to be administered. The two compounds did however achieve similar IC₅₀ values and showed comparable dose-response curves (Figure 2.3).

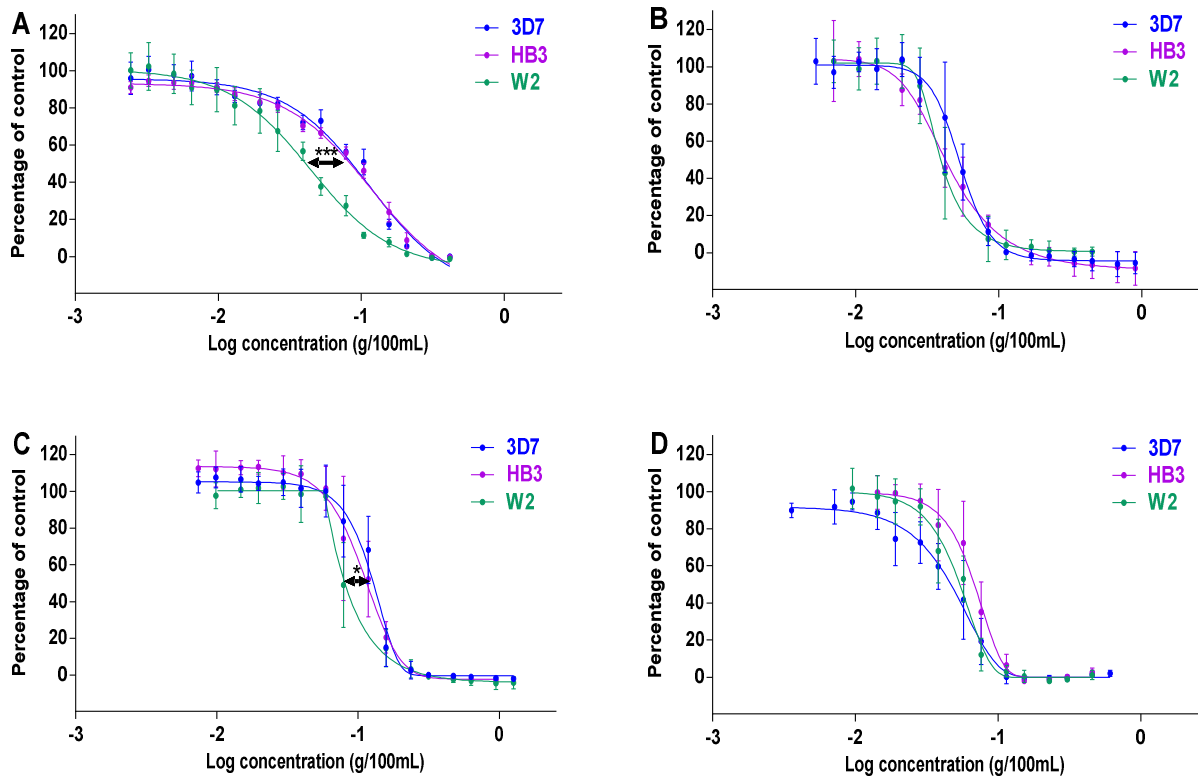


Figure 2.3 The mean growth inhibition of *Plasmodium falciparum* strains exposed to humic compounds

Strains are 3D7 (blue), HB3 (purple) and W2 (green) exposed to (A) humic acid, (B) fulvic acid #390, (C) fulvic acid #377/11 and (D) fulvic acid #391/11 as indicated by the Malaria SYBR Green-1[®] Assisted Fluorometric (MSF) assay. All graphs are standardized to 120% of control and show up to log (g/100mL) = 0. Note the high concentrations required to elicit a cytotoxic effect which cannot be achieved physiologically. Significant differences in IC₅₀ values between strains for each drug was calculated, One-way ANOVA, * at $p < 0.05$, and *** at $p < 0.001$

Significantly decreased IC₅₀ values were detected for W2 strains in comparison to 3D7 and HB3 strains exposed to humic acid and fulvic acid #337/11 which is apparent in Figure 2.3.

2.4 Discussion

Previous research has found that artemisinin inhibited growth (IC₅₀) of *Plasmodium* species at 1.2 – 19.5 nM in field isolates from the Thai-Myanmar border (Veiga *et al.*, 2011), and at 3.97 ± 0.08 nM in the 3D7 laboratory adapted strain (Bhattacharya *et al.*, 2008). These reported inhibitory values are low in comparison to the IC₅₀ values obtained in this study (Table 2.4), supporting the existence of genomic shifts in culture-adapted strains.

Chloroquine has been found to inhibit growth of the laboratory adapted W2 (chloroquine resistant strain) at 249.55 IC₅₀ nM, and in the 3D7 (chloroquine sensitive strain) at 16.79 nM (Chorattanakawee *et al.*, 2013). These previous findings suggest a 10 fold increase in sensitivity to chloroquine by 3D7 strains in comparison to W2 strains, which is supported by the current findings for chloroquine (Table 2.4).

Barteselli *et al.* screened the antiplasmodial ability of various analogues of clofazimine, and determined its IC₅₀ concentration to be approximately 7.02 x 10³ nM in W2 parasites (Barteselli *et al.*, 2015), significantly higher than the inhibitory concentration obtained in this study (Table 2.4). The SI value for chloroquine on W2 parasites, as obtained in this study, is lower than previously determined to be 4200 (Boechat *et al.*, 2012).

Even though the selectivity values for clofazimine are from *in vitro* testing on mammalian HepG2 cells similar toxicity values can be assumed *in vivo* due to various clinical trial findings supporting the accumulation of clofazimine in the tissues of patients being administered therapeutic doses for the treatment of *Mycobacterium leprae* infections (Cholo *et al.*, 2012; Hastings *et al.*, 1976). Although clofazimine exhibits gastrointestinal and dermal side effects, these are not believed to outweigh the antimicrobial benefits the drug possesses (Hastings *et al.*, 1976).

The HMG-CoA reductase inhibitor, mevinolin, has been claimed to decrease the incidence of malaria infection in patients treated for elevated cholesterol levels and decrease neurocognitive damage after cerebral malaria (Reis *et al.*, 2012). Previous studies determined mevinolin to achieve 50% inhibition in growth of *P. falciparum* strains (F32 and FcB.1) at 10 – 20 µg/mL; equating to 247 – 494 nM, with mevinolin's molecular weight of 404.54 g/mol. These concentration values are approximately 300x less than obtained in our study (Grellier *et al.*,

1994). Mevinolin is equally toxic to mammalian and protozoan cells (Figure 2.1, C). Hepatocytes synthesise cholesterol from acetyl-CoA requiring HMG-CoA reductase as a rate-limiting enzyme (Goldstein & Brown, 1990). Hepatocytes also internalise serum cholesterol by receptor mediated endocytosis (Goldstein *et al.*, 1985). This method is employed by erythrocytes, as they are unable to undergo *de novo* synthesis or esterification (Gold & Phillips, 1990; Gottlieb, 1980; Schick & Schick, 1985; Yeagle, 1985). The expression of HMG-CoA in *Plasmodium* parasites has not yet been established, but it is known that parasites do have an active isoprenoid pathway which is generally regulated by HMG-CoA synthase and HMG-CoA reductase in eukaryotic and prokaryotic species (Couto *et al.*, 1999; Grellier *et al.*, 1994). Intra-erythrocytic malaria parasites do not produce cholesterol, rather they internalise cholesterol, specifically during hepatic merozoite formation in initial stages of infection (Labaied *et al.*, 2011; Tokumasu *et al.*, 2014).

Humic and fulvic acid compounds have been shown by others to have anti-inflammatory activity, possibly through release of nitric oxide by macrophages at doses of 0.02 g/100mL (Gandy *et al.*, 2012; Schepetkin *et al.*, 2003). The observed humic acid, fulvic acid #390, fulvic acid #377/11 and fulvic acid #391/11 concentrations required to show antimalarial efficacy are not clinically achievable, and this dose administration limitation has been previously established, therefore no further testing was done on these compounds (Gandy *et al.*, 2012).

When assessing dose-response curves obtained for HB3 versus 3D7 parasites, no significant IC₅₀ shifts were detected for humic acid, the fulvic acids, mevinolin, and clofazimine (Figures 2.1; 2.2; 2.3). These insignificant differences were taken as an indication that 3D7 strains were adequate to continue with parasite stage specificity analysis, and that HB3 parasite strains were not necessary to be used in further investigations performed in this research project.

2.5 Conclusion

P. falciparum 3D7 and HB3 strains showed comparable IC₅₀ concentrations for all drug compounds tested, therefore the HB3 strain was not retained for further assessment in this research study. *P. falciparum* W2 strains showed decreased susceptibility to chloroquine, as expected from its previously established susceptibility profile and origin.

Mevinolin has been shown to express poor selective toxicity for *Plasmodium* parasites over mammalian cells. Findings suggest mevinolin acts on a vital and unknown target that is common to both the parasite and the hepatocytes. From literature it can be postulated that this target may be involved in the anchoring of essential invasion and/or adhesion proteins on the membranes of infected erythrocytes. Further investigation may confirm if mevinolin expresses favourable results for *in vivo* or clinical tests. Due to the high concentrations required to elicit antimalarial activity, mevinolin's effects on life-cycle progression was not assessed.

Humic acid and fulvic acid have been shown to elicit antiplasmodial effects at concentrations unachievable *in vivo*. These findings do not dissuade from the possible antimalarial efficacy of these substances as there may be numerous physiological responses induced by humic compounds resulting in enhanced inflammatory and/or immune responses in the human host. These physiological responses could decrease an individual's probability of contracting malaria.

Clofazimine showed remarkable antimalarial efficacy across all *Plasmodium* strains tested, with average selectivity, indicating that the antimycobacterial action is comparable to *Plasmodium* species. The concerns over the lipophilic profile of clofazimine and its accumulation in patient tissues may hinder its acceptance as an adjunct to current antimalarial therapies.

Chapter 3: Stage specificity (parasite life-cycle progression) analysis of drugs

3.1 Introduction

Healthy *Plasmodium* parasites progress through their entire life-cycle in 48 h. Observing parasites from ring stage till the next cycle ring stage allows for the possible detection of delayed death effects. These effects may be attributable to the inhibition of apicoplast development as observed with antibiotics, such as doxycycline treatment (Dahl & Rosenthal, 2008; Pradel & Schlitzer, 2010).

The cell cycle of mammalian and yeast cells is distinct from those of *P. falciparum*, which undergo endomitotic division with centriolar plaques that are equivalent to centrosomes in mammalian cells (Arnot *et al.*, 2011). Parasites in the ring or early trophozoite stages of intra-erythrocytic development contain a single nucleus (1N), with late stage trophozoites being doubly nucleated (2N), and mature schizonts having multiple nuclei (>2N) due to the formation of independent merozoites (Niemand *et al.*, 2013; Verlinden *et al.*, 2011). SYBR green-1® dye has been shown previously to adhere to DNA and RNA residues, and to fluoresce under the correct wavelength selection (Dragan *et al.*, 2012). This allowed for the use of flow cytometry (specifically Channel FL1) to determine the percentage parasitaemia of samples given their degree of fluorescence relative to controls.

DFMO is an antitrypanosomal agent, which is applied clinically for its beneficial effects on hair growth (Burchmore *et al.*, 2002). The effects of this drug on the *Plasmodium* parasite life-cycle have been studied in depth by other researchers. DFMO is able to irreversibly inactivate ornithine decarboxylase preventing the formation of putrescine and spermidine (Assaraf *et al.*, 1987a). DFMO thereby inhibits polyamine synthesis in young trophozoites (in the G₀ phase of

the cell cycle), preventing further nuclear divisions required for progression into later trophozoite and schizont stages of the *Plasmodium* life-cycle (Arnot *et al.*, 2011).

3.2 Materials and methods

3.2.1 Determination of inhibition in *P. falciparum* intra-erythrocytic life-cycle progression

Life-cycle progression was not assessed on the HB3 strain, as this strain showed similar dose-response curves compared to 3D7 parasites for all compounds. Therefore, test compounds were screened for their ability to halt 3D7 and W2 progression through specific life-cycle stages as reported previously (Niemand *et al.*, 2013; Verlinden *et al.*, 2011). Briefly, synchronous ring stage parasite suspensions (2% hct, 2% parasitaemia) were pipetted into a 96 well microplate and exposed to approximately IC₅₀ or 4 x IC₅₀ concentrations of test compounds for up to 48 h.

Table 3.1 Test compound concentrations (in nM) for life-cycle progression study

		Artemisinin	Chloroquine	Clofazimine	DFMO
3D7	IC₅₀	32.6	8.9	336.2	5.04 x 10 ⁵
	4 x IC₅₀	130.5	35.5	1.345 x 10 ³	2.016 x 10 ⁶
W2	IC₅₀	24.4	72.2	271	3.386 x 10 ⁵
	4 x IC₅₀	97.6	288.8	1.084 x 10 ³	1.354 x 10 ⁶

Uninfected erythrocytes and untreated but infected erythrocytes were included in control wells to perform flow cytometric assay gating (CXP version 2.2 Acquisition and Data analysis Software). *P. falciparum* infected erythrocytes exposed to chloroquine (0.5 µM) served as a positive control for parasite death; used as the blank. Samples were isolated 6 h, 24 h, and 48 h after initiating drug exposure. Samples from each time point (50 µL) and control samples (50 µL) were fixed by addition of glutaraldehyde (0.025% v/v, 1 mL). These samples were stored at 4°C, for a maximum of two days, prior to commencement of flow cytometric analysis. Fixed samples were washed with PBS, microfuged for 5 min at 500 g, resuspended in SYBR® green dye (diluted 1:10⁴ in PBS) and allowed to incubate in the dark at room temperature for 30 min.

Samples were centrifuged, and after the removal of the supernatant the pellet was resuspended in 750 μ L PBS before transferal into flow cytometry tubes. A minimum of 5×10^5 were measured on the channel 1 of a Beckman Coulter Cytomics FC500, whilst gating to include infected erythrocytes only.

3.2.2 Interpretation of intra-erythrocytic life-cycle progression results

All experiments were performed in triplicate for each concentration tested. The percentage parasitaemia at each time point was calculated in Excel, Microsoft Office 2010 with the following equation:

$$\% \text{ Parasitaemia} = \left(\frac{\text{Mean sample readings} - \text{Mean blank (0.5 } \mu\text{M CQ)}}{\text{Mean positive control readings(untreated parasites)} - \text{Mean blank}} \right) \times 100$$

Data with respect to percentage parasitaemia versus test compound concentration was plotted using GraphPad Prism version 5.0 software (GraphPad Software, San Diego California USA, www.graphpad.com) as dose-response curves using the non-linear curve fit method to visualise the change in parasitaemia of the different parasite strains exposed to concentrations of test compounds for 48 h. The standard error of the mean was also calculated. Statistical analysis was also performed using GraphPad Prism version 5.0 to determine the statistical significance of shifts in percentage parasitaemia of *P. falciparum* strains exposed to test compounds. The mean values were analysed by two-way ANOVA (non-parametric) with Tukey's *post-hoc* multiple comparisons test performed to compare intergroup differences. Results were considered to be significant if a *p*-value of less than 0.05 was indicated.

3.3 Results

P. falciparum 3D7 and W2 parasites were exposed to drug compounds at time “0” when parasites were at 2% parasitaemia in the ring stage of development. At the 24 h time point, parasites were observed to be in the early to late-trophozoite stage (Figure 3.1, light microscopy, images not shown). The effects of the drugs on cell-cycle progression of HB3 parasites were not assessed, as discussed earlier under antiplasmodial screening of the substances.

Statistical significance in Figure 3.1 was determined for drug treated strains versus uninfected erythrocytes, as well as for drug treated strains versus infected erythrocytes. Where no significance is indicated the drug samples have percentage parasitaemia values comparable to the closest control population of cells. For example, in 3D7 strains all drug compounds have low percentage parasitaemia that are not significantly different from uninfected erythrocyte controls, but are significantly different from infected, untreated erythrocytes as seen in Figure 3.1, A.

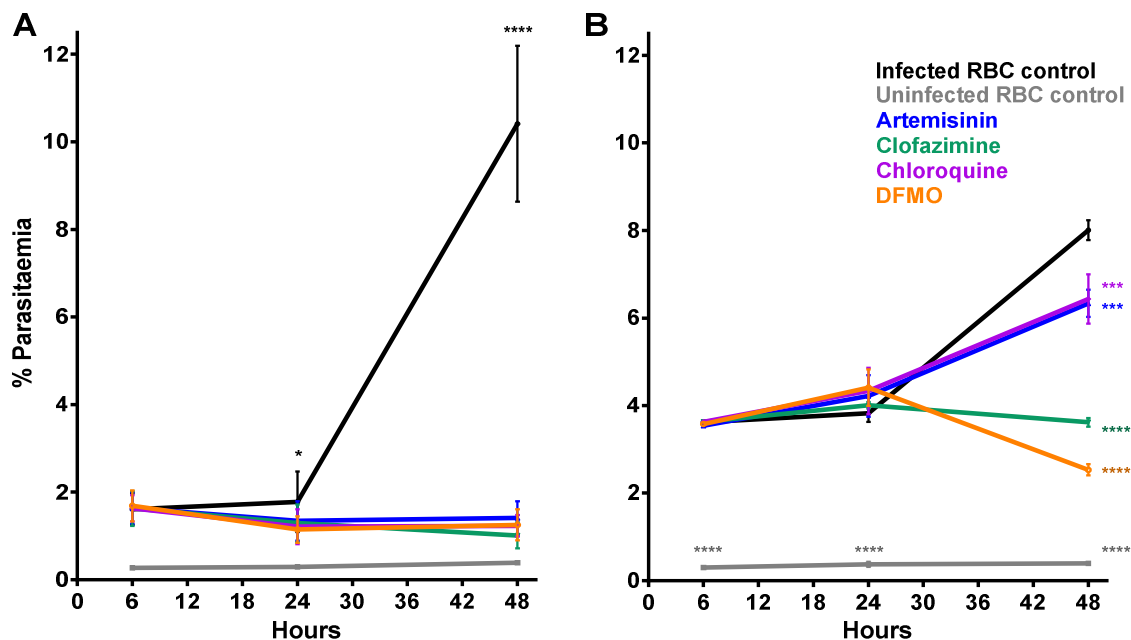


Figure 3.1 The change in parasitaemia of *Plasmodium* 3D7 and W2 strains

(A) 3D7 and (B) W2 exposed to artemisinin (blue), clofazimine (green), chloroquine (purple) and DFMO (orange) at 4 x IC50 values as outlined in Table 4.1 after a complete life-cycle of *P. falciparum* (48 h) as detected by SYBR Green-1® fluorescence. Statistical deviations indicated as *, ***, or **** are at $p < 0.05$, < 0.001 and < 0.0001 respectively as determined by two-way ANOVA and Tukey's multiple comparisons test for test drugs and uninfected erythrocyte (RBC) controls in comparison to infected erythrocytes. Results show the mean \pm SEM, $n=3$.

From Figure 3.1 (A) it is clear that 3D7 strains exposed to artemisinin (130.5 nM), chloroquine (35.5 nM), clofazimine (1.345×10^3 nM) or DFMO (2.016×10^6 nM) were unable to recover from exposure to these drugs. The parasites were also unable to undergo nuclear replication and produce viable schizonts and merozoites (approximately 36 h on graph) as indicated by the low percentage parasitaemia at the 48 h time point (no significant difference detected in comparison to uninfected, untreated, RBC control). Statistically significant deviations were observed in the 3D7 strain only between the uninfected, untreated RBC control in comparison to all other drug exposed, or untreated uninfected erythrocytes ($p < 0.0001$, Figure 3.1, A), indicating the susceptibility of the 3D7 parasites to all test compounds screened.

A significant difference in parasitaemia was observed between uninfected RBC cells and infected, untreated RBC controls, at 0.39% and $10.4 \pm 3.09\%$, respectively ($p < 0.05$ at 24 h and $p < 0.0001$ at 48 h, Figure 3.1, A).

More significant variations were detected for the W2 strain. All parasites exposed to test compounds had parasitaemias significantly less than untreated infected controls and greater than uninfected, untreated controls (Figure 3.1, B; $p < 0.05$). W2 strains treated with clofazimine (1.084×10^3 nM) and DFMO (1.354×10^6 nM) showed a noteworthy decrease in parasitaemia, from $4 \pm 0.13\%$ to $3.16 \pm 0.17\%$ and $4.41 \pm 0.73\%$ to $2.53 \pm 0.22\%$, respectively between the 24 h and the 48 h time points.

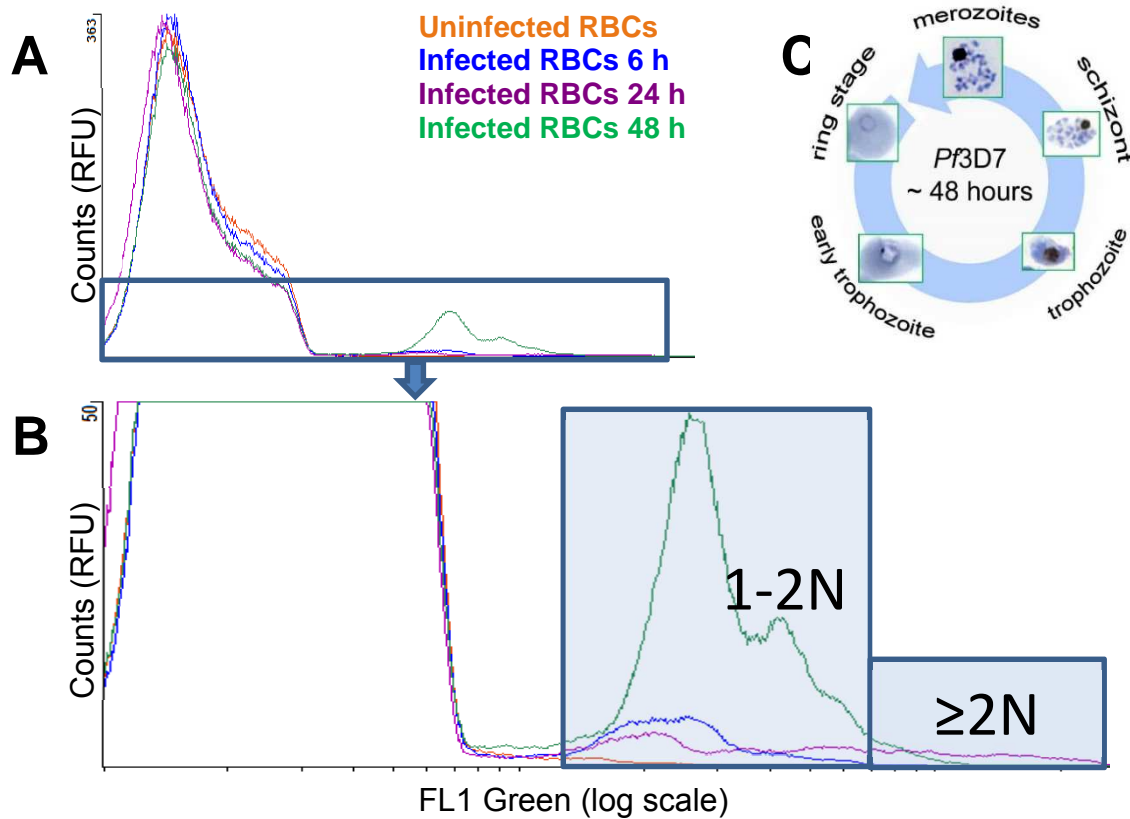


Figure 3.2 Overlay histogram of fluorescent DNA content in parasites over time

“Events” counts as detected by flow cytometry (FL1 Channel) at excitation 488 nm (**A**) of uninfected RBCs (orange) and *P. falciparum* 3D7 infected RBCs after 6 h (blue), 24 h (purple), and 48 h (green) and the same histogram (**B**) enlarged to observe infected RBC populations more clearly, specifically the increase in nuclear content from 1-2N to $\geq 2N$. Image (**C**) depicts the life-cycle progression of *P. falciparum* 3D7 parasites.

Plasmodium 3D7 parasites treated with DFMO and clofazimine follow the trend of *Plasmodium* infected RBCs in their life-cycle progression; at the 6 h and 48 h time point parasites have 1-2N nuclear content indicative of the ring stage (Figure 3.2, Figure 3.1). At the 48 h time point the number of counts increases, due to merozoite egression and invasion of healthy RBCs (Figure 3.2, Figure 3.3).

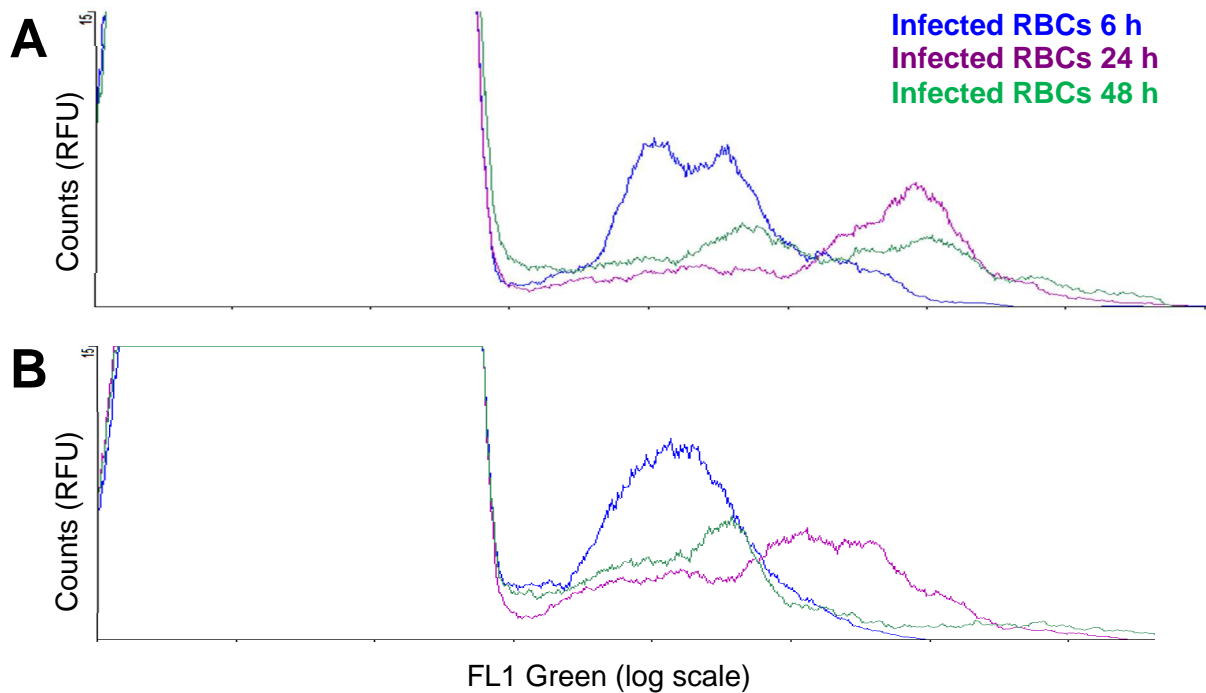


Figure 3.3 Overlay histogram of fluorescent DNA content of “events” as detected by flow cytometry

(FL1 Channel) at excitation 488 nm **(A)** of *P. falciparum* 3D7 infected RBCs exposed to 2.016×10^6 nM DFMO and **(B)** 1.345×10^3 nM clofazimine after 6 h (blue), 24 h (purple), and 48 h (green).

At the 24 h time point, nuclear content is increased above 2N, as expected during DNA replication of trophozoites and early schizonts (Figure 3.2, Figure 3.3).

W2 strains exposed to artemisinin (97.6 nM) and chloroquine (288.8 nM) showed a significant decline in parasitaemia in comparison to the infected RBC controls ($8.01 \pm 0.39\%$, $p < 0.001$), at $6.33 \pm 0.54\%$ and $6.44 \pm 0.98\%$ respectively (Figure 3.1, B). This drop in parasitaemia is however to a much lesser degree than seen with DFMO and clofazimine ($p < 0.0001$), at a parasitaemia of $2.53 \pm 0.22\%$ and $3.62 \pm 0.17\%$, respectively.

Fluorescence of trophozoite and schizont DNA was confirmed by fluorescent microscopy (Figure 3.4). Egressed merozoites, purified by magnetic separation, were also visible with this technique (Figure 3.4, C).

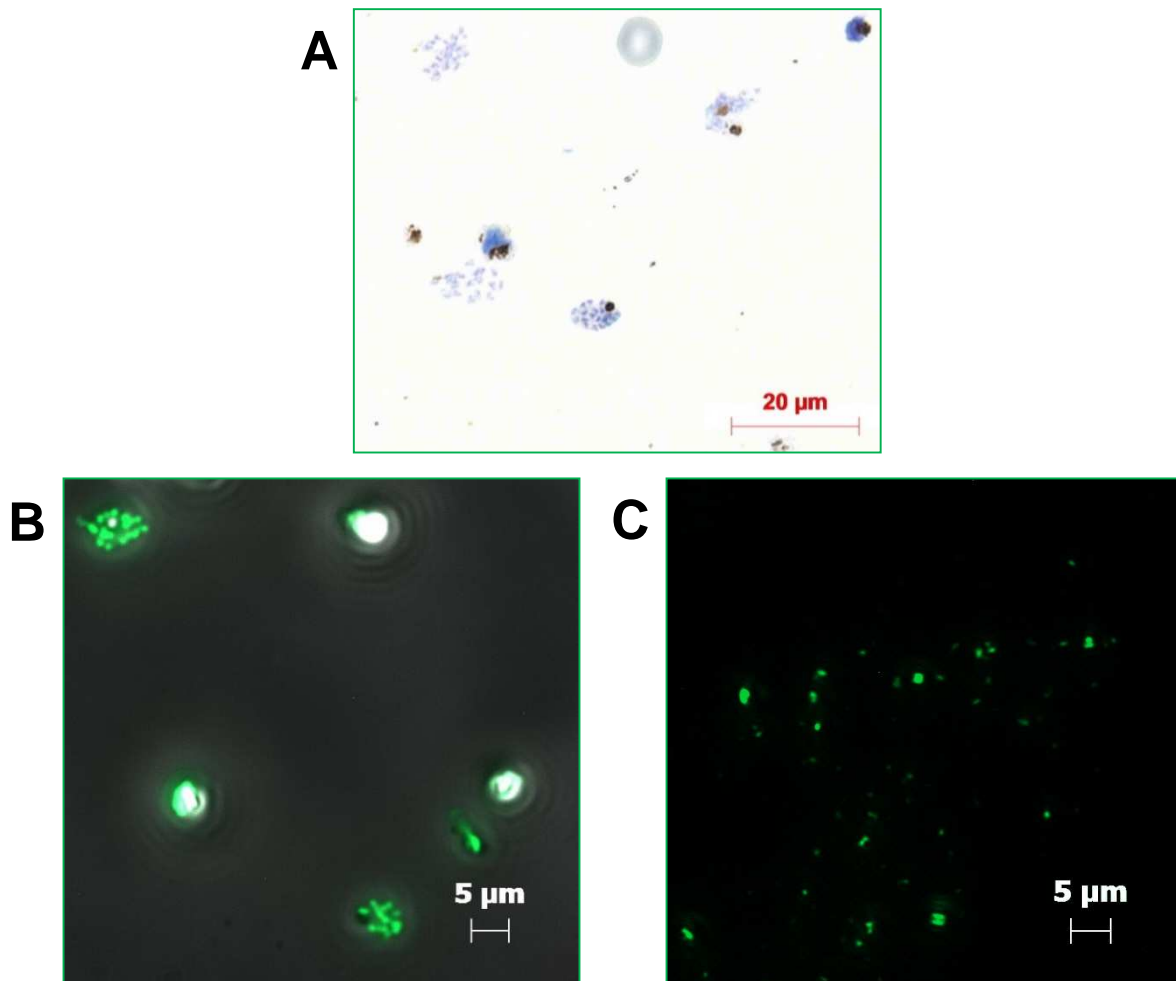


Figure 3.4 Microcopy images of schizonts and their fluorescent DNA

Light micrograph at 100x magnification of **(A)** 3D7 schizonts and egressing merozoites at approximately 48 h in life-cycle. Fluorescent micrographs overlaid with white light images of **(B)** SYBR green-1® treated schizonts and **(C)** egressed merozoites at 63 x magnification, fluorescing DNA was visualised under FITC filter (excitation 470 nm, emission 520 nm).

Confirmation of the successful isolation of merozoites by the sorbitol synchronisation and magnetic isolation methods implemented within this study formed the basis for further research on erythrocyte invasion proteins of merozoites by other researchers within the faculty.

3.4 Discussion

From Figure 3.1 (A, B) it can be discerned that artemisinin and chloroquine elicit their antimalarial effects on the parasites at an estimated life cycle stage of the late ring and/or early trophozoite as seen in the drop in viable parasites from the 6 h to 24 h time point. This observation is most likely due to chloroquine's alteration of parasitic food vacuole pH and inhibition of haemozoin formation (Wilson *et al.*, 2013) and the interaction of endoperoxide moieties of artemisinin with iron containing haemoglobin by-products in the food vacuole (Goldberg *et al.*, 1991).

The shift in clofazimine susceptibility of W2 strains at 24 versus 48 h shows that the drug inhibits parasite proliferation. A similar trend is observed for DFMO which is known to inhibit ornithine decarboxylase from producing polyamines from putrescine (Andrews *et al.*, 2014), required by parasites for development. This inhibition by DFMO generally results in a delayed death effect, which is not distinctly discernible in these findings (Clark *et al.*, 2010). Clofazimine, at 10 µg/mL, has been shown to elicit cell death in mammalian macrophages *in vitro* by decreasing metabolic activity, decreasing cell sizes, and causing karyorrhexis (Fukutomi *et al.*, 2011).

The flow cytometry results for W2 strains are indicative of resistance to chloroquine, as expected, and possibly even a controversial decline in the parasites' susceptibility to artemisinin. This is not expected for laboratory adapted strains, but has been reported for field isolates from Asia (Mok *et al.*, 2011).

An intriguing occurrence is that DFMO has a significant distribution of parasite counts with a >2N nuclear content at the 48 h time point (Figure 3.3, A). If invasion occurs successfully a higher peak would have been observed in the <2N range on the RFU axis. The observed drop in RFU in the <2N and the remaining RFU content in the >2N range on the x-axis (FL 1 Channel

Scale) suggests that DFMO has a slight ability to halt the development of late trophozoites and the egression of merozoites indicating some cytostatic potential. Previous studies confirmed DFMO to block parasites in the early trophozoite stages in the quiescent stage of the cell cycle (Assaraf *et al.*, 1987b). Clofazimine appeared unable to block parasite progression, and all surviving parasites were able to complete their life-cycles and re-invade erythrocytes (Figure 3.3, B).

3.5 Conclusion

P. falciparum 3D7 parasites showed susceptibility to all test compounds at all time points screened, at parasitaemias so low that they are not significantly different from the background fluorescence observed by uninfected erythrocyte controls. W2 strains showed interesting distributions of drug susceptibility at the 48 h timepoint, with chloroquine and artemisinin percentage parasitaemias significantly different from uninfected and infected untreated erythrocyte controls. W2 parasites were most susceptible to DFMO followed by clofazimine in these assays.

Flow cytometry proved to be an effective technique in assessing stage of drug specificity on the *Plasmodium* IE life-cycle in these analyses, showing a very slight blockade or delay in life-cycle progression in DFMO treated parasites as reported previously (Assaraf *et al.*, 1987a).

Chapter 4: Chloroquine sensitisation of resistant *Plasmodium falciparum*

4.1 Introduction

Reversal of chloroquine resistance in *Plasmodium falciparum* parasites has been studied in-depth, and is an area of intense interest for the research community. This is due to the past success of chloroquine as an antimalarial therapy, the lower cost for production, the relevant safety profile exhibited by the drug in patients and the ease of administration thereof. Furthermore, understanding the mechanisms by which parasites elicit their resistance to chloroquine can aid in the design of new chemical substances that are less affected by the parasite's adaptable genomic and proteomic variability.

A number of chemosensitisers have been identified to enhance plasmodial susceptibility to chloroquine, including the calcium channel blocker verapamil, the tricyclic anti-depressant desipramine and the phenothiazine antipsychotic, trifluoperazine (van Schalkwyk *et al.*, 2001). The antihistamine chlorpheniramine has also been shown to be effective as a chloroquine resistance reversal agent (Egan & Kaschula, 2007). These drugs have been shown to enhance chloroquine accumulation in food vacuoles of chloroquine resistant *P. falciparum* strains (van Schalkwyk *et al.*, 2001). Researchers confirmed that these drugs did not alter the action of chloroquine, but only affected the access to its target site and accumulation.

The IC₅₀ shift assay, an adaptation of the Malaria SYBR Green-1® fluorescence was used to establish whether co-administration of low doses of clofazimine, previously described as a chemotherapeutic sensitizing agent assay (Bennett *et al.*, 2004; Saliba *et al.*, 2008; Smilkstein *et al.*, 2004; Van Rensburg *et al.*, 1998; Verlinden *et al.*, 2011), could induce susceptibility of *P. falciparum* W2 (chloroquine resistant) strains to chloroquine.

4.2 Materials and methods

4.2.1 Sensitisation of the *Plasmodium falciparum* W2 strain to chloroquine by the IC₅₀ shift assay

The IC₅₀ shift assay was implemented to establish whether the *Plasmodium falciparum* W2 (chloroquine resistant) strain could be made more susceptible to chloroquine following exposure to clofazimine, as adapted from the Malaria SYBR Green-1® fluorescence assay that has been described above (Bennett *et al.*, 2004; Smilkstein *et al.*, 2004).

Briefly, two identical 96 well microplates were prepared with a series of concentrations of chloroquine to provide a dose-response curve using a parasite suspension obtained from a single culture flask (as discussed under the *P. falciparum* viability testing methods). The first microplate, was set-up as previously described under the MSF assay method while the second microplate was spiked with a clofazimine concentration required (375nM or 495 nM)). The dose-response curves of the chloroquine treated and chloroquine plus clofazimine combination treated parasites were plotted on the same axes to highlight any noticeable shift in the chloroquine IC₅₀ values. A shift to the left (lower IC₅₀ values) was considered to be indicative of an increase in parasite susceptibility to chloroquine.

4.2.2 Interpretation of IC₅₀ shift assay results

All microplate experiments for IC₃₀ concentrations with clofazimine were performed in triplicate with three replicate wells for each concentration tested, IC₄₀ concentrations of clofazimine were screened in a single experiment with triplicate wells only. The percentage inhibition of the test compounds at various concentrations was expressed as a percentage relative to untreated parasites (i.e. the average of positive control wells) and was calculated in Excel, Microsoft Office 2010 using the following equation:

$$\% \text{ Inhibition of parasite growth} = \left(\frac{\text{Mean sample readings} - \text{Mean blank}}{\text{Mean positive control readings} - \text{Mean blank}} \right) \times 100$$

Data were plotted using GraphPad Prism version 5.0 software (GraphPad Software, San Diego California USA, www.graphpad.com) applying a non-linear LOWESS spline fit method to determine shifts in 50% inhibitory concentrations. The standard error of the mean of the IC_{50} was also calculated, and reported sample sizes (n) are from technical and biological repeats. Statistical analysis was performed with GraphPad Prism version 5.0. To establish whether shifts in IC_{50} values were statistically significant, multiple Student t-test was performed with adjustment for multiple comparison by Tukey's *post hoc* analysis, data were considered significant if a *p*-value of less than 0.05 was indicated. All the drug concentrations on the axes of the dose-response curves were plotted on a logarithmic scale in order to visualise a wider range of concentrations.

4.3 Results

The aim of these experiments was to establish if clofazimine could increase the chloroquine susceptibility of a *Plasmodium falciparum* W2 strain, previously shown to be chloroquine resistant. This was assessed by the IC_{50} shift assay, an adaptation from the Malaria SYBR-Green-1 Fluorescent assay. Figure 4.1 depicts the resultant dose-response curve with chloroquine only (green) versus chloroquine in combination with a fixed dose of clofazimine (blue). The concentration of clofazimine added to obtain the shift were screened on a trial-and-error basis, with ascending doses of clofazimine used consecutively until a visible shift in chloroquine susceptibility was observed (a shift to the left of the dose-response curve, indicating a decreased 50% inhibitory concentration).

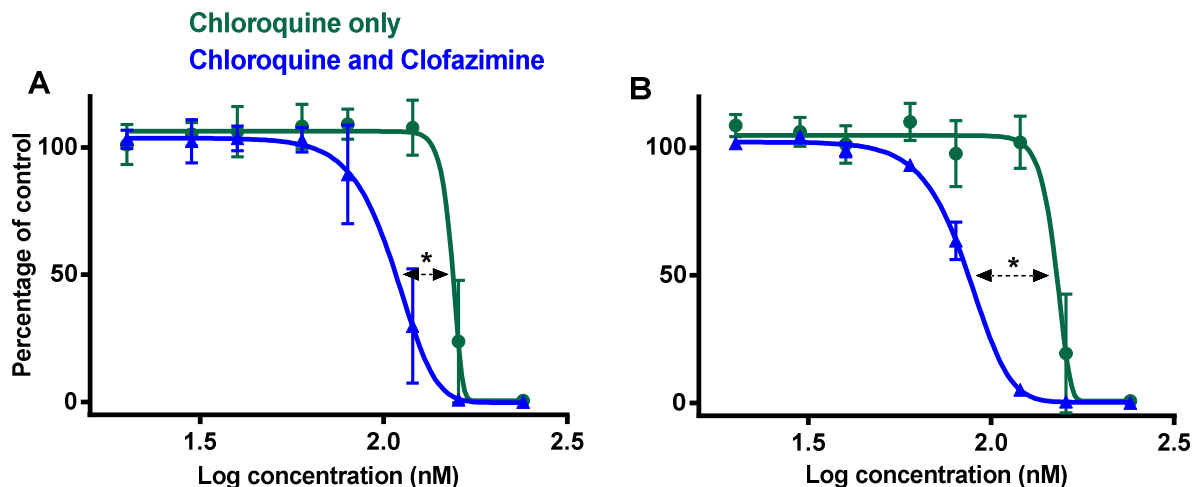


Figure 4.1 Dose-response curves of W2 parasites exposed to chloroquine alone or with clofazimine

Serial dilutions of chloroquine only (green) or in combination with clofazimine (blue) **(A)** at 375 nM (n=9) or **(B)** at 495 nM (n=3). Clofazimine concentrations are 75% and 80% inhibitory concentrations (IC_{75} and IC_{80}), respectively, as determined by MSF assay. Statistically significant deviations are indicated by * at $p < 0.05$, as determined by Student t-tests, and Tukey's multiple comparisons test. Results show the mean \pm SEM.

Three independent experiments were conducted to assess the shift in potency of a constant low dose of clofazimine ($IC_{75} = 375$ nM) in combination with 2-fold serial dilutions of chloroquine (starting dose 240 nM) against W2 strains (Figure 4.1, A); a similar experiment was also conducted but with a slightly higher constant low dose of clofazimine ($IC_{80} = 495$ nM) (Figure 4.1, B).

It is evident that the addition of low doses of clofazimine causes a statistically significant shift to lower concentrations to achieve IC_{50} values, as is visible in a shift to the left in dose-response curves (visible in Figure 4.1, $p < 0.05$), thereby suggesting that co-administration of clofazimine and chloroquine enhances antiplasmodial potency. Inhibitory concentrations of 50% of parasite growth were obtained at 151.8 ± 14.52 nM for chloroquine only, in comparison to 107.2 ± 1.03 nM for chloroquine and clofazimine (IC_{75}) (Figure 4.1, A), and at 141.9 ± 1.03 nM for chloroquine

only in comparison to 85.97 ± 1.01 nM for chloroquine and clofazimine (IC_{80}) (Figure 4.1, B). It is exciting to note that in both graphs there is an estimated drop in effective antiplasmodial concentrations by at least 40 nM of chloroquine. The exact mechanism by which the increase in W2 parasite susceptibility is achieved still requires further investigation.

4.4 Discussion

Chloroquine sensitisizers, are synonymously referred to as reversed chloroquines or chloroquine reversers and have been shown to enhance the action of chloroquine in resistant phenotypes of the *Plasmodium* parasite. These substances elicit their mechanism of action in diverse ways (Egan & Kaschula, 2007). Interesting, studies report the necessity for elevated concentrations of chloroquine reversers, possibly due to excessive binding of these substances to α 1-acid glycoproteins in the serum (Gross *et al.*, 1988).

The proposed mechanism of action of clofazimine is said to be two-fold: by binding to DNA thereby disrupting the cell cycle and by inhibition of potassium transporters mediated by membrane lysophospholipids of the target organism (Cholo *et al.*, 2006). Concerningly, a study has found that the use of resistance reversers with weak antiplasmodial activity, such as verapamil, also confers drug resistance in the *pfmdr1* gene of these parasites (Hayward *et al.*, 2005a). This may not be of such a great concern for clofazimine, which has been shown in this study to possess considerable antiplasmodial efficacy *in vitro*. Clofazimine doses used in this assay, 375 and 495 nM, were expected to inhibit parasite growth by 75 and 80%, respectively, which is unusually high. Additive effects of clofazimine with chloroquine are highly likely, and shifts observed may not be due to logistical enhancement of chloroquine action in these resistant parasites. In order to confirm this hypothesis, it would be essential to conduct isobolic plots and analysis on varying concentration combinations of chloroquine and clofazimine, as discussed previously (Bell, 2005) (Fivelman *et al.*, 2004) (Van Schalkwyk *et al.*, 2008).

4.5 Conclusion

It has been shown that clofazimine in combination with chloroquine causes favourable increase in the susceptibility profile of W2 strains to chloroquine. It is however, important to note that the cause of this observed shift has not been determined. It could be that clofazimine has an additive effect only or potentially a synergistic effect on parasite growth inhibition. It is not possible to comment on the ability of clofazimine to alter chloroquine efflux from the food vacuole or parasitorous vacuole of the parasite from the results of this assay. Further investigation is required to establish whether the dose-response curve shift to the left is due to the addition of the *Plasmodium* parasite cytotoxic clofazimine or if the clofazimine results in higher accumulation of the chloroquine in the parasite food vacuole. This will need to be established by isobole analysis and by determining the absolute accumulation of chloroquine in the food vacuole of the parasite after clofazimine treatment.

Chapter 5: Harvesting trophozoite food vacuole membrane proteins

5.1 Introduction

Previously, in Section 2.2.2, methods of synchronisation of *Plasmodium* parasites were discussed. Another method of synchronisation is by magnetic purification of late stage trophozoite infected erythrocytes by CS+ magnetic columns (Miltenyi Biotech) and returning these isolated parasite infected erythrocytes into culture media with adjusted haematocrits (Ribaut *et al.*, 2008).

In this study, this isolation method was however used to harvest a large number of trophozoites at high parasitaemias. This method exploits the magnetic properties of the haemozoin crystals to retain late stage trophozoites with developed food vacuoles containing these haemozoin crystals in a column packed with a magnetic sponge material, whilst eluting non-magnetic cell debris and earlier life-cycle stages of parasites together with the uninfected erythrocytes (Butykai *et al.*, 2013). It has been established that rings and early trophozoites accumulate little haemozoin, but that 50-70% of an erythrocytes haemoglobin is converted to haemozoin in the late trophozoite and early shizont stages of parasite IE development (Francis *et al.*, 1997).

Food vacuoles are visible under a light microscope as dark brown stained pigments. Clearer images with greater resolution of food vacuoles have been captured previously by electron microscopy (Lamarque *et al.*, 2008).

The aim of this experiment was to enrich and isolate late-stage trophozoite infected erythrocytes from other IE life-cycle stages and uninfected erythrocytes by magnetic separation, and to further process these cells to harvest the intact parasite food vacuoles for further downstream proteomic analysis of food vacuole membrane proteins.

5.2 Materials and methods

5.2.1 Exposure of *P. falciparum* to clofazimine prior to food vacuole purification

The aim of food vacuole isolation was to establish whether any changes in protein expression occurred after exposure of *P. falciparum* W2 strains to constant doses of clofazimine. Sorbitol synchronised W2 rings (approximately 6 – 10 h into new life-cycle) were exposed to 375 nM clofazimine in culture for 96 h prior to isolation of food vacuoles. Untreated W2 and 3D7 parasites were also maintained under similar conditions to serve as control samples, in order to establish significant changes in protein expression of treated W2 strains to these controls.

5.2.2. Isolation of late-stage trophozoites

Parasite suspensions (6-8% parasitaemia, late stage trophozoites/schizonts) were passed through a culture media preconditioned MACS column (CS⁺, Miltenyi Biotech) connected to a VarioMACS apparatus. A CS⁺ column was installed in VarioMACS apparatus as described in the Miltenyi Biotech cell separation protocol, and pre-treated from the bottom up with incomplete culture medium to displace all trapped air. The suspension of infected erythrocytes was then passed through the column and washed with incomplete RPMI-1640 medium to wash out cell debris and uninfected erythrocytes while retaining late trophozoite stage infected erythrocytes on the column. The flow through contained the uninfected and non-parametric ring-stage parasites, whereas the haemozoin crystals resulted in trapping of the late-stage trophozoites and early schizonts in the magnetised column. Once saturated and washed, the column was disconnected from the VarioMACS magnet and fitted into a burette stand. The magnetically-trapped erythrocytes were then eluted with incomplete RPMI-1640 medium. The percentage parasitaemia was determined from a small aliquot of the column eluent that was used to make a thin smear, stained with Giemsa dye for microscopic examination and the percentage of purified trophozoite infected erythrocytes confirmed. Isolation of food vacuoles was conducted immediately thereafter (approximate 2 min time delay).

5.2.3 Isolation of trophozoite food vacuoles and endocytic vesicles

Isolated late-stage trophozoite or alternately cultures of approximately 8% parasitaemia and 5% hct were centrifuged, exposed to saponin (1 g/100mL PBS containing 1% w/v bovine serum albumin (BSA) and 1 mM phenylmethylsulphonyl fluoride (PMSF) and vortex mixed to lyse erythrocyte membranes. The parasites were centrifuged at 2500 g for 5 min and the supernatant aspirated. The parasite pellet was then resuspended in PBS (1% w/v BSA) and placed in an Eppendorf tube containing a phthalate oil mixture (dibutyl phthalate and dioctyl phthalate in a ratio of 5:4). Eppendorf tubes were centrifuged at 14 000 g for 5 min, the oil mixture carefully aspirated, and the pellets washed with PBS (with no BSA) and then resuspended in a potassium chloride (KCl) buffer (140 mM KCl, 25 mM HEPES, 1 mM PMSF pH 7.2). The parasites were filtered through a 3 µm filter (filters and apparatus donated to the Department of Biochemistry of Rhodes University); and a drop of this filtrate viewed under a compact light microscope (1000x magnification, NIS elements F3.0 software, normal mode, manual exposure 30 ms, gain of 1.2 x, colour contrast medium) to confirm presence of haemozoin crystals enclosed within food vacuole membranes.

5.2.4 Purification of trophozoite food vacuoles

The lysed trophozoites and food vacuole filtrate was passed through a smaller volume Miltenyi LS⁺ magnetic column and washed with KCl buffer while connected to a midi-MACS magnet (Miltenyi Biotech) to elute any remaining erythrocyte debris and endocytic vesicles. Once removed from the midi-MACS, the column was flushed with 1 mL KCl buffer to elute the magnetically retained food vacuoles (black/dark brown in appearance). The endocytic vesicles and food vacuole samples were stored at -20°C until proteomic analysis.

5.3 Results

Two independent starting cultures were pooled and passed through a VarioMACS to remove ring stage parasites and uninfected erythrocytes, resulting in approximately 95% purified late trophozoite infected erythrocytes (Figure 5.1, C; D). Parasitaemia was allowed to increase up to 8% before harvesting to ensure maximum yield of trophozoites. Three separate harvests of food vacuoles (two x 30 mL cultures each) were pooled to obtain adequate protein quantities for further proteomic analysis.

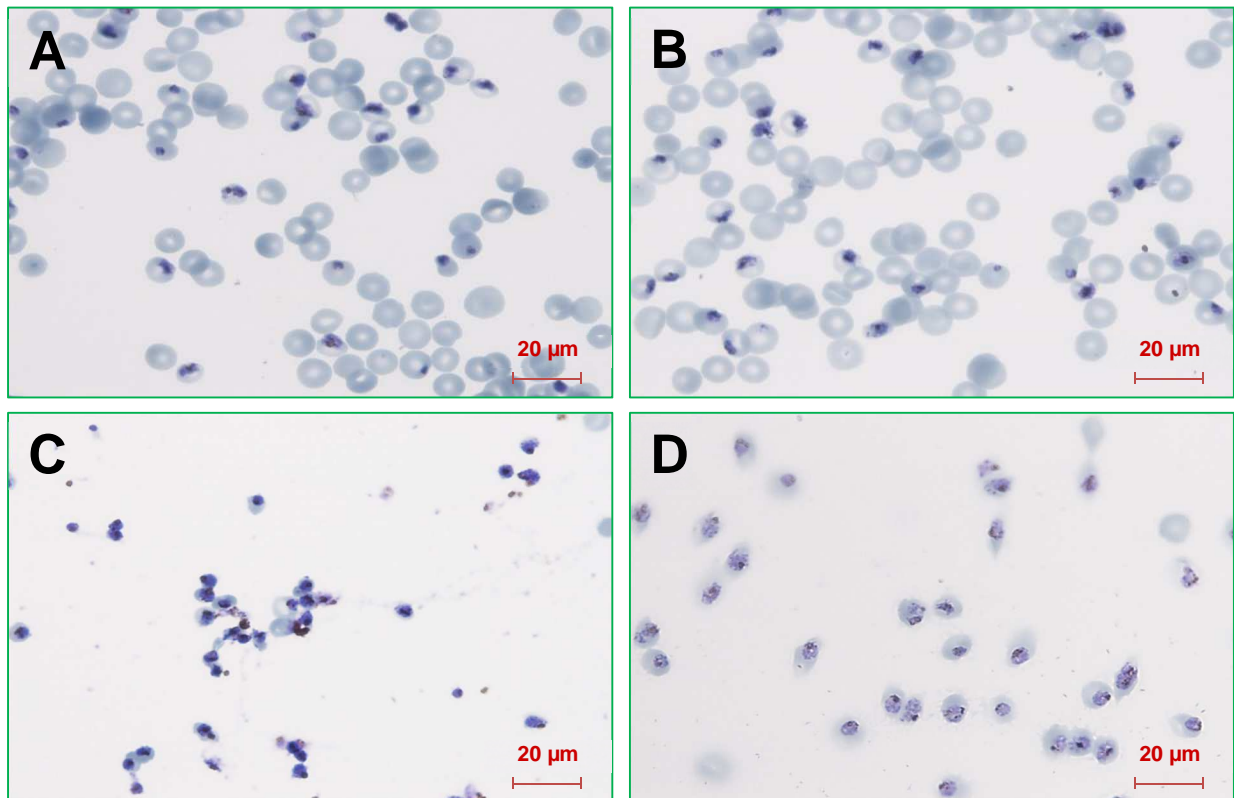


Figure 5.1 Light microscope images of Giemsa stained clofazimine (un)treated W2 strains (A) untreated (control) and (B) clofazimine (375 nM) treated *P. falciparum* W2 infected erythrocytes at 8% parasitaemia, followed by CS+ magnetic purification (VarioMACS) of trophozoite infected erythrocytes (C) untreated (control) and (D) clofazimine (375 nM) treated samples.

These independent isolations were performed for W2 parasites treated with 375 nM clofazimine for 96 h, as well as untreated W2 and 3D7 parasite cultures. Some variation in the life-cycle

stage of isolated samples was noted; following VarioMACS purification a number of merozoites were observed for one of the isolation performed (image not shown).

Other than a slight drop in percentage parasitaemia for clofazimine treated samples prior to isolation, no distinction could be made between morphology or development stage of treated parasites in comparison to untreated controls (Figure 5.1, A; B).

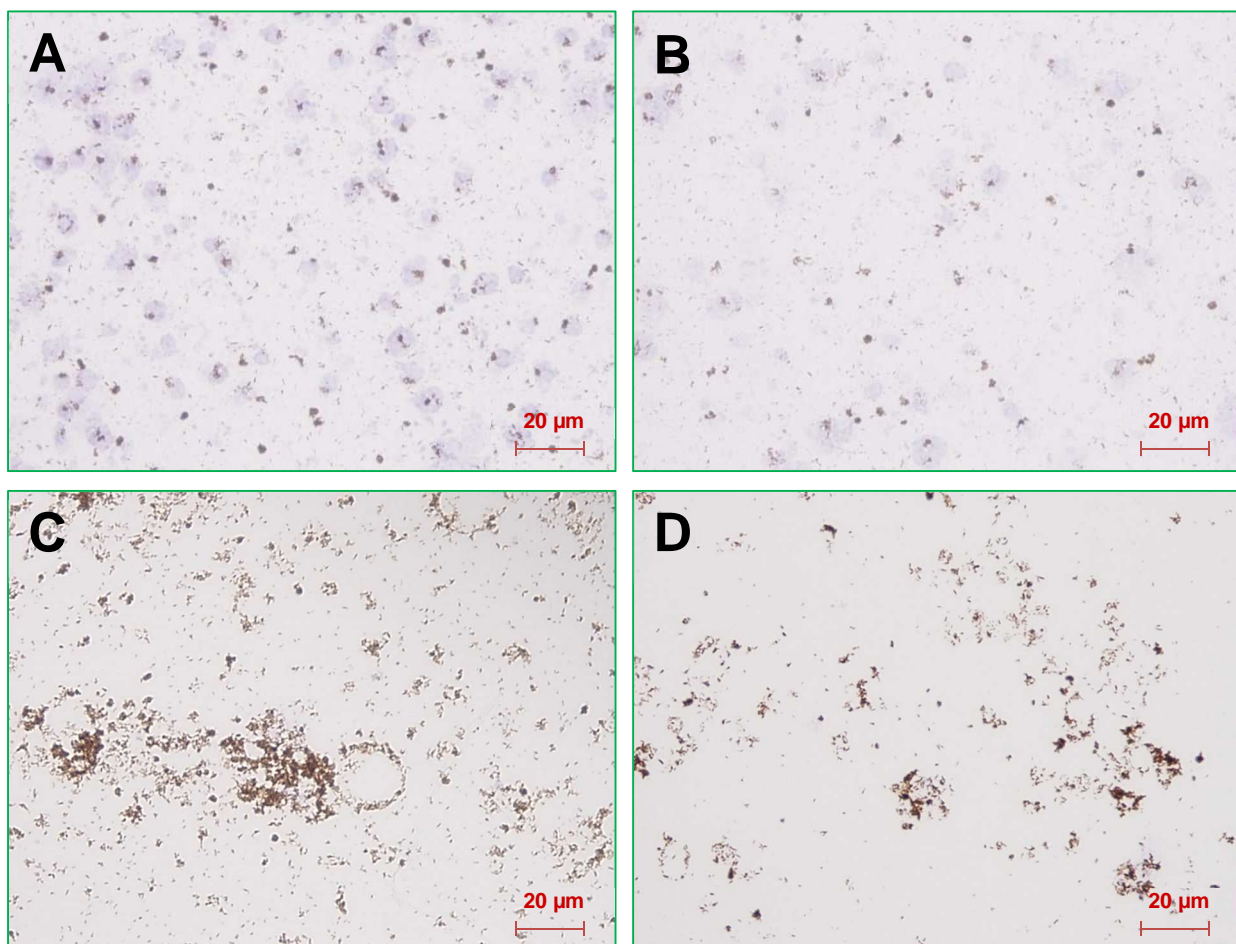


Figure 5.2 Light microscope images of food vacuole isolation steps

Saponin lysed, Giemsa stained (A) untreated (control) and (B) clofazimine (375 nM) treated *P. falciparum* W2 infected, purified trophozoites, and food vacuoles isolated by centrifugation and filtration from (C) untreated (control) and (D) clofazimine treated (375 nM) samples.

Purified food vacuoles appeared brown in colour (Figure 5.2, C; D), due to the presence of haemozoin pigments contained within them (Goldberg *et al.*, 1991). Samples of wash steps were stored for SDS-page analysis in order to assess the degree of protein waste.

5.4 Discussion

The presence of haemozoin crystals on Giemsa smears of food vacuole preparations (Figure 5.2) suggests that food vacuoles were isolated successfully. However, it has been found previously that crystals present in a sample does not conclude that vacuolar membranes and its content is intact and present (Azimzadeh *et al.*, 2010). Possible protein degradation by the release of proteolytic enzymes after lyses of erythrocyte and parasite membranes, and filtration of samples was counteracted by the addition of phenylmethylsulphonyl fluoride (PMSF), a non-selective inhibitor of a majority of serine proteases, to all resuspension and elution buffers (Sharma & Radha Kishan, 2011). It has been noted previously that even with meticulous care, cellular debris and other contaminants are still present in the food vacuole isolates and attempts to further purify these samples leads to significant loss of valuable sample (Lamarque *et al.*, 2008).

5.5 Conclusion

Parasitic food vacuoles were isolated from late trophozoite stage parasites by using highly synchronised parasite cultures followed by isolation and harvesting of the infected erythrocytes in high yield using magnetic capture techniques. Despite culturing and combining large volumes of parasite cultures, the protein yield of food vacuole membrane proteins was sub-optimal and the concentration of the low abundance proteins present in the isolated protein samples negatively affected the downline proteomics analysis. The presence and integrity of isolated food vacuole membranes could have been confirmed by electron microscopy or Western blotting techniques with the use of antibodies.

Chapter 6: Proteomic analysis

6.1 Introduction

It has previously been established that resistant isoforms of parasites have decreased accumulation of drug compounds within their food vacuoles due to an amino acid substitution in the 76th residue of the *PfCRT* membrane protein (Fidock *et al.*, 2000).

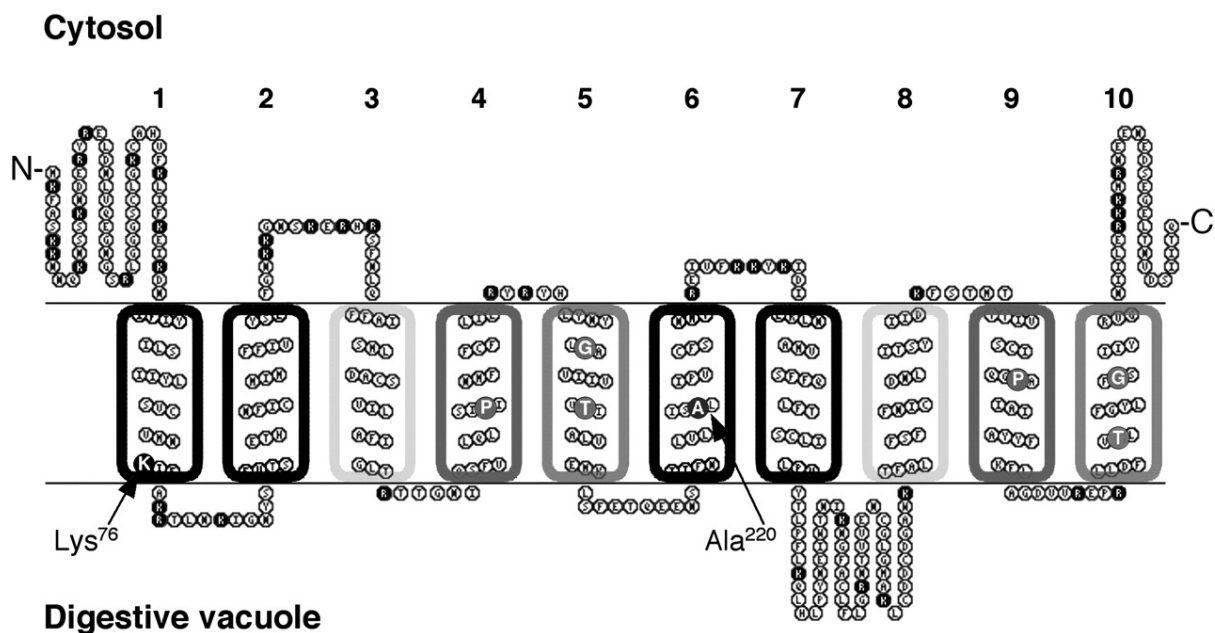


Figure 6.1 *Plasmodium falciparum* Chloroquine Resistance Transporter (*PfCRT*) topology of the transmembrane domains

The protein has 10 predicted hydrophobic transmembrane binding domains. Predicted lysine and arginine, positively charged residues are shown in black. The chloroquine-resistance associated K76T mutation is shown in black in TMD-1 on the left of the image. TMDs 3 and 8 bind and translocate substrates. TMDs 1-3 and 6-8 determine substrate specificity. Image taken from (Martin & Kirk, 2004) with permission.

PfCRT is a transmembrane protein that transports drugs from the lumen of the food vacuole into the cytoplasm of the parasite, it has 10 transmembrane domains (TMDs), made up of 424 amino acids (Martin *et al.*, 2009). Other functions of this protein includes the efflux of alkaloids, amine compounds, amino acids and peptides from digestion of haemoglobin molecules' globin constituents for reuse by the parasite (Singh Sidhu *et al.*, 2002). Mutations in this protein alter intravacuolar pH, as this protein acts as an ion channel, but most significantly these enhance chloroquine efflux transport (Papakrivos *et al.*, 2012).

Increases in copy number of the gene coding for *Pf*MDR1 membrane protein localized to the food vacuole has also been linked to decreased drug susceptibility of these parasites (Cowman *et al.*, 1991).

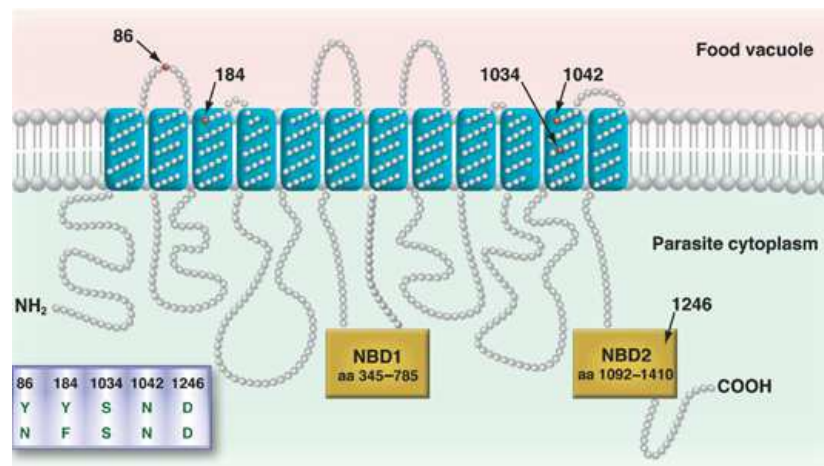


Figure 6.2 *Plasmodium falciparum* Multi-drug resistance transporter (*Pf*MDR1 or Pgh-1) topology of transmembrane domains

The protein has 12 predicted hydrophobic transmembrane binding domains. NBD: nucleotide-binding domain. Polymorphisms associated with alteration of drug movement across food vacuole membranes are indicated. Image taken from (Rohrbach *et al.*, 2006).

*Pf*MDR1, containing 12 TMDs, has been shown to actively remove drugs from the cytoplasm and store them within food vacuoles, protecting parasites against antimalarials that are active in the cytoplasm (Cowman *et al.*, 1991). Mutations in this protein alter substrate specificity and have been linked to artemisinin and chloroquine resistance *in vitro* (Hayward *et al.*, 2005b).

The aim of the proteomic analysis was to conduct comparative proteomics on resistance proteins harvested from food vacuole membranes of clofazimine treated (possibly chloroquine sensitised) W2 parasites, untreated W2 and 3D7 strains by spectral counting and emPAI analysis.

6.2 Materials and methods

6.2.1 Food vacuole protein precipitation

The isolated and frozen food vacuole samples were allowed to thaw, and then precipitated by addition of 1 volume of 100% (w/v) trichloroacetic acid (TCA) to 4 volumes of protein sample. After a 10 min incubation period, the samples were centrifuged at 15 000 g for 5 min in Eppendorf lo-bind tubes and the supernatant aspirated. The pellet was suspended in 200 μ L chilled acetone, sonicated (5 min), centrifuged and the supernatant aspirated. This acetone wash procedure was repeated three times, the acetone was aspirated and the final residual acetone was left to evaporate at 60°C for 5-10 min.

6.2.2 Protein quantitation

The protein concentration of samples was determined by the bicinchoninic acid (BCA) method (Smith *et al.*, 1985). Briefly, a non-sterile 96 well plate was used to create a bovine serum albumin (BSA) standard curve with concentrations ranging between 0.1 mg/ml and 2.5 mg/ml, with two quality control concentrations of 0.4 mg/ml and 2 mg/ml. A blank of PBS was incorporated to eliminate background from measurements obtained. The samples were added to BCA reagents (50 parts of reagent A to 1 part reagent B, composed of, 1% w/v BCA, 5.4% w/v Na₂CO₃, 0.209% w/v disodium tartrate dehydrate, 0.4% w/v NaOH and 0.95% w/v NaHCO₃ at pH 11.25 and 2.56% w/v cupric sulphate, respectively) in a ratio of 1:49 in well. The plate was placed on a microplate shaker for 2-3 min before incubation at 60°C for 1 h. The microplate was allowed to cool for 10 min and absorbance was measured at 570 nm on a plate reader (ELX 800, BioTek, with BioTek's Gen5™ software to calculate calibrations and extrapolations using best fit formulae). Microsoft Office 2010, Excel software was used to extrapolate unknown protein concentrations from the BSA standard curve.

6.2.3 Protein preparation for Sodium Dodecyl Sulphate – Polyacrylamide Gel Electrophoresis (SDS-PAGE)

Protein samples were treated with radioimmunoprecipitation assay (RIPA) buffer (10 mM Tris-HCl, pH 8, 2 mM EDTA, 1% v/v Triton X-100, 0.1% w/v SDS, 0.1% w/v sodium deoxycholate, 140 mM NaCl and 1 mM PMSF added just prior to use) in a ratio of 1:5 to prevent proteolytic activity that may have occurred in the remaining sample preparation activities. Then samples were exposed to ultrasonic homogeniser pulses of approximately 700 W for 1 min pulse intervals for a total of 5 min whilst being kept on ice. Homogenised protein samples were stored at 4°C for 1 h, then centrifuged at 15 000 g for 20 min. One part Laemmli buffer (0.188 M Tris HCl, pH 6.8, 6% w/v SDS, 15% v/v β-mercaptoethanol, 30% v/v glycerol, 0.006% w/v bromophenol blue) was added to two parts protein sample, boiled (10 min, 95°C) and centrifuged (16 000 g, 5 min). The supernatant was loaded into wells of the SDS-PAGE gel.

6.2.4 One-dimensional gel electrophoresis

For one dimensional gel electrophoresis (1DE) a 4-20% gradient, 12+2 well, Midi size Criterion™ TGX Stain-Free™ Precast Gel (Bio-Rad) was used. Protein standards were loaded in well 1 and 12 for mass calibration (Precision Plus Protein™ Standard, BioRad). The protein samples were diluted to approximately 1 mg/mL with Laemmli buffer and 20-30 ug protein loaded per sample well. The gel was loaded into a running chamber, filled with running buffer (0.124 M Tris, pH 6.8, 14.5% v/v glycine, 1% w/v SDS) and the power source was set at 60 V for approximately 3 h. Thereafter the gel was carefully removed from its cassettes and stored in a fixing solution in a new, sealable plastic container (50% v/v Methanol, 10% v/v glacial acetic acid, 40% v/v distilled water) until needed.

6.2.5 Protein band detection by imaging

Protein bands were detected by the Stain Free process using a Gel Doc™ EZ System (Bio-Rad) to activate and image the gel using Image Lab™ Software to conduct image analysis. For reference purposes, e.g. when excising protein bands for in-gel trypsinisation, gels were stained with Oriole™ fluorescent gel stain (Bio-Rad) for 90 minutes and visualised under ultra violet light.

6.2.6 In-gel trypsinisation

In-gel trypsinisation was performed by adapting methods described previously (Rosenfeld *et al.*, 1992). Gel pieces were destained with acetonitrile, chemical reagents were added to aid in reduction and alkylation of low abundance proteins and finally proteins were trypsinised and peptides extracted as discussed below.

6.2.7 Destaining of gel pieces

Protein bands of interest were excised from gels using new scalpel blades per band to avoid contamination and cubed before de-staining with 50 mM NH_4HCO_3 / 50% MeOH (vortex mixed, then left to settle for 20 min). The supernatant was removed before repeating the de-staining procedure. Acetonitrile (ACN, 75% v/v) was added to cover gel pieces (vortex mixed, then left to stand for 20 min), after which the supernatant was discarded and destained gel bits were allowed to dry in a water bath (60°C, 30 min).

6.2.8 Reduction and alkylation of low-level proteins

The samples were reduced and alkylated by addition of enough 10 mM DTT in 25 mM NH_4HCO_3 to cover gel pieces, samples were incubated at 60°C for 1 h, followed by addition of acetonitrile (75% v/v, 10 min, then the supernatant was discarded), and 55mM iodoacetamide in 25 mM NH_4HCO_3 (regular vortex mixing, with a 20 min reaction time, in dark, then the supernatant was

discarded). Then gel cubes were washed twice in 25 mM NH_4HCO_3 (vortex mixed 10 min, discarded supernatant) before samples were placed in a “Speedy Vac” to dry, then sealed and stored at -20°C .

6.2.9 Trypsinisation and extraction of peptides

Dehydrated gel pieces from selected bands cut from the SDS-PAGE gel containing protein samples of interest were rehydrated (by addition of 25 mM NH_4HCO_3) and vortex mixed before enzymatic digestion at 37°C , cleavage (by 10 ng/ μL activated sequence grade trypsin in 22.5 mM NH_4HCO_3) overnight. These gel digests could be stored at -20°C for a few weeks if no peptide extraction was performed.

In order to extract the peptides from the digested gel samples, the gel pieces were centrifuged (500 g, 2 min) before transfer of the digest solutions (supernatant) to 0.5 mL Protein Lo-Bind tubes (Eppendorf®, Sigma). Gel pieces were submerged in 50% (v/v) ACN / 5% (v/v) formic acid solution, vortex mixed 25 min, sonicated 5 min) before the supernatant was transferred to Lo-bind tubes. This process was repeated twice, combining the gel washes with the first extract then drying the total peptide extracts perband using a “Speedy Vac” and stored at -20°C for about 2 months.

6.2.10 Sample Stage-tip clean-up and MALDI-TOF/TOF protein sequencing

Three proteins bands of different intensity were analysed at the Council for Scientific and Industrial Research (CSIR) to assess whether low band intensities were adequate for detection of peptides by Matrix Assisted Laser Desorption Ionisation- Time of Flight (MALDI-TOF) mass spectrometry. This pilot assay confirmed the ability to perform this type of analysis on relatively low abundance proteins separated using gel electrophoresis. Digested proteins from six bands isolated from the gel were forwarded to the Proteomics Research and Service unit of the

Department of Biotechnology, at the University of Western Cape for assessment by a more sensitive and advanced MALDI-TOF/TOF system and to apply the peptide mass fingerprinting (PMF) approach. Significant MASCOT scores for protein identification were however not obtained, despite using the dedicated PlasmaDB protein database for *Plasmodium* species.

The same digested protein samples were then re-analysed by a more tedious but more efficient approach where peptide samples of each trypsin digested band was separated into 192 fractions by nano Liquid Chromatography (nLC) and 3 μL fractions sequentially spotted onto a pre-prepared MALDI-target plate (Bruker MTP AnchorChip™, 384-well plate). This reduced the complexity of individual samples for analysis by MALDI-TOF/TOF. Methods used to prepare samples for mass spectrometry varied only with regards to method of addition of the α -Cyano-4-hydroxy-cinnamic acid matrix (HCCA) used to enhance the ionisation during analysis.

For MALDI-TOF analysis at the CSIR peptide extracts were suspended with equilibration solvent (5% v/v formic acid) (vortex mixed for 1 min, sonicated for 5 min) and Stage-tip aided peptide desalting was performed with a 2.5 mL Eppendorf Combi-Tip syringe as adapted from previous publications (Rappsilber *et al.*, 2003). Briefly, the tip was activated with a preconditioning solvent (50% v/v methanol, 5% v/v formic acid) and prepared for sample loading by washing with 10 μL of equilibration solvent (5% v/v formic acid). Sample proteins were loaded, washed (as above) and then eluted into polymerase chain reaction (PCR) tube lids with an elution solvent (70% v/v acetonitrile, 0.1% v/v formic acid) containing α -Cyano-4-hydroxy-cinnamic acid matrix (HCCA) (5 mg/mL) described previously as the dried droplet method (Spengler *et al.*, 1990). Protein samples were then spotted (1.5 μL) onto a mass spectrometer MALDI plate in duplicate. The MALDI target plate was air-dried and analysed in a Bruker Daltonics, Ultraflex MALDI-TOF system to establish the signal intensities of the different protein bands selected from the gel and to assess whether the signal intensity would be able to provide usable peptide mass fingerprint information to identify the proteins present in the bands cut from the gel.

For MALDI-TOF/TOF analysis at UWC samples were purified and concentrated as described above however using C₁₈ZipTip® columns for the sample cleanup, and run on an UltrafleXtreme MALDI-TOF/TOF system (Bruker Daltonics, Bremen, Germany). Speedy Vac dried samples were suspended in 0.1% v/v formic acid for nLC on a Thermo Scientific EASY-nLC II connected to a Proteiner fc II protein spotter controlled through HyStar software. Samples were separated into fractions on an EASY C18 pre-column (Dimension 2 cm, 75 µm internal diameter, 5 µm), passed through a C18 analytical column (Dimension 10 cm, 75 µm internal diameter, 3 µm) and co-eluted with HCCA matrix on a MTP AnchorChip™ 800/384 (Bruker Daltonics) at a flow rate of 300 nL/min using a 48 min solvent gradient (Table 6.1).

Table 6.1 Gradient Run for nLC on a Thermo Scientific EASY-nLC II

Time (min)	Function	Value
0	Solvent Mix	98% A , 2% B
44	Solvent Mix	65% A , 35% B
48	Solvent Mix	60% A , 40% B
48.10	Solvent Mix	0% A , 100% B
60	Solvent Mix	0% A , 100% B
60.10	Solvent Mix	98% A , 2% B
70	Solvent Mix	98% A , 2% B

Solvent A: 0.05% (v/v) Trifluoroacetic acid (TFA) in LC-MS grade water, Solvent B: 0.05% TFA in acetonitrile. Performed at a flow rate of 300 nL/min.

The Bruker MTP AnchorChip™ MALDI target plate with dried sample fractions was loaded into the UltrafleXtreme II MALDI-TOF/TOF system for protein sequencing with Flex Control 3.4 software. Peptides were ionised with a nitrogen laser at 337 nm, and spectra were obtained in reflector positive mode (28kV, 1000 lasershots per spectrum, scan range 700-4000 m/z). Calibration was done using peptide calibration standard II (Bruker Daltonics). Peptide spectra accumulated from 4000 shots were automatically processed in WARP LC 3.2 software (Bruker Daltonics).

6.2.11 Proteomic analysis and interpretation of results

The Proteomics Research and Service unit of UWC conducted in-house proteomics analysis using a SwissProt database using a ProteinScape 3.0 workstation, with MASCOT algorithms. Search parameters were: *Plasmodium falciparum* (taxonomy), trypsin (enzyme), 1 missed cleavage allowed, carbamidomethyl (C) fixed modifications, oxidation (M) variable modifications, 50 ppm precursor tolerance, and 0.7 Da fragment tolerance. Protein matches were considered valid if a molecular weight search score (MOWSE) of greater than 11 was obtained.

Raw spectral data were obtained from the Proteomics Research and Service unit of UWC and re-analysed with SearchGUI version 1.24.0 using proteomics identification search engines X!Tandem, MS-GF+, MS Amanda, MyriMatch, Comet, Tide and OMSSA (Vaudel *et al.*, 2011). Proteomic analysis was done against a *Plasmodium falciparum* 3D7 proteome sequence from UniProt, enriched with Max Planck Institute of Biochemistry Martinsried (MPI) common protein contaminants database and the UniProt proteome for *Cordyceps militaris* strain CM01 in order to reduce false positives for proteins identified. Settings were adjusted as follows: fragmentation method of high-energy collisional dissociation (HCD) for all search engines, trypsin (enzyme), 1 missed cleavage allowed, carbamidomethyl (C) fixed modifications, oxidation (M) variable modifications, 50 ppm precursor tolerance, and 0.7 Da fragment tolerance, precursor charge 1 to 1 (singly charged only).

Peptide Shaker (version 0.36.1) was used as post-processing software to identify *Plasmodium* proteins with a high confidence (Vaudel *et al.*, 2015). Exponentially modified protein abundance index (EmPAI) scores provided per protein by the software, as described by Ishihama *et al.*, were used as a “label-free” quantitation method of similar proteins identified between samples in order to assess the effect of clofazimine on food vacuole proteins (Ishihama *et al.*, 2005).

6.3 Results

6.3.2 SDS-PAGE results

Stored food vacuole samples were thawed, protein was precipitated, quantified and then homogenised prior to SDS-page (1DE 4-20% gradient, 12+2 well, Midi size Criterion™ TGX Stain-Free™ Precast Gel, BioRad). An R^2 value of 0.98 was obtained for the albumin calibration curve used to extrapolate the protein concentration of treated food vacuoles and untreated controls (either W2 or 3D7). A sample volume was loaded to obtain between 8.2 μg and 10.4 μg protein per well (Table 6.2). However, due to low protein yield from the isolated food vacuoles, a final concentration of only 2.3 μg could be loaded for the food vacuoles isolated from clofazimine treated W2 parasites (Table 6.2, Clofazimine FV).

Table 6.2 Protein sample concentrations and quantities loaded to SDS-PAGE wells

<i>P. falciparum</i> strain	Sample description	Concentration in Laemmli buffer (in $\mu\text{g}/\mu\text{L}$)	Volume loaded on SDS-PAGE
W2	Clof FV	0.05	50
	Control FV	0.15	55
	Clof Wash	0.21	50
	Control Wash	0.17	50
3D7	Control FV	0.29	30
	Control Wash	0.34	24

Concentration values are as determined by the BCA method, sample volumes are in μL . FV = Food Vacuole, Clof = Clofazimine treated (375 nM), Control = Untreated, *P. falciparum*-infected erythrocytes, Wash = Endocytotic vesicles and non-haemozoin debris eluted from LS⁺ magnetic columns (Midi-MACS).

Literature suggests that larger quantities of *P. falciparum* cultures are essential to obtain enough protein, for example Larmarque *et al.* pooled four food vacuole fractions from 30 x 175 cm² culture flasks (approximately 5-12 L starting culture) to obtain a maximum of 500 μg protein for proteomic analysis (Larmarque *et al.*, 2008). This roughly equates to three 175 cm² culture flasks for 10 μg final food vacuole protein, depending on the hct, volume of culture medium and parasitaemia of samples. Consequently, in this study, duplicate adjacent wells were run for this

sample, and bands were excised across both lanes and trypsinised together to increase peptide yield.

It has been determined that chloroquine resistance occurs partly through the actions of *PfCRT* and *PfMDR1*, proteins that are localised in the food vacuole membrane of trophozoites, with calculated masses of 45 and 162 kDa, respectively (Duraisingh & Cowman, 2005; Raj *et al.*, 2009; Valderramos & Fidock, 2006). No bands were visualised in the 162 kDa region on the gel obtained (Figure 6.3), therefore sample bands at approximately 40 and 65 kDa estimated mass ranges were isolated for MALDI-TOF/TOF screening at the Proteomics Department of UWC. Table 6.3 indicates the bands assessed by MALDI-MS/MS at the BioSciences division of the CSIR (in bold).

Table 6.3 Description of sample treatment and location on SDS-PAGE gel

Strain	Code	Mass estimate (kDa)	Fraction	Treatment
W2	A1	65	Food Vacuoles	Clofazimine
	B1	40		
	C1	23		
	A2	65	Food Vacuoles	Untreated
	B2	40		
		A4	65	Wash step
3D7	A5	65	Food Vacuoles	Untreated
	B5	40		
	D5	15		

Samples in bold were analysed at CSIR on MALDI-TOF, remaining samples were analysed by the Proteomics Unit at UWC with nLC MALDI-TOF/TOF.

Proteins separated by 1D SDS-PAGE resulted in very low intensity bands. Staining with Oriole™ ultraviolet activated fluorescent dye enhanced the visibility of a few faint bands, especially in the lower kDa mass ranges (Figure 6.3, B). Bands were excised, worked up as described above and trypsin digested, and the peptide extracts per band were analysed by mass spectrometry to characterise proteins (Figure 6.3, B).

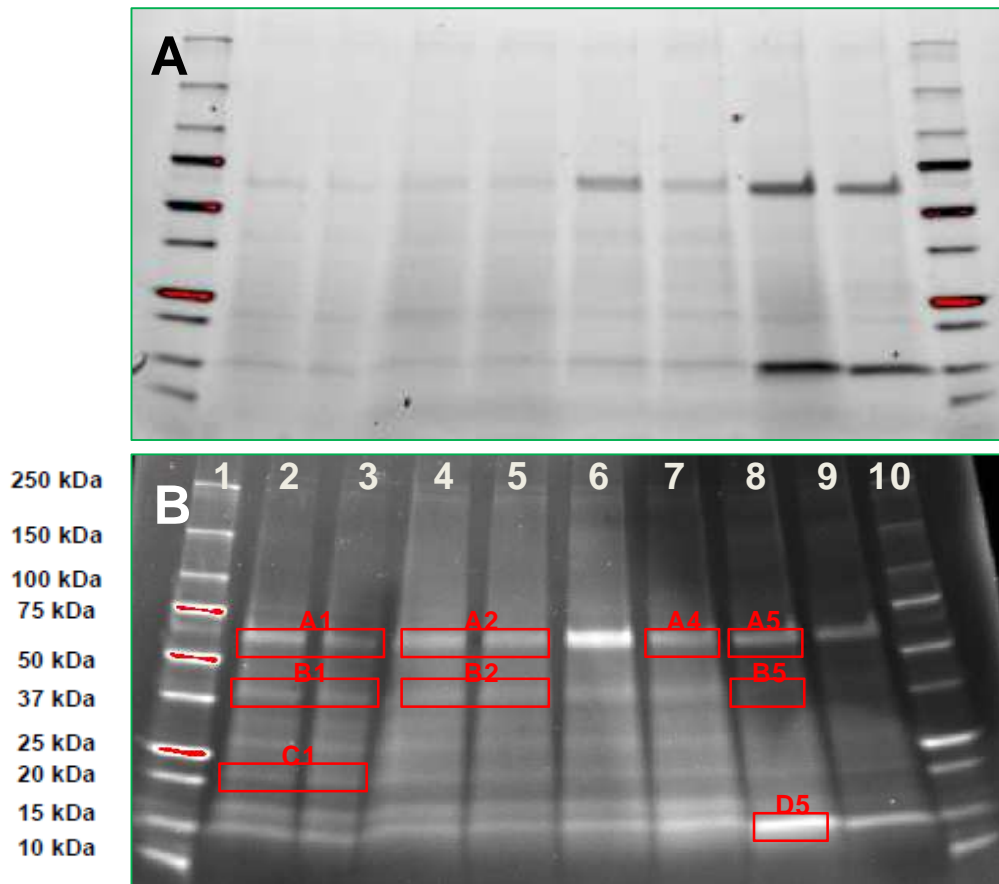


Figure 6.3 SDS-PAGE of *Plasmodium falciparum* food vacuole protein samples

(A) as observed under stain-free gel settings, or (B) with the fluorescent protein dye Oriole™ stain under UV light. Protein bands were labelled and codes (e.g. A1) were used for subsequent proteomic analysis with standard masses on the right and present in lane 1 and 10 (Precision Plus Protein™, BioRad). Lane 2&3: W2 clofazimine exposed food vacuoles (FV), lane 4&5: W2 untreated FVs, lane 6&7: wash debris of W2s, lane 8: 3D7 untreated FVs and lane 9: 3D7 wash debris. Images are from a Gel Doc™ EZ System (Bio-Rad) gel imaging system and Image Lab™ Software, where red indicates high intensity protein bands.

In Figure 6.3 (B) it is clear that the higher intensity bands are seen for samples A and D. With Lane 6 and 9 representing wash steps for W2 and 3D7 food vacuole isolation, respectively, in which erythrocyte cellular debris and endocytic vesicles are expected to be present. Lane 1 and 10 were loaded with protein standards (Precision Plus Protein™, BioRad). Lane 7 and 8 contained 3D7 untreated controls, and lanes 2-5 contained treated and untreated food vacuoles from W2 strains.

6.3.3 Peptide mass fingerprinting

Clofazimine treated food vacuoles from W2 (C1) with a light band intensity, W2 untreated endocytic vesicles and cell debris (A4- wash step) with a medium band intensity, and 3D7 untreated food vacuoles (D5) with a dark band intensity were screened at the BioSciences Division of CSIR to establish whether peptide mass fingerprinting on MALDI-TOF was possible from the concentrations of protein recovered (Table 6.3). A limited number of peptide peaks were detected in all three samples, which allowed for protein identification with with insignificant Mascot scores (<100). Below if a mass spectrum of the medium intensity band's peptide extracts (Figure 6.4).

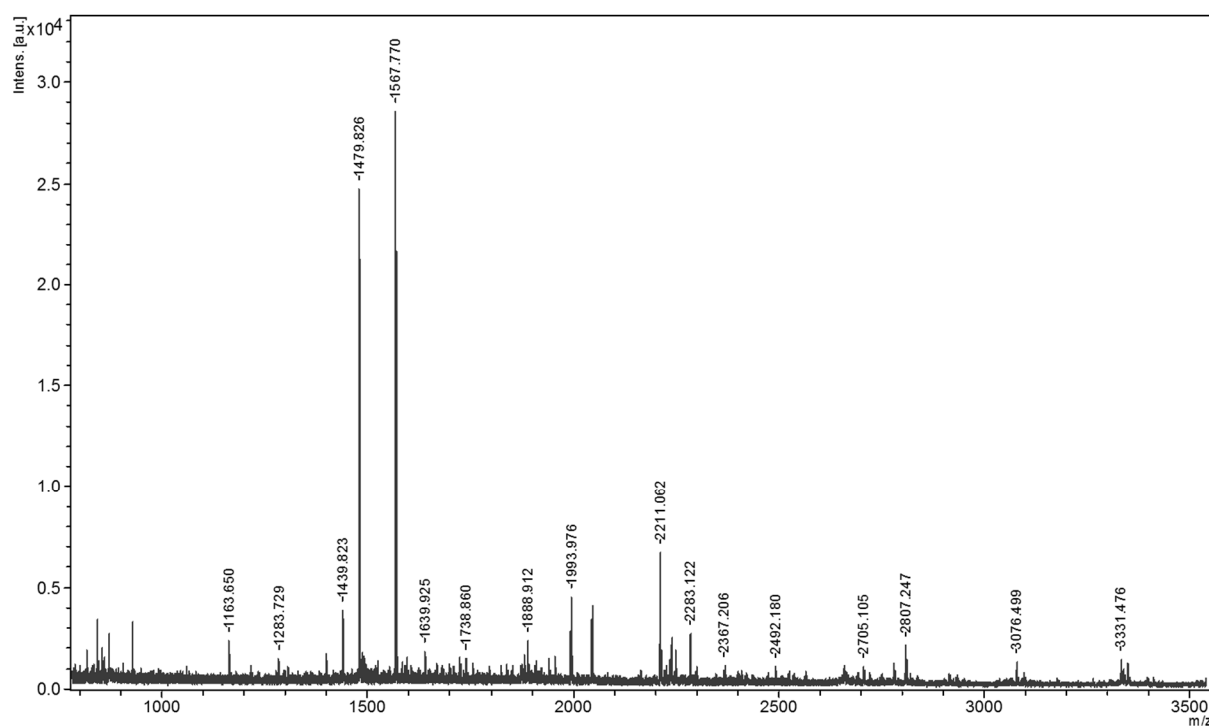


Figure 6.4 Mass spectrum of untreated *Plasmodium falciparum* W2 endocytic vesicles and cell debris (wash step)

Sample A4 spectrum as obtained by an Ultraflex MALDI-TOF system (Bruker Daltonics), ionisation by nitrogen laser at 337nm in reflector positive mode (28 kV, 1000 lasershots per spectrum, scan range 700-3500 m/z). Calibration was done using peptide calibration standard II (Bruker Daltonics).

From this mass spectrum it is evident that there are a number peptide ions present in the sample with the majority being present with low abundance as indicated by the ion peaks in the lower orders of magnitude (<2 x 10⁴). Consequently peptide sequencing by MALDI-TOF/TOF was performed on all remaining samples at the Proteomics unit of the UWC to

provide enhanced ms/ms ion yield and peptide spectra. The following mass spectrum was obtained for an untreated 3D7 food vacuole sample (B5) (Figure 6.5).

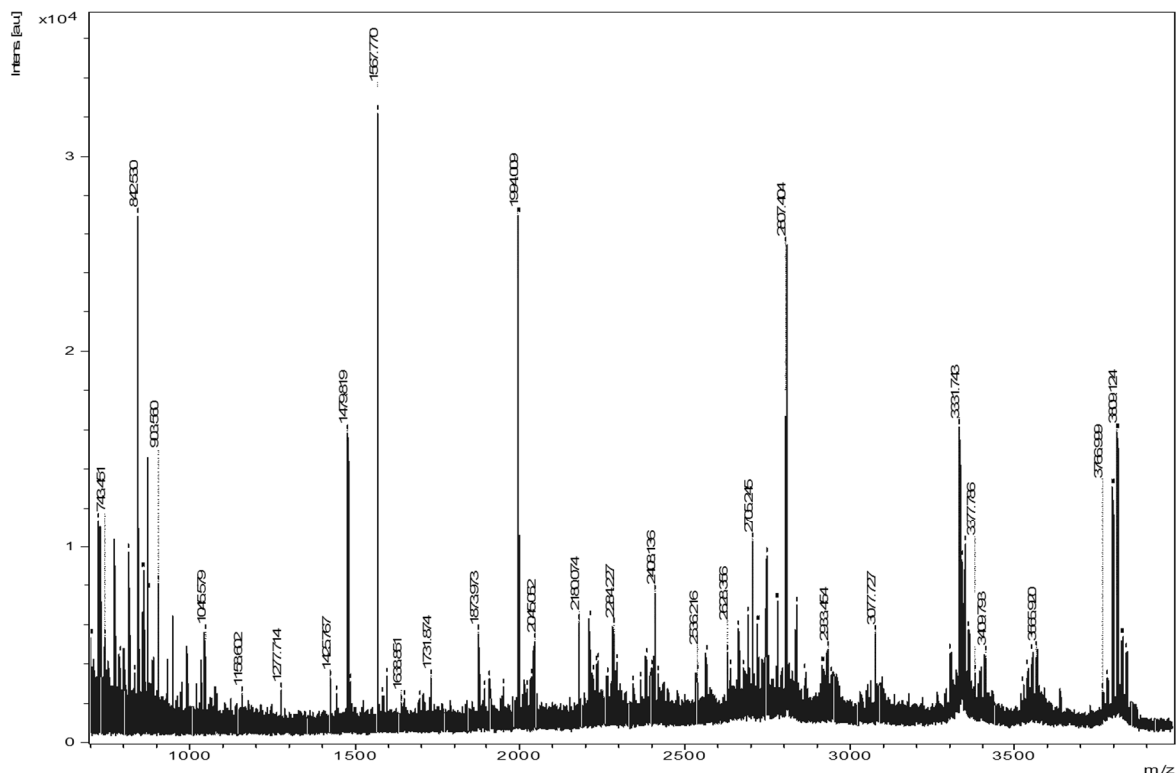


Figure 6.5 Mass spectrum of untreated *Plasmodium falciparum* 3D7 food vacuoles

Sample B5 spectrum as obtained by an UltrafleXtreme II MALDI-TOF/TOF system (Bruker Daltonics), ionisation by nitrogen laser at 337 nm in reflector positive mode (28 kV, 1000 lasershots per spectrum, scan range 700-4000 m/z). Calibration was done using peptide calibration standard II (Bruker Daltonics).

Due to the complexity of the samples obtained mass spectra of peptide fragments showed poor peak resolution leading to no proteins being identified with an acceptably high confidence. In an attempt to decrease sample complexity and enhance identification of low abundance proteins nano-liquid chromatography was employed to fractionate samples prior to peptide analysis and sequencing by MALDI TOF/TOF mass spectrometry.

6.3.4 Peptide sequencing and protein identification

Samples were then re-run with nLC in order to enhance separation of peptides prior to mass spectrometry. Raw spectra were initially analysed in ProteinScape 3.0 software to search *P. falciparum* protein databases on SwissProt, with MASCOT algorithms. This resulted in a number of significant protein identifications (Table 6.4), however no proteins could be identified for untreated 3D7 food vacuoles (Sample A5). Significant hits for mostly theoretical proteins were obtained for the remaining samples (A1, B1, A2, B2, B5), and none of these proteins were previously found to elicit drug resistance in any *Plasmodium* species.

Unfortunately no proteins previously identified to confer *Plasmodium* resistance were identified in the raw spectra of samples screened with PeptideShaker.

The majority of proteins were linked to protein trafficking (e.g. *P. falciparum* 3D7 surface protein, Pf113; erythrocyte membrane protein 1, PfEMP1; skeleton binding protein 1; and early transcribed membrane protein 5, ETRAMP5) or invasion and motility mechanisms (e.g. merozoite surface protein 1 precursor; rhoptry-associated protein 2, RAP2; glideosome-associated protein 45; and rifin-like protein RAMA) (Table 6.4, Table 6.5).

Table 6.4 ProteinScape (3.0) and Swissprot database identification of proteins

Sample	Swissprot Accession Number	Protein Description	Sequence Coverage (%)	No. of Peptides	MW (kDa)	Score
A1	MSP1_PLAFM	Merozoite surface protein 1 OS= <i>Plasmodium falciparum</i> (isolate mad20 / Papua New Guinea)	20.90	30	195.60	1534.93
	MSP1_PLAF3	Merozoite surface protein 1 OS= <i>Plasmodium falciparum</i> (isolate ro-33 / Ghana)	18.80	29	192.30	1433.68
	MSP1_PLAFP	Merozoite surface protein 1 OS= <i>Plasmodium falciparum</i> (isolate Palo Alto / Uganda)	17.30	27	196.10	1278.07
	MSA2_PLAFF	Merozoite surface antigen 2 OS= <i>Plasmodium falciparum</i> (isolate FC27 / Papua New Guinea)	33.30	6	27.90	602.25
	GRP78_PLAF O	78 kDa glucose-regulated protein homolog OS= <i>Plasmodium falciparum</i> (isolate NF54)	18.60	12	72.70	482.84
	MLRR1_PLAF 7	MATH and LRR domain-containing protein PFE0570w OS= <i>Plasmodium falciparum</i> (isolate 3D7)	2.30	9	1186.80	260.63
	YPF11_PLAF7	Uncharacterized protein PFB0765w OS= <i>Plasmodium falciparum</i> (isolate 3D7)	6.90	5	166.90	260.63
	DYHC1_PLAF 7	Dynein heavy chain-like protein MAL7P1.162 OS= <i>Plasmodium falciparum</i> (isolate 3D7)	3.00	7	582.00	257.19
	SEY1_PLAF7	Protein SEY1 homolog OS= <i>Plasmodium falciparum</i> (isolate 3D7)	5.00	3	110.50	148.44
HSP70_PLAF A	Heat shock 70 kDa protein OS= <i>Plasmodium falciparum</i>	10.60	5	74.20	141.02	
A2	MSP1_PLAFP	Merozoite surface protein 1 OS= <i>Plasmodium falciparum</i> (isolate Palo Alto / Uganda)	8.70	18	196.10	626.84
	MSP1_PLAFM	Merozoite surface protein 1 OS= <i>Plasmodium falciparum</i> (isolate mad20 / Papua New Guinea)	8.30	18	193.60	623.63
	MSP1_PLAF3	Merozoite surface protein 1 OS= <i>Plasmodium falciparum</i> (isolate ro-33 / Ghana)	8.20	18	192.30	621.45
B1	MSP1_PLAF3	Merozoite surface protein 1 OS= <i>Plasmodium falciparum</i> (isolate ro-33 / Ghana)	8.30	11	192.30	513.56
	MSP1_PLAFF	Merozoite surface protein 1 OS= <i>Plasmodium falciparum</i> (isolate FC27 / Papua New Guinea)	7.90	11	193.60	489.15
	MSA2_PLAFF	Merozoite surface antigen 2 OS= <i>Plasmodium falciparum</i> (isolate FC27 / Papua New Guinea)	7.20	1	27.90	121.80
B2	MSP1_PLAFF	Merozoite surface protein 1 OS= <i>Plasmodium falciparum</i> (isolate FC27 / Papua New Guinea)	17.00	28	193.60	1365.15
	MSP1_PLAF3	Merozoite surface protein 1 OS= <i>Plasmodium falciparum</i> (isolate ro-33 / Ghana)	15.70	24	192.30	1263.75
	MSA2_PLAFF	Merozoite surface antigen 2 OS= <i>Plasmodium falciparum</i> (isolate FC27 / Papua New Guinea)	19.30	2	27.90	206.90
B5	MSP1_PLAFF	Merozoite surface protein 1 OS= <i>Plasmodium falciparum</i> (isolate FC27 / Papua New Guinea)	9.30	13	193.60	426.50
	MSP1_PLAF3	Merozoite surface protein 1 OS= <i>Plasmodium falciparum</i> (isolate ro-33 / Ghana)	8.40	12	192.30	367.06

Data obtained from **ProteinScape 3.0**, Swissprot databases and MASCOT algorithms (score), confidence >99.9%. Protein hits with a score greater than 100 are shown. MW=Molecular weight. A1=65kDa clofazimine treated W2, A2=65kDa untreated W2, B1=40kDa clofazimine treated W2, B2=40kDa untreated W2, B5=40kDa untreated 3D7

Re-analysis of raw spectra on SearchGui (v. 1.24.0) and PeptideShaker (v. 0.36.1) (Table 6.5) allowed for successful identification of proteins linked to erythrocyte invasion by merozoites, folding and transport of proteins within the healthy trophozoite for sample A5.

Table 6.5 PeptideShaker (0.36.1) and UniProt database identification of proteins

Sample	UniProt Accession Number	Protein Description	Sequence Coverage	emPAI	MW (kDa)
A1	Q8I0U8	Merozoite surface protein 1 precursor	10.12	0.15	195.60
	Q8II24	Heat shock protein hsp70 homologue	7.24	0.08	73.25
	Q8I2X4	Heat shock protein 70 (HSP70) homologue	13.19	0.25	72.34
	O97291	Conserved <i>Plasmodium</i> protein, unknown function	0.82	0.01	231.65
	Q8IJN9	Heat shock protein 60	4.31	0.07	62.51
	Q8IB24	Heat shock 70 kDa protein	2.36	0.03	73.87
	Q8ILA1	Conserved <i>Plasmodium</i> protein, unknown function	5.04	0.07	112.34
	Q8ILP3	<i>Plasmodium falciparum</i> 3D7 surface protein, Pf113	11.35	0.10	112.50
A2	Q8I0U8	Merozoite surface protein 1 precursor	4.30	0.06	195.60
	G3JI18	<i>Plasmodium falciparum</i> 3D7 surface protein, Pf113	1.79	0.05	49.25
	Q8I207	<i>Plasmodium</i> exported protein (PHISTb), unknown function	1.96	0.03	60.23
	Q8ILP3	<i>Plasmodium falciparum</i> 3D7 surface protein, Pf113	4.64	0.04	112.50
A5	C6S3L1	Erythrocyte membrane protein 1, PEMP1	0.91	0.01	247.16
	Q8IE49	DNA-directed RNA polymerase	1.02	0.01	274.66
	Q9U0K8	Conserved <i>Plasmodium</i> protein, unknown function	0.82	0.01	229.98
	C6KSX6	<i>Plasmodium falciparum</i> 3D7 integral membrane protein, putative	1.90	0.01	171.91
	C0H5F7	Conserved <i>Plasmodium</i> protein, unknown function	0.48	0.01	393.01
	Q8I5N9	DNA-binding chaperone, putative	1.06	0.02	111.00
	Q8I207	<i>Plasmodium</i> exported protein (PHISTb), unknown function	1.96	0.03	60.23
	Q8ILP3	<i>Plasmodium falciparum</i> 3D7 surface protein, Pf113	4.64	0.04	112.50
B1	Q8I487	Skeleton-binding protein 1	2.67	0.12	36.28
	Q8I484	Rhoptry-associated protein 2, RAP2	5.28	0.10	46.71
	Q8I3F3	Early transcribed membrane protein 5, ETRAMP5	13.26	0.12	19.02
	Q8IIR7	Endoplasmic reticulum-resident calcium binding protein	21.28	0.28	39.35
	Q8I5I8	Glideosome-associated protein 45	7.35	0.09	23.62
	Q8I0U8	Merozoite surface protein 1 precursor	4.19	0.06	195.60
	Q8I4X0	Actin-1	4.79	0.06	41.84
	C0H4Y6	Protein disulfide-isomerase	1.86	0.04	55.48
	C0H4M0	Rifin-like protein (RAMA protein)	7.08	0.09	103.58
	Q8IBN1	Conserved <i>Plasmodium</i> protein, unknown function	1.87	0.02	87.83

Data obtained from **PeptideShaker**, UniProt databases and the algorithms applied were X!Tandem, MS-GF+, MS Amanda, MyriMatch, Comet, Tide and OMSSA. Protein hits with a confidence of 100 are shown, confidence >99.9%. emPAI= Exponentially Modified Protein Abundance Index. MW=Molecular weight. A1=65kDa clofazimine treated W2, A2=65kDa untreated W2, A5=65kDa untreated 3D7, B1=40kDa clofazimine treated W2, B2=40kDa untreated W2, B5=40kDa untreated 3D7

Table 6.5 PeptideShaker (0.36.1) and UniProt database identification of proteins (Continued)

Sample	UniProt Accession Number	Protein Description	Sequence Coverage	emPAI	MW (kDa)
	Q8I485	Rhoptry-associated protein 3, RAP3	13.00	0.24	46.97
	Q8ILA1	Conserved <i>Plasmodium</i> protein, unknown function	5.04	0.07	112.34
	C0H4Y6	Protein disulfide-isomerase	14.29	0.20	55.48
	C0H5L9	Membrane associated histidine-rich protein, MAHRP-1	5.62	0.23	28.93
	Q8I0U8	Merozoite surface protein 1 precursor	11.05	0.19	195.60
	Q8I484	Rhoptry-associated protein 2, RAP2	18.59	0.32	46.71
	Q8IE67	Phosphoribosylpyrophosphate synthetase	11.44	0.12	49.35
	Q8IDH5	Thioredoxin-related protein, putative	5.77	0.08	23.97
	Q8I487	Skeleton-binding protein 1	2.67	0.12	36.28
B2	Q8IJN7	Enolase	3.59	0.04	48.65
	Q8I2X3	Glideosome-associated protein 50	4.04	0.06	44.58
	Q8I468	Ser/Arg-rich splicing factor, putative	3.57	0.03	37.68
	Q8IIV1	Histone H2B	8.55	0.10	13.12
	Q8IIR7	Endoplasmic reticulum-resident calcium binding protein	24.49	0.34	39.35
	Q8I4R5	Rhoptry neck protein 3, putative	0.45	0.01	262.99
	Q8I5I8	Glideosome-associated protein 45	19.12	0.29	23.62
	C0H4M0	Rifin-like protein (RAMA protein)	8.83	0.11	103.58
	Q8I0P6	Elongation factor 1-alpha	2.71	0.04	48.93
	Q8I206	<i>Plasmodium</i> exported protein (PHISTa), unknown function	2.80	0.02	49.71
B5	Q8I0U8	Merozoite surface protein 1 precursor	6.28	0.08	195.60

Data obtained from **PeptideShaker**, UniProt databases and the algorithms applied were X!Tandem, MS-GF+, MS Amanda, MyriMatch, Comet, Tide and OMSSA. Protein hits with a confidence of 100 are shown, confidence >99.9%.. emPAI= Exponentially Modified Protein Abundance Index. MW=Molecular weight. A1=65kDa clofazimine treated W2, A2=65kDa untreated W2, A5=65kDa untreated 3D7, B1=40kDa clofazimine treated W2, B2=40kDa untreated W2, B5=40kDa untreated 3D7

All proteins listed were identified at a confidence level of 100, except for the theoretical protein merozoite surface protein 1 (MSP1, Accession number Q8I0U8) in sample B5. Proteins identified were linked to metabolic pathways and functional groups with the help of PlasmoDB release 24 (<http://plasmodb.org/plasmo/>) and MPMP: Malaria Parasite Metabolic Pathways (<http://mpmp.huji.ac.il/>). Numerous “Conserved *Plasmodium* proteins” with unknown functions were identified from all samples.

Other functional pathways that were identified were those for chaperone assisted protein folding (e.g. Heat shock protein 70 (HSP70) homologue; HSP60, DNA-binding chaperone), metabolism of the apicoplast (e.g. Disulfide-isomerase), histone modification (e.g. Histone H2B), redox metabolism (e.g. Thioredoxin-related protein), and transcription and RNA metabolism (e.g. DNA-directed RNA polymerase; Serine/Arginine-rich splicing factor, putative). Interestingly, disulfide isomerase and skeleton-binding protein 1 identified in combination in sample B1 (clofazimine treated W2 parasites) have both been found to be involved in the formation of Maurer's clefts on the surface of infected erythrocytes (Kats *et al.*, 2015).

Exponentially Modified Protein Abundance Index (emPAI) scores are of interest in that it provides an implied label-free method of protein quantitation, in terms of spectral abundance (Neilson *et al.*, 2011). The emPAI scores obtained for protein hits were very low, due to the limited number of spectra that were positively matched to identified proteins.

The most abundant proteins were heat shock protein 20 (HSP70) homologue present only in clofazimine treated food vacuoles of W2 parasites (emPAI=0.25). Endoplasmic reticulum-resident calcium binding protein was present in both clofazimine treated (emPAI=0.28) and untreated food vacuoles of W2 parasites (emPAI=0.34), but was not detected in 3D7 controls. A number of proteins were identified that are not expected considering the mass ranges of the bands excised from the 1D SDS-PAGE gel, however *Pf*HSP70 and endoplasmic reticulum-resident calcium binding protein are sensible hits with molecular weights of 73.24 and 39.35 kDa respectively. In contrast to current findings, *Pf*HSP70 possibly plays a role in protein foldings and tends to be localised along the edges of the cytosol or in the nucleus of the parasite, and is not in the food vacuole (Pesce *et al.*, 2008).

Other abundant proteins included rho-try-associated proteins 2 and 3 (emPAI= 0.32 and 0.24, respectively; from untreated W2 parasites), membrane associated histidine-rich protein (emPAI=0.23, from untreated W2 parasites), and glideosome-associated protein 45 (emPAI=0.29). However, there are no evident shifts in the abundance of protein expression between 3D7 controls, W2 controls and clofazimine exposed parasites. All proteins identified suggest normal metabolic function and replication patterns within the parasite.

6.4 Discussion

It is of note that the bands excised for proteomic analysis (Samples A and D) are very close to bands where BSA (MW of 66.5 kDa) and haemoglobin (MW of 64 kDa for the tetramer and 16 kDa for each subunit) are expected to separate to during electrophoresis (Figure 6.3, B). Proteomic searches were performed on *Plasmodium* species and not on *Homo sapiens* or other mammalian species, as the aim was to detect the low abundance *Plasmodium* proteins expected to fall in those mass ranges also. It is likely that the majority of intense bands in these mass ranges are in fact BSA present in Albumax-II enriched culture medium and buffers used in wash steps in food vacuole isolation and/or haemoglobin from the infected erythrocytes. It must be reiterated from the methods, that final sample collection and washing was performed in PBS and collection of sample by filtration in a potassium chloride (KCl) buffer (140 mM KCl, 25 mM HEPES, 1 mM PMSF pH 7.2) both without BSA enrichment. The highest intensity band is visible in well 6, where W2 cellular debris is loaded, in the 50-75 kDa range. This is indicative that the majority of haemoglobin and BSA was removed from food vacuole samples of W2 strains during wash steps.

Some limitations to two-dimensional gel electrophoresis have been highlighted in this study and include low loading ability and poor representation and separation of hydrophobic proteins (Bunai & Yamane, 2005). This method also produces a lot of variation in bands with similar

preparation techniques. The latter two limitations have been the deciding factors for choosing 1D over 2D electrophoresis.

Another alternative to 2D gel electrophoresis that could have been implemented is the OFFGEL™ solution-based isoelectric focussing (IEF) and gel-eluted liquid fraction entrapment electrophoresis (GELFrEE) followed by mass spectrometry methods (Lee *et al.*, 2009; O'Cualain *et al.*, 2010). The GELFrEE method elutes intact proteins for top-down proteomics and is compatible with nanocapillary-LC-MS/MS. The IEF method exploits the migration of zwitterionic molecules in electric fields and allows solution-based focussing, but requires electrophoresis and in-gel trypsin digestion if GELFrEE methods are not implemented. GELFrEE offers decreased run-times over SDS-PAGE gels and are sensitive to low-mass proteomes and low abundance proteins, with reproducible results (Lee *et al.*, 2009).

No proteins previously linked to chloroquine or other antimalarial drug resistance in *Plasmodium* parasites were identified by the methods employed in this study. It is noteworthy how the change in analysis software, and proteomic databases allows for such great variability in protein identification as seen with sample A5 that initially yielded no protein hits (ProteinScope, SwissProt) but with reanalysis, showed many hits (PeptideShaker, UniProt) comparable to the other samples. It is possible that sample A5 was not exposed to adequate quantities of trypsin, or that trypsin did not have access the cleavage sites within the protein possibly due to enhanced folding caused by the presence of inappropriate quantities of detergents in solution (Zardeneta & Horowitz, 1994).

Given that bands of molecular weights between 45-65 kDa were excised, the majority of identified proteins were not expected to be present. The majority of the identified proteins are also not predicted to be localised in the food vacuole suggesting that the purification processes implemented in this study were inadequate. Further washing was however not practical as there was already a large sample loss from isolation at the beginning of analysis. The ability

to quantitate using label-free techniques was also an issue and this could be ascribed to the low concentrations of the peptides in the samples and this in turn could have been due to a number of possibilities. There was very little protein to start out with for the analysis, with at least two storage periods of the samples and there may have been sample loss due to degradation, poor stability or binding of the more lipophilic peptides to the storage tube surfaces. All these factors may result in a small protein loss but a potentially large accumulated sample loss when all taken into account.

Membrane proteins of the parasite food vacuole that were expected to be involved in drug resistance were not identified or quantified in this project, however other researchers have been able to identify them successfully by alternate methods. Immunofluorescence and immunoelectron microscopy techniques have been employed by Cowman *et al.* to establish that the *PfMDR1* protein is localized in the membrane of food vacuoles of late stage parasites (Cowman *et al.*, 1991). Gene studies encompassing the transfection of the *PfCRT* gene into plasmids and amoeba have been performed extensively, but not much research has been done to attempt the isolation and quantification of the *PfCRT* or *PfMDR* proteins from lab-adapted strains or field isolates of *Plasmodium falciparum* parasites (Papakrivos *et al.*, 2012). Therefore information on the expected relative abundance of these proteins is lacking.

From allelic analysis, it can be concluded that the relative abundance of the genes and gene transcripts coding for *PfCRT* is generally low with dynamic within-host variability in expression, independent of the drug-susceptibility profile of the *Plasmodium* strains (Gadalla *et al.*, 2010). Contrary to expectations Veiga *et al.* showed that *PfCRT* was less expressed in W2 compared to 3D7 clones with a 0.5 fold difference, suggesting that resistance is not dominantly inferred by expression and action of *PfCRT* on the food vacuole surface of these parasites (Veiga *et al.*, 2010).

It is possible that low abundance proteins were subjected to enzymatic cleavage, denaturation or loss of activity, not counteracted by the addition of PMSF or that this protease inhibitor, or alternately EDTA or E-64, should have been added at other timepoints in order to stabilise the solubilised membrane proteins (Yasui *et al.*, 2010). The fact that these proteins are multipass membrane proteins adds difficulty in terms of appropriate solubilisation, which may have been overcome by addition of alkylamines or polyamines, such as spermidine, which has been shown to enhance solubilisation of plant membrane proteins and animal Golgi-localized proteins (Yasui *et al.*, 2010).

Label-free quantification in proteomics offers a number of advantages, most-importantly is does not require expensive or tedious metabolic, chemical or enzymatic labelling procedures and it is compatible with a number of different work-flows (Arike & Peil, 2014). However, due to the nature of label-free proteomics, either standards or “house-keeper” proteins are required to be present (“spiked-in” or naturally occurring) in samples in order to draw a comparison in terms of relative abundance. Absolute quantification is possible with APEX, or Absolute Protein Expression levels based on learned correction factors and MS/MS spectral counts, but this required access to probability values of identifying the selected peptides (Lu *et al.*, 2007). The relative abundance of proteins is determined either by comparing the number of peptide sequences (Peak intensities) or spectra (counting or Total Ion Current- TIC) by which the proteins were identified. This method is made more subjective by the requirement for normalisation. The emPAI is an established method for estimation of protein abundance by performing peptide counts (Lasonder *et al.*, 2002).

In this project, the inconsistencies in protein quantities loaded per well, number of wells excised per band, and the absence of a common proteins across all samples subjected to MS/MS has made it seemingly impossible to draw an accurate comparison between the relative abundance of identified proteins in this study. Furthermore, the abundance of the

proteins that were identified is too low to draw reasonable conclusion based on Exponentially Modified Protein Abundance Index (emPAI) mass spectrometric scores of identified proteins.

6.5 Conclusion

A number of challenges have been identified in terms of the isolation, solubilisation and separation of multipass membrane proteins such as the non-selective drug efflux pump proteins (Bledi *et al.*, 2003). Each of these processes are essential for accurate identification of proteins embedded in membranes. Other hindrances to effective proteomic analysis of membranes proteins similar to *PfMDR1* and *PfCRT* are their inherent hydrophobicity in the transmembrane regions of their structures, and the general low abundance of these proteins in the membranes of parasites which are potentially already contaminated with host cell proteins that are present in higher concentrations.

The major shortcoming to the procedures implemented in the proteomic analysis performed here was the quantities of protein samples harvested and the isolation of these samples from the trophozoite food vacuole membranes in which they are postulated to reside. These methods have also not allowed for the detection of downregulation of resistance mediators in other locations of the parasite, or even resistance caused by point mutations instead of alterations in level of expression. An advantage of the approach taken in this study is the possibility of identifying proteins that to date have not been linked to resistance of *Plasmodium* parasites, however this is very dependent on which bands are excised from SDS-PAGE gels.

Future optimisation of the methods implemented in this study are essential in order to insure improved isolation and identification of proteins of interest, and to allow for reliable label-free quantification of these.

Concluding discussion

The reported spread of resistance to the current arsenal of antimalarials has the implication of severe loss of human life. There is hope on the horizon for a vaccine, however the sustained efficacy of this vaccine candidate over the long term (especially in adults and children over the age of two) still needs to be established before it is approved for the market (Agnandji *et al.*, 2012; Boes *et al.*, 2015). In parallel to the vaccine development, the Medicines for Malaria Venture (MVV) is collaborating with a number of research institutions in order to design new antimalarial drugs with enhanced efficacy and decreased costs for production. However, re-allocation of existing medicines indicated for other conditions, but with favourable antiplasmodial profiles is still more economical.

This research project set out to confirm whether clofazimine, an antimycobacterial agent forming part of the leprosy drug treatment, could reverse the susceptibility profile of resistant *Plasmodium* strains. It was postulated that if clofazimine could alter susceptibility of resistant *Plasmodium* strains to chloroquine, this effect was possibly elicited by down-regulation of membrane transporter proteins previously linked to efflux of antimalarials from food vacuoles or parasite parasitophorous vacuoles of *Plasmodium* trophozoite stages.

It has been established that clofazimine is able to selectively inhibit *P. falciparum* growth without harming mammalian cells, with a promising selectivity index (SI) comparable to that of DFMO (also known as eflornithine). DFMO is a medicine most commonly prescribed for other ailments, and it was originally approved for African sleeping sickness and hirsutism. More recently, DFMO has been shown to effectively inhibit polyamine synthesis in *Plasmodium* species and has been coined the “resurrecting drug” for its toxicity in late-stage, cerebral malaria (Birkholtz *et al.*, 2011; Wickware, 2002). In this study DFMO has been shown to slow the life cycle progression by halting some parasites’ development in the trophozoite stage of

the *Plasmodium* life-cycle, to some extent supporting previous findings that DFMO is cytostatic and not cytotoxic (Assaraf *et al.*, 1987b).

Clofazimine was shown to enhance the susceptibility to chloroquine in *P. falciparum* parasites showing resistance to chloroquine, however the proteomic analyses conducted in this study were unable to establish whether this was achieved through altering the expression or the activity of previously identified resistance proteins. A number of improvements in the methods used for isolation and purification of food vacuoles are required in order to increase the yield of food vacuole membrane proteins and to remove contaminating host cell components.

An evident shortcoming in the sample preparation for proteomic analyses was the inadequate amount of food vacuole proteins harvested. SDS-PAGE was conducted to separate food vacuole proteins for mass spectrometry. The pooling of excised bands from wells increased the variability of proteomics results, and decreased the comparability of protein abundance by label-free techniques. For future reference, possibly five times the quantities of starting cultures used in this project may be required. Methods established in the laboratories of Boyle *et al.* have been shown to drastically enhance the yield of isolated parasites by significantly decreasing culture haematocrits allowing parasitaemias to exceed well above the 8% norm for trophozoite stage parasites (Boyle *et al.*, 2010a; Boyle *et al.*, 2010b). Implementation of these or similar techniques could have enhanced the yield of magnetically harvested trophozoites, without significant increases in the cost or duration of culture. Enhanced sample yields could reduce the requirement for highly sensitive downstream analysis equipment and sample fractionation required for mass spectrometric analysis.

More traditional ways of detecting the levels of expression of known proteins could have yielded more favourable results. Western blotting could have been performed using anti-chloroquine resistance transporter antibodies available for purchase from a few biotechnology companies. Alternatively quantitative RT-PCR or microarrays could have been performed to

detect changes in transporter-encoding mRNA levels or changes in the transcriptome, respectively. However the last two methods would not indicate changes in protein expression levels solely in food vacuoles and their membranes.

More technical and biological repeats of the proteomic analysis employed is required in future studies to be conducted in order to demonstrate the reproducibility of results. These and further method optimisations may increase the intensity of bands, and possibly eliminate the need to identify protein hits by the costly protein sequencing route, as peptide mass fingerprinting may be adequate. Proteins that were identified from all samples were mostly linked to protein trafficking, invasion and motility which could indicate that even clofazimine exposed parasites were not terminally stressed and were still performing normal metabolic functions.

To improve the standard of the results obtained, validation of all findings is required. A number of the experimental findings were not validated by reputable methods. It would have been valuable to characterise the total carbohydrate content in fractions of humic and fulvic acid, and to establish the abundance of polar and non-polar entities to assess the solubility of these substances in culture medium, as discussed previously (Schepetkin *et al.*, 2003). Incorporation of this tests would have improved the reliability of the Malaria SYBR Green-1® Fluorescence assay results obtained for humic and fulvic substances screened.

Similarly testing for the linearity, detection limit and level of sequestration for parasitaemia values obtained by the use of SYBR Green-1® Fluorescent dye in antiplasmodial and life-cycle specificity screening could have been addressed, as proposed previously (Chorattanakawee *et al.*, 2013).

The most concerning lack of validation has been in the determination of food vacuole number isolated for proteomic analysis, as well as the characterisation of the purity and homogeneity of the food vacuole samples. Although disputable as to their value, techniques to quantify food

vacuoles, such as haemocytometric counting or suspension of food vacuoles in PBS, setting up a standard curve and determining vacuole concentration by spectrophotometer (Saliba *et al.*, 1998) could have been used. The purity and composition of food vacuole samples could have been determined by Western blotting, using Malaria Research and Reference Reagent Resource Center (MR4) antibodies and secondary antibodies coupled to horseradish peroxidase, as described previously (Lamarque *et al.*, 2008). These methods would have enabled improved uniformity in loading of protein samples onto SDS-PAGE gels, for more accurate conclusions to be drawn on the altered abundance of proteins of interest from spectral data.

Another aim of this study was to screen the antiplasmodial potential of humic acid and fulvic acid. These substances were shown to be poorly selective antimalarials, with limited efficacy in comparison to the standard treatment artemisinin, chloroquine and even DFMO. Furthermore, the concentrations of humic and fulvic acid substances found to possess antiplasmodial efficacy were observed to be above doses that are clinically acceptable and safe for administration to human patients. It can therefore be postulated that humic substances may elicit their anecdotal decrease in the probability to contract malaria by beneficially altering the immune response of exposed patients. Therefore further *in vivo* analyses may highlight other mechanisms by which these substances are active in a model-biological system.

Mevinolin was assessed for its antiplasmodial specificity, and low selectivity index (SI) values led to the conclusion that this drug exerts its toxic effect by a similar mechanism in mammalian and plasmodial cells; indicative of poor species specificity. Further research is required to establish whether the anecdotal claims of decreased probability of contracting malaria in patients treated with mevinolin and similar HMG-CoA reductase inhibitors is warranted. This can be concluded by research assessing whether the possible beneficial effect of these drugs are due to altered expression, structure and/or functionality of adhesion molecules on the surface membranes of *Plasmodium* infected erythrocytes.

In this research there was great variance observed in the susceptibility of the same *P. falciparum* parasite strains to antimalarial agents over a short period of time, resulting in ranges of effective inhibitory concentrations, which vary slightly from literature. A controversial finding from flow cytometric data hints that chloroquine resistant W2 strains may also have decreased susceptibility to artemisin. Yet, it would be of value to ascertain the degree of genomic shift, if any, which may occur in laboratory adapted strains of *P. falciparum in vitro*, possibly by Polymerase Chain Reaction (PCR) or Microarray experimentation. From further cytometric analysis to determine the life-cycle specificity of clofazimine, this drug was shown to possess similar efficacy to DFMO in decreasing the parasite load of W2 parasites after the same exposure time. Clofazimine did not halt DNA division and the life-cycle progression of *P. falciparum* parasites as seen with DFMO.

The most significant finding was the ability of clofazimine to enhance the apparent susceptibility of chloroquine resistant *P. falciparum* W2 strains to the actions of chloroquine. Overall this study's findings warrant further investigation to determine the exact mechanism by which clofazimine exerts its effects in combination with chloroquine. There is a possibility that clofazimine, or derivatives thereof, may be exploited as an adjunct to current antimalarial therapies to prevent active efflux of antimalarial substances. Due to the pharmacokinetic profile of clofazimine, and its excessive accumulation in tissues of patients treated clinically, it is not likely that clofazimine will be adopted for this function. Alternatively, further analysis of clofazimine could enhance our understanding of chloroquine sensitizers aiding in the design of drugs with improved resilience to the genetic variability of *Plasmodium* parasites to improve the longevity of our current antimalarial drug arsenal.

References

- Aditya NP, Vathsala PG, Vieira V, Murthy RSR, Souto EB, 2013. Advances in nanomedicines for malaria treatment. *Advances in Colloid and Interface Science* **201-202**, 1-17.
- Agnandji ST, Lell B, Fernandes JF, Abossolo BP, Methogo BGNO, Kabwende AL, Adegnikaa AA, Mordmüller B, Issifou S, Kreamsner PG, Sacarlal J, Aide P, Lanaspaa M, Apontee JJ, Machevo S, Acacio S, Buloo H, Sigauque B, Macete E, Alonso P, Abdulla S, Salim N, Minjaa R, Mpina M, Ahmed S, Ali AM, Mtoroo AT, Hamad AS, Mutani P, Tanner M, Tinto H, D'alessandro U, Sorghoo H, Valea I, Bihoun B, Guiraud I, Kaboré B, Sombié O, Guiguemdé RT, Ouédraogoo JB, Hamel MJ, Kariuki S, Oneko M, Odero C, Otieno K, Awino N, Mcmorrow M, Muturi-Kioi V, Laserson KF, Slutsker L, Otieno W, Otieno L, Otsyula N, Gondi S, Otieno A, Owira V, Oguk E, Odongoo G, Ben Woods J, Ogutuu B, Njugunaa P, Chilengi R, Akoo P, Keruboo C, Maingii C, Lang T, Olotuu A, Bejoo P, Marsh K, Mwambinguu G, Owusu-Agyeii S, Asante KP, Osei-Kwakyyee K, Boahen O, Dosoo D, Asante I, Adjei G, Kwara E, Chandramohan D, Greenwood B, Lusinguu J, Gesase S, Malabejaa A, Abdul O, Mahende C, Liheluka E, Malle L, Lemnge M, Theander TG, Drakeley C, Ansong D, Agbenyegaa T, Adjei S, Boateng HO, Rettig T, Bawaa J, Sylverken J, Sambian D, Sarfo A, Agyekum A, Martinson F, Hoffman I, Mvaloo T, Kamthunzii P, Nkomoo R, Tembo T, Tegha G, Tsidyya M, Kileembe J, Chawingaa C, Ballou WR, Cohen J, Guerra Y, Jongert E, Lapierree D, Leach A, Lievens M, Ofori-Anyinam O, Olivier A, Vekemans J, Carter T, Kaslow D, Leboulleux D, Loucq C, Radford A, Savarese B, Schellenberg D, Sillman M, Vansadia P, Mian-Mccarthy S, 2012. A phase 3 trial of RTS,S/AS01 malaria vaccine in African infants. *New England Journal of Medicine* **367**, 2284-2295.
- Allen RJW, Kirk K, 2010. *Plasmodium falciparum* culture: The benefits of shaking. *Molecular and Biochemical Parasitology* **169**, 63-65.
- Amazigo UV, Leak SGA, Zoure HGM, Njepuome N, Lusamba-Dikassa PS, 2012. Community-driven interventions can revolutionise control of neglected tropical diseases. *Trends in Parasitology* **28**, 231-238.
- Andrews KT, Fisher G, Skinner-Adams TS, 2014. Drug repurposing and human parasitic protozoan diseases. *International Journal for Parasitology: Drugs and Drug Resistance* **4**, 95-111.
- Arikee L, Peil L, 2014. Spectral Counting Label-Free Proteomics. In. *Methods in Molecular Biology*. 213-222. (1156.)
- Arnot DE, Ronander E, Bengtsson DC, 2011. The progression of the intra-erythrocytic cell cycle of *Plasmodium falciparum* and the role of the centriolar plaques in asynchronous mitotic division during schizogony. *International Journal for Parasitology* **41**, 71-80.
- Ashley EA, Dhordaa M, Fairhurst RM, Amaratungaa C, Lim P, Suon S, Sreng S, Anderson JM, Mao S, Sam B, Sopha C, Chuor CM, Nguon C, Sovannarothee S, Pukrittayakamee S, Jittamala P, Chotivanich K, Chutasmit K, Suchatsoonthorn C, Runcharoen R, Hien TT, Thuy-Nhien NT, Thanh NV, Phu NH, Htut Y, Han KT, Aye KH, Mokuoluu OA, Olaosebikaa RR, Folaranmii OO, Mayxay M, Khanthavong M, Hongvanthong B, Newton PN, Onyambokoo MA, Fanello CI, Tshefu AK, Mishra N, Valecha N, Phyo AP, Nosten F, Yi P, Tripuraa R, Borrmann S, Bashraheil M, Peshu J, Faiz MA, Ghose A, Hossain MA, Samad R, Rahman MR, Hasan MM, Islam A, Miotto O, Amato R, Macinnis B, Stalker J, Kwiatkowski DP, Bozdech Z, Jeeyapant A, Cheah PY, Sakulthaew T, Chalk J, Intharabut B, Silamut K, Lee SJ, Vihokhern B, Kunasol C, Imwong M, Tarning J, Taylor WJ, Yeung S, Woodrow CJ, Flegg JA, Das D, Smith J, Venkatesan M, Plowe CV, Stepniiewska K, Guerin PJ, Dondorpp AM, Day NP, White NJ, 2014. Spread of artemisinin resistance in *Plasmodium falciparum* malaria. *New England Journal of Medicine* **371**, 411-423.
- Assaraf YG, Abu-Elheiga L, Spira DT, Desser H, Bachrach U, 1987a. Effect of polyamine depletion on macromolecular synthesis of the malarial parasite, *Plasmodium falciparum*, cultured in human erythrocytes. *Biochemical Journal* **242**, 221-226.

- Assaraf YG, Golenser J, Spira DT, Messer G, Bachrach U, 1987b. Cytostatic effect of DL- α -difluoromethylornithine against *Plasmodium falciparum* and its reversal by diamines and spermidine. *Parasitology Research* **73**, 313-318.
- Assaraf YG, Kahana C, Spira DT, Bachrach U, 1988. *Plasmodium falciparum*: Purification, properties, and immunochemical study of ornithine decarboxylase, the key enzyme in polyamine biosynthesis. *Experimental Parasitology* **67**, 20-30.
- Avery VM, Bashyam S, Burrows JN, Duffy S, Papadatos G, Puthukkuti S, Sambandan Y, Singh S, Spangenberg T, Waterson D, Willis P, 2014. Screening and hit evaluation of a chemical library against blood-stage *Plasmodium falciparum*. *Malaria Journal* **13**.
- Azimzadeh O, Sow C, Gèze M, Nyalwidhe J, Florent I, 2010. *Plasmodium falciparum* PfA-M1 aminopeptidase is trafficked via the parasitophorous vacuole and marginally delivered to the food vacuole. *Malaria Journal* **9**, 189-189.
- Bannister LH, Hopkins JM, Fowler RE, Krishna S, Mitchell GH, 2000. A brief illustrated guide to the ultrastructure of *Plasmodium falciparum* asexual blood stages. *Parasitology Today* **16**, 427-433.
- Barteselli A, Casagrande M, Basilico N, Parapini S, Rusconi CM, Tonelli M, Boido V, Taramelli D, Sparatore F, Sparatore A, 2015. Clofazimine analogs with antileishmanial and antiplasmodial activity. *Bioorganic and Medicinal Chemistry* **23**, 55-65.
- Bartoloni A, Zammarchi L, 2012. Clinical aspects of uncomplicated and severe malaria. *Mediterranean Journal of Hematology and Infectious Diseases* **4**.
- Basco LK, De Pecoulas PE, Le Bras J, Wilson CM, 1996. *Plasmodium falciparum*: Molecular characterization of multidrug-resistant Cambodian isolates. *Experimental Parasitology* **82**, 97-103.
- Basco LK, Ringwald P, 1998. Molecular epidemiology of malaria in Yaounde, Cameroon II. Baseline frequency of point mutations in the dihydropteroate synthase gene of *Plasmodium falciparum*. *American Journal of Tropical Medicine and Hygiene* **58**, 374-377.
- Beckett R, Jue Z, Giddings JC, 1987. Determination of molecular weight distributions of fulvic and humic acids using flow field-flow fractionation. *Environmental Science & Technology* **21**, 289-295.
- Bell A, 2005. Antimalarial drug synergism and antagonism: Mechanistic and clinical significance. *FEMS Microbiology Letters* **253**, 171-184.
- Bennett TN, Paguio M, Gligorijevic B, Seudieu C, Kosar AD, Davidson E, Roepe PD, 2004. Novel, Rapid, and Inexpensive Cell-Based Quantification of Antimalarial Drug Efficacy. *Antimicrobial Agents and Chemotherapy* **48**, 1807-1810.
- Bhatia R, Rastogi RM, Ortega L, 2013. Malaria successes and challenges in Asia. *J Vector Borne Dis* **50**, 239-247.
- Bhattacharya A, Mishra LC, Bhasin VK, 2008. In vitro activity of artemisinin in combination with clotrimazole or heat-treated amphotericin B against *Plasmodium falciparum*. *American Journal of Tropical Medicine and Hygiene* **78**, 721-728.
- Bhowmick IP, Kumar N, Sharma S, Coppens I, Jarori GK, 2009. Immuno-gold electron microscopic (IEM) imaging for the localization of enolase in mid and late stage trophozoites of *P. falciparum*. In.: National Institute of Health.
- Birkholtz L-M, Williams M, Niemand J, Louw Abraham i, Persson L, Heby O, 2011. Polyamine homeostasis as a drug target in pathogenic protozoa: peculiarities and possibilities. *Biochemical Journal* **438**, 229-244.
- Bledi Y, Inberg A, Linial M, 2003. PROCEED: A proteomic method for analysing plasma membrane proteins in living mammalian cells. *Briefings in Functional Genomics and Proteomics* **2**, 254-265.
- Boechat N, Pinheiro LCS, Silva TS, Aguiar ACC, Carvalho AS, Bastos MM, Costa CCP, Pinheiro S, Pinto AC, Mendonça JS, Dutra KDB, Valverde AL, Santos-Filho OA, Ceravolo IP, Krettli AU, 2012.

- New trifluoromethyl triazolopyrimidines as anti-*Plasmodium falciparum* agents. *Molecules* **17**, 8285-8302.
- Boes A, Spiegel H, Voepel N, Edgue G, Beiss V, Kapelski S, Fendel R, Scheuermayer M, Pradel G, Bolscher JM, Behet MC, Dechering KJ, Hermsen CC, Sauerwein RW, Schillberg S, Reimann A, Fischer R, 2015. Analysis of a Multi-component Multi-stage Malaria Vaccine Candidate—Tackling the Cocktail Challenge. *PLoS ONE* **10**, e0131456.
- Boyle MJ, Richards JS, Gilson PR, Chai W, Beeson JG, 2010a. Interactions with heparin-like molecules during erythrocyte invasion by *Plasmodium falciparum* merozoites. *Blood* **115**, 4559-4568.
- Boyle MJ, Wilson DW, Richards JS, Riglar DT, Tetteh KKA, Conway DJ, Ralph SA, Baum J, Beeson JG, 2010b. Isolation of viable *Plasmodium falciparum* merozoites to define erythrocyte invasion events and advance vaccine and drug development. *Proceedings of the National Academy of Sciences of the United States of America* **107**, 14378-14383.
- Bunai K, Yamane K, 2005. Effectiveness and limitation of two-dimensional gel electrophoresis in bacterial membrane protein proteomics and perspectives. *Journal of Chromatography B: Analytical Technologies in the Biomedical and Life Sciences* **815**, 227-236.
- Burchmore RJS, Ogbunude POJ, Enanga B, Barrett MP, 2002. Chemotherapy of human African trypanosomiasis. *Current Pharmaceutical Design* **8**, 257-267.
- Butykai A, Orbán A, Kocsis V, Szaller D, Bordács S, Tátrai-Szekeres E, Kiss LF, Bóta A, Vértessy BG, Zelles T, Kézsmárki I, 2013. Malaria pigment crystals as magnetic micro-rotors: Key for high-sensitivity diagnosis. *Scientific Reports* **3**.
- Caminade C, Kovats S, Rocklov J, Tompkins AM, Morse AP, Colón-González FJ, Stenlund H, Martens P, Lloyd SJ, 2014. Impact of climate change on global malaria distribution. *Proceedings of the National Academy of Sciences* **111**, 3286-3291.
- Casares S, Brumeanu TD, Richie TL, 2010. The RTS,S malaria vaccine. *Vaccine* **28**, 4880-4894.
- Castellini MA, Buguliskis JS, Casta LJ, Butz CE, Clark AB, Kunkel TA, Taraschi TF, 2011. Malaria drug resistance is associated with defective DNA mismatch repair. *Molecular and Biochemical Parasitology* **177**, 143-147.
- Catron D, Lange Y, Borenztajn J, Sylvester MD, Jones BD, Haldar K, 2004. Salmonella enterica serovar typhimurium requires nonsterol precursors of the cholesterol biosynthetic pathway for intracellular proliferation. *Infection and Immunity* **72**, 1036-1031-1042.
- Chaorattanakawee S, Tyner SD, Lon C, Yingyuen K, Ruttvisutinunt W, Sundrakes S, Sai-Gnam P, Johnson JD, Walsh DS, Saunders DL, Lanteri CA, 2013. Direct comparison of the histidine-rich protein-2 enzyme-linked immunosorbent assay (HRP-2 ELISA) and malaria SYBR green i fluorescence (MSF) drug sensitivity tests in *Plasmodium falciparum* reference clones and fresh ex vivo field isolates from Cambodia. *Malaria Journal* **12**.
- Childs RA, Miao J, Gowda C, Cui L, 2013. An alternative protocol for *Plasmodium falciparum* culture synchronization and a new method for synchrony confirmation. *Malaria Journal* **12**.
- Cholo MC, Boshoff HI, Steel HC, Cockeran R, Matlola NM, Downing KJ, Mizrahi V, Anderson R, 2006. Effects of clofazimine on potassium uptake by a Trk-deletion mutant of Mycobacterium tuberculosis. *Journal of Antimicrobial Chemotherapy* **57**, 79-84.
- Cholo MC, Steel HC, Fourie PB, Gerimshuizen WA, Anderson R, 2012. Clofazimine: current status and future prospects. *The Journal of Antimicrobial Chemotherapy* **67**, 290-298.
- Clark K, Niemand J, Reeksting S, Smit S, Van Brummelen AC, Williams M, Louw AI, Birkholtz L, 2010. Functional consequences of perturbing polyamine metabolism in the malaria parasite, *Plasmodium falciparum*. *Amino Acids* **38**, 633-644.
- Cohuet A, Harris C, Robert V, Fontenille D, 2010. Evolutionary forces on Anopheles: what makes a malaria vector? *Trends in Parasitology* **26**, 130-136.
- Coppens I, Bastin P, Levade T, Courtot P, 1995. Activity, pharmacological inhibition and biological regulation of 3-hydroxy-3-methylglutarul coenzyme A reductase in Trypanosoma brucei. *Molecular and Biochemical Parasitology* **69**, 29-40.

- Couto AS, Kimura EA, Peres VJ, Uhrig ML, Katzin AM, 1999. Active isoprenoid pathway in the intra-erythrocytic stages of *Plasmodium falciparum*: presence of dolichols of 11 and 12 isoprene units. *Biochemical Journal* **341**, 629-637.
- Cowman AF, Crabb BS, 2006. Invasion of red blood cells by malaria parasites. *Cell* **124**, 755-766.
- Cowman AF, Karcz S, Galatis D, Culvenor JG, 1991. A P-glycoprotein homologue of *Plasmodium falciparum* is localized on the digestive vacuole. *Journal of Cell Biology* **113**, 1033-1042.
- Cowman AF, Morry MJ, Biggs BA, Cross GA, Foote SJ, 1988. Amino acid changes linked to pyrimethamine resistance in the dihydrofolate reductase-thymidylate synthase gene of *Plasmodium falciparum*. *Proceedings of the National Academy of Sciences of the United States of America* **85**, 9109-9113.
- Croft SL, 1999. Antiparasitic agents: Challenges of sleeping sickness, hopes for malaria. *Current Opinion in Infectious Diseases* **12**, 557-558.
- Cui L, Su X-Z, 2009. Discovery, mechanisms of action and combination therapy of artemisinin. *Expert Review of Anti-Infective Therapy* **7**, 999-1013.
- Cullen KA, Arguin PM, 2014. Malaria surveillance - United States, 2012. *MMWR Surveillance Summaries* **63**, 1-22.
- D'hulst A, Augustijns P, Arens S, Van Parijs L, Colson S, Verbeke N, Kinget R, 1996. Determination of Artesunate by Capillary Electrophoresis with Low UV Detection and Possible Applications to Analogues. *Journal of Chromatographic Science* **34**, 276-281.
- Dahl EL, Rosenthal PJ, 2008. Apicoplast translation, transcription and genome replication: targets for antimalarial antibiotics. *Trends in Parasitology* **24**, 279-284.
- Dame JB, Williams JL, Mccutchan TF, Weber JL, Wirtz RA, Hockmeyer WT, Lee Maloy W, David Haynes J, Schneider I, Roberts D, Sanders GS, Premkumar Reddy E, Diggs CL, Miller LH, 1984. Structure of the gene encoding the immunodominant surface antigen on the sporozoite of the human malaria parasite *Plasmodium falciparum*. *Science* **225**, 587-593.
- Das B, Gupta R, Madhubala R, 1995. Combined action of inhibitors of polyamine biosynthetic pathway with a known antimalarial drug chloroquine on *Plasmodium falciparum*. *Pharmacological Research* **31**, 189-193.
- Diggs C, Joseph K, Flemmings B, Snodgrass R, Hines F, 1975. Protein synthesis in vitro by cryopreserved *Plasmodium falciparum*. *American Journal of Tropical Medicine and Hygiene* **24**, 760-763.
- Dixon MWA, Dearnley MK, Hanssen E, Gilberger T, Tilley L, 2012. Shape-shifting gametocytes: How and why does *P. falciparum* go banana-shaped? *Trends in Parasitology* **28**, 471-478.
- Dragan AI, Pavlovic R, Mcgivney JB, Casas-Finet JR, Bishop ES, Strouse RJ, Schenerman MA, Geddes CD, 2012. SYBR Green I: Fluorescence properties and interaction with DNA. *Journal of Fluorescence* **22**, 1189-1199.
- Duraisingh MT, Cowman AF, 2005. Contribution of the pfmdr1 gene to antimalarial drug-resistance. *Acta Tropica* **94**, 181-190.
- Dwek RD, Kobrin LH, Grossman N, Ron EZ, 1980. Synchronization of cell division in microorganisms by Percoll gradients. *Journal of Bacteriology* **144**, 17-21.
- Egan TJ, Kaschula CH, 2007. Strategies to reverse drug resistance in malaria. *Current Opinion in Infectious Diseases* **20**, 598-604.
- Ehlgen F, Pham JS, De Koning-Ward T, Cowman AF, Ralph SA, 2012. Investigation of the *Plasmodium falciparum* food vacuole through inducible expression of the chloroquine resistance transporter (PfCRT). *PLoS ONE* **7**.
- Elsohly HN, Croom EM, El-Ferally FS, El-Sherei MM, 1990. A Large-Scale Extraction Technique of Artemisinin from *Artemisia annua*. *Journal of Natural Products* **53**, 1560-1564.
- Fidock DA, Nomura T, Talley AK, Cooper RA, Dzekunov SM, Ferdig MT, Ursos LMB, Bir Singh Sidhu A, Naudé B, Deitsch KW, Su XZ, Wootton JC, Roepe PD, Wellems TE, 2000. Mutations in the *P. falciparum* digestive vacuole transmembrane protein PfCRT and evidence for their role in chloroquine resistance. *Molecular Cell* **6**, 861-871.

- Fivelman QL, Adagu IS, Warhurst DC, 2004. Modified fixed-ratio isobologram method for studying in vitro interactions between atovaquone and proguanil or dihydroartemisinin against drug-resistant strains of *Plasmodium falciparum*. *Antimicrobial Agents and Chemotherapy* **48**, 4097-4102.
- Florens L, Washburn M, Muster N, Wolters D, Gardner M, Anthony R, Haynes D, Moch K, Sacci J, Witney A, Grainger N, Holder A, Wu Y, Yates Iii J, Carucci D. A proteomic view of the malaria parasite life cycle. *Proceedings of the Proceedings 50th ASMS Conference on Mass Spectrometry and Allied Topics, 2002*, 59-60.
- Francis SE, Sullivan Jr DJ, Goldberg DE, 1997. Hemoglobin metabolism in the malaria parasite *Plasmodium falciparum*. In. *Annual Review of Microbiology*. 97-123. (51.)
- Frevert U, Nacer A, 2014. Fatal cerebral malaria: A venous efflux problem. *Frontiers in Cellular and Infection Microbiology* **4**.
- Fukutomi Y, Maeda Y, Makino M, 2011. Apoptosis-inducing activity of clofazimine in macrophages. *Antimicrobial Agents and Chemotherapy* **55**, 4000-4005.
- Gadalla NB, Elzaki SE, Mukhtar E, Warhurst DC, El-Sayed B, Sutherland CJ, 2010. Dynamics of *pfprt* alleles CVMNK and CVIET in chloroquine-treated Sudanese patients infected with *Plasmodium falciparum*. *Malaria Journal* **9**, 74-74.
- Gandy JJ, Meeding JP, Snyman JR, Van Rensburg CEJ, 2012. Phase 1 clinical study of the acute and subacute safety and proof-of-concept efficacy of carbohydrate-derived fulvic acid. *Clinical Pharmacology: Advances and Applications* **4**, 7-11.
- Garner P, 2004. Artesunate combinations for treatment of malaria: Meta-analysis. *Lancet* **363**, 9-17.
- Gatton ML, Cheng Q, 2004. Modeling the development of acquired clinical immunity to *Plasmodium falciparum* malaria. *Infection and Immunity* **72**, 6538-6545.
- Gerald N, Mahajan B, Kumar S, 2011. Mitosis in the human malaria parasite *Plasmodium falciparum*. *Eukaryotic Cell* **10**, 474-482.
- Gething PW, Patil AP, Smith DL, Guerra CA, Elyazar IRF, Johnston GL, Tatem AJ, Hay SI, 2011. A new world malaria map: *Plasmodium falciparum* endemicity in 2010. *Malaria Journal* **10**.
- Gold JC, Phillips MC, 1990. Effects of membrane lipid composition on the kinetics of cholesterol exchange between lipoproteins and different species of red blood cells. *BBA - Biomembranes* **1027**, 85-92.
- Goldberg DE, Slater AFG, Beavis R, Chait B, Cerami A, Henderson GB, 1991. Hemoglobin degradation in the human malaria pathogen *Plasmodium falciparum*: A catabolic pathway initiated by a specific aspartic protease. *Journal of Experimental Medicine* **173**, 961-969.
- Goldstein JL, Brown MS, 1990. Regulation of the mevalonate pathway. *Nature* **343**, 425-430.
- Goldstein JL, Brown MS, Anderson RG, Russell DW, Schneider WJ, 1985. Receptor-mediated endocytosis: concepts emerging from the LDL receptor system. *Annual review of cell biology* **1**, 1-39.
- González R, Ataíde R, Naniche D, Menéndez C, Mayor A, 2012. HIV and malaria interactions: Where do we stand? *Expert Review of Anti-Infective Therapy* **10**, 153-165.
- Gottlieb MH, 1980. Rates of cholesterol exchange between human erythrocytes and plasma lipoproteins. *Biochimica et Biophysica Acta* **600**, 530-541.
- Grellier P, Valentin A, Millerieux V, Schrevel J, Rigomier D, 1994. 3-Hydroxy-3-methylglutaryl coenzyme A reductase inhibitors lovastatin and simvastatin inhibit in vitro development of *Plasmodium falciparum* and *Babesia divergens* in human erythrocytes. *Antimicrobial Agents and Chemotherapy* **38**, 1144-1148.
- Gross AS, Heuer B, Eichelbaum M, 1988. Stereoselective protein binding of verapamil enantiomers. *Biochemical Pharmacology* **37**, 4623-4627.
- Hanssen E, Mcmillan PJ, Tilley L, 2010. Cellular architecture of *Plasmodium falciparum*-infected erythrocytes. *International Journal for Parasitology* **40**, 1127-1135.
- Hastings RC, Jacobson RR, Trautman JR, 1976. Long term clinical toxicity studies with clofazimine (B663) in leprosy. *International Journal of Leprosy* **44**, 287-293.

- Hayward R, Saliba KJ, Kirk K, 2005a. Mutations in *pfmdr1* modulate the sensitivity of *Plasmodium falciparum* to the intrinsic antiplasmodial activity of verapamil. *Antimicrobial Agents and Chemotherapy* **49**, 840-842.
- Hayward R, Saliba KJ, Kirk K, 2005b. *pfmdr1* mutations associated with chloroquine resistance incur a fitness cost in *Plasmodium falciparum*. *Molecular Microbiology* **55**, 1285-1295.
- Hikosaka K, Hirai M, Komatsuya K, Ono Y, Kita K, 2015. Lactate retards the development of erythrocytic stages of the human malaria parasite *Plasmodium falciparum*. *Parasitology International* **64**, 301-303.
- Ishihama Y, Oda Y, Tabata T, Sato T, Nagasu T, Rappsilber J, Mann M, 2005. Exponentially modified protein abundance index (emPAI) for estimation of absolute protein amount in proteomics by the number of sequenced peptides per protein. *Molecular and Cellular Proteomics* **4**, 1265-1272.
- Izumiyama S, Omura M, Takasaki T, Ohmae H, Asahi H, 2009. *Plasmodium falciparum*: Development and validation of a measure of intraerythrocytic growth using SYBR Green I in a flow cytometer. *Experimental Parasitology* **121**, 144-150.
- Kapishnikov S, Weiner A, Shimoni E, Schneider G, Elbaum M, Leiserowitz L, 2013. Digestive Vacuole Membrane in *Plasmodium falciparum*-Infected Erythrocytes: Relevance to Templated Nucleation of Hemozoin. *Langmuir* **29**, 14595-14602.
- Kats LM, Proellocks NI, Buckingham DW, Blanc L, Hale J, Guo X, Pei X, Herrmann S, Hanssen EG, Coppel RL, Mohandas N, An X, Cooke BM, 2015. Interactions between *Plasmodium falciparum* skeleton-binding protein 1 and the membrane skeleton of malaria-infected red blood cells. *Biochimica et Biophysica Acta - Biomembranes* **1848**, 1619-1628.
- Killeen GF, Seyoum A, Sikaala C, Zomboko AS, Gimnig JE, Govella NJ, White MT, 2013. Eliminating malaria vectors. *Parasites and Vectors* **6**.
- Koval AV, Vlasov P, Shichkova P, Khunderyakova S, Markov Y, Panchenko J, Volodina A, Kondrashov FA, Katanaev VL, 2014. Anti-leprosy drug clofazimine inhibits growth of triple-negative breast cancer cells via inhibition of canonical Wnt signaling. *Biochemical Pharmacology* **87**, 571-578.
- Kreidenweiss A, Kreamsner PG, Mordmüller B, 2008. Comprehensive study of proteasome inhibitors against *Plasmodium falciparum* laboratory strains and field isolates from Gabon. *Malaria Journal* **7**.
- Labaied M, Jayabalasingham B, Bano N, Cha S-J, Sandoval J, Guan G, Coppens I, 2011. *Plasmodium* salvages cholesterol internalized by LDL and synthesized de novo in the liver. *Cellular Microbiology* **13**, 569-586.
- Lamarque M, Tastet C, Poncet J, Demette E, Jouin P, Vial H, Dubremetz JF, 2008. Food vacuole proteome of the malarial parasite *Plasmodium falciparum*. *Proteomics - Clinical Applications* **2**, 1361-1374.
- Lambros C, Vanderberg JP, 1979. Synchronization of *Plasmodium falciparum* erythrocytic stages in culture. *Journal of Parasitology* **65**, 418-420.
- Lasonder E, Ishihama Y, Andersen JS, Vermunt AMW, Pain A, Sauerwein RW, Eling WMC, Hall N, Waters AP, Stunnenberg HG, Mann M, 2002. Analysis of the *Plasmodium falciparum* proteome by high-accuracy mass spectrometry. *Nature* **419**, 537-542.
- Laveran CL, 1982. Classics in infectious diseases: A newly discovered parasite in the blood of patients suffering from malaria. Parasitic etiology of attacks of malaria: Charles Louis Alphonse Laveran (1845-1922). *Reviews of Infectious Diseases* **4**, 908-911.
- Le Port A, Watier L, Cottrell G, Ouédraogo S, Dechavanne C, Pierrat C, Rachas A, Bouscaillou J, Bouraima A, Massougbdji A, Fayomi B, Thiébaud A, Chandre F, Migot-Nabias F, Martin-Prevel Y, Garcia A, Cot M, 2011. Infections in infants during the first 12 months of life: Role of placental malaria and environmental factors. *PLoS ONE* **6**.
- Lee J, Kellie J, Tran J, Tipton J, Catherman A, Thomas H, Ahlf D, Durbin K, Vellaichamy A, Ntai I, Marshall A, Kelleher N, 2009. A robust two-dimensional separation for top-down tandem

- mass spectrometry of the low-mass proteome. *Journal of the American Society for Mass Spectrometry* **20**, 2183-2191.
- Lemieux JE, Gomez-Escobar N, Feller A, Carret C, Amambua-Ngwa A, Pinches R, Day F, Kyes SA, Conway DJ, Holmes CC, Newbold CI, 2009. Statistical estimation of cell-cycle progression and lineage commitment in *Plasmodium falciparum* reveals a homogeneous pattern of transcription in ex vivo culture. *Proceedings of the National Academy of Sciences of the United States of America* **106**, 7559-7564.
- Life-Cycle of the Malaria Parasite, 2011. In.: National Institute of Health.
- Lu P, Vogel C, Wang R, Yao X, Marcotte EM, 2007. Absolute protein expression profiling estimates the relative contributions of transcriptional and translational regulation. *Nature Biotechnology* **25**, 117-124.
- Macchi G, 1999. Camillo Golgi: A clinical pathologist. *Journal of the History of the Neurosciences* **8**, 141-150.
- Maeno Y, Toyoshima T, Fujioka H, Ito Y, Meshnick SR, Benakis A, Milhous WK, Aikawa M, 1993. Morphologic effects of artemisinin in *Plasmodium falciparum*. *American Journal of Tropical Medicine and Hygiene* **49**, 485-491.
- Makgatho ME, Anderson R, O'sullivan JF, Egan TJ, Freese JA, Cornelius N, 2000. Tetramethylpiperidine-substituted phenazines as novel anti-plasmodial agents. *Drug development research* **50**, 195-202.
- Manning L, Laman M, Davis WA, Davis TME, 2014. Clinical features and outcome in children with severe *Plasmodium falciparum* malaria: A meta-analysis. *PLoS ONE* **9**.
- Martin RE, Kirk K, 2004. The Malaria Parasite's Chloroquine Resistance Transporter is a Member of the Drug/Metabolite Transporter Superfamily. *Molecular Biology and Evolution* **21**, 1938-1949.
- Martin RE, Marchetti RV, Cowan AI, Howitt SM, Bröer S, Kirk K, 2009. Chloroquine transport via the malaria parasite's chloroquine resistance transporter. *Science* **325**, 1680-1682.
- Matthews H, Usman-Idris M, Khan F, Read M, Nirmalan N, 2013. Drug repositioning as a route to anti-malarial drug discovery: Preliminary investigation of the in vitro anti-malarial efficacy of emetine dihydrochloride hydrate. *Malaria Journal* **12**.
- Mauritz JMA, Esposito A, Ginsburg H, Kaminski CF, Tiffert T, Lew VL, 2009. The Homeostasis of *Plasmodium falciparum*-Infected Red Blood Cells. *PLoS Computational Biology* **5**.
- Miao J, Wang Z, Liu M, Parker D, Li X, Chen X, Cui L, 2013. *Plasmodium falciparum*: Generation of pure gametocyte culture by heparin treatment. *Experimental Parasitology* **135**, 541-545.
- Mita T, Tanabe K, 2012. Evolution of *Plasmodium falciparum* drug resistance: Implications for the development and containment of artemisinin resistance. *Japanese Journal of Infectious Diseases* **65**, 465-475.
- Mok S, Imwong M, Mackinnon MJ, Sim J, Ramadoss R, Yi P, Mayxay M, Chotivanich K, Liong KY, Russell B, Socheat D, Newton PN, Day NPJ, White NJ, Preiser PR, Nosten F, Dondorp AM, Bozdech Z, 2011. Artemisinin resistance in *Plasmodium falciparum* is associated with an altered temporal pattern of transcription. *BMC Genomics* **12**.
- Montalvetti A, Pana-Diaz J, Hurtado R, Ruiz-Perez LM, Gonzalez-Pacanowska D, 2000. Characterization and regulation of Leishmania major 3-hydroxy-methyl-glutaryl-CoA reductase. *Biochemistry Journal* **349**, 27-34.
- Moya-Alvarez V, Abellana R, Cot M, 2014. Pregnancy-associated malaria and malaria in infants: An old problem with present consequences. *Malaria Journal* **13**.
- Mutuku FM, King CH, Mungai P, Mbogo C, Mwangangi J, Muchiri EM, Walker ED, Kitron U, 2011. Impact of insecticide-treated bed nets on malaria transmission indices on the south coast of Kenya. *Malaria Journal* **10**.
- Mwangoka G, Ogutu B, Msambichaka B, Mzee T, Salim N, Kafuruki S, Mpina M, Shekalaghe S, Tanner M, Abdulla S, 2013. Experience and challenges from clinical trials with malaria vaccines in Africa. *Malaria Journal* **12**.

- Neilson KA, Ali NA, Muralidharan S, Mirzaei M, Mariani M, Assadourian G, Lee A, Van Sluyter SC, Haynes PA, 2011. Less label, more free: Approaches in label-free quantitative mass spectrometry. *Proteomics* **11**, 535-553.
- Niemand J, Burger P, Verlinden BK, Reader J, Joubert AM, Kaiser A, Louw AI, Kirk K, Phanstiel IV O, Birkholtz LM, 2013. Anthracene-polyamine conjugates inhibit in vitro proliferation of intraerythrocytic *Plasmodium falciparum* parasites. *Antimicrobial Agents and Chemotherapy* **57**, 2874-2877.
- Noor AM, Kinyoki DK, Mundia CW, Kabaria CW, Mutua JW, Alegana VA, Fall IS, Snow RW, 2014. The changing risk of *Plasmodium falciparum* malaria infection in Africa: 2000-10: A spatial and temporal analysis of transmission intensity. *The Lancet* **383**, 1739-1747.
- O'cualain R, Hyde J, Sims P, 2010. A protein-centric approach for the identification of folate enzymes from the malarial parasite, *Plasmodium falciparum*, using OFFGEL™ solution-based isoelectric focussing and mass spectrometry. *Malaria Journal* **9**, 1-12.
- Olliaro P, 1998. Safety of artemisinin and its derivatives a review of published and unpublished clinical trials. *Medecine Tropicale* **58**, 50-53.
- Omosun YO, Adoro S, Anumudu CI, Odaibo AB, Uthiapibull C, Holder AA, Nwagwu M, Nwuba RI, 2009. Antibody specificities of children living in a malaria endemic area to inhibitory and blocking epitopes on MSP-119 of *Plasmodium falciparum*. *Acta Tropica* **109**, 208-212.
- Papakrivos J, Sá JM, Wellem TE, 2012. Functional characterization of the *Plasmodium falciparum* chloroquine-resistance transporter (PfCRT) in transformed Dictyostelium discoideum vesicles. *PLoS ONE* **7**.
- Partnership Clinical Trials R.T.S./S., 2015. Efficacy and safety of RTS,S/AS01 malaria vaccine with or without a booster dose in infants and children in Africa: final results of a phase 3, individually randomised, controlled trial. *The Lancet* **386**, 31-45.
- Penny MA, Galactionova K, Tarantino M, Tanner M, Smith TA, 2015. The public health impact of malaria vaccine RTS,S in malaria endemic Africa: Country-specific predictions using 18 month follow-up Phase III data and simulation models. *BMC Medicine* **13**.
- Pesce ER, Acharya P, Tatu U, Nicoll WS, Shonhai A, Hoppe HC, Blatch GL, 2008. The *Plasmodium falciparum* heat shock protein 40, Pfj4, associates with heat shock protein 70 and shows similar heat induction and localisation patterns. *International Journal of Biochemistry and Cell Biology* **40**, 2914-2926.
- Peters PJ, Thigpen MC, Parise ME, Newman RD, 2007. Safety and toxicity of sulfadoxine/pyrimethamine: Implications for malaria prevention in pregnancy using intermittent preventive treatment. *Drug Safety* **30**, 481-501.
- Pradel G, Schlitzer M, 2010. Antibiotics in malaria therapy and their effect on the parasite apicoplast. *Current Molecular Medicine* **10**, 335-349.
- Pradines B, Torrentino-Madamet M, Fontaine A, Henry M, Baret E, Mosnier J, 2007. Atorvastatin is 10-fold more active in vitro than other statins against *Plasmodium falciparum*. *Antimicrobial Agents and Chemotherapy* **51**, 2654-2655.
- Raj DK, Mu J, Jiang H, Kabat J, Singh S, Sullivan M, Fay MP, Mccutchan TF, Su XZ, 2009. Disruption of a *Plasmodium falciparum* multidrug resistance-associated protein (PfMRP) alters its fitness and transport of antimalarial drugs and glutathione. *Journal of Biological Chemistry* **284**, 7687-7696.
- Raman J, Mauff K, Muianga P, Mussa A, Maharaj R, Barnes KI, 2011. Five years of antimalarial resistance marker surveillance in Gaza Province, Mozambique, following artemisinin-based combination therapy roll out. *PLoS ONE* **6**.
- Rappsilber J, Ishihama Y, Mann M, 2003. Stop And Go Extraction tips for matrix-assisted laser desorption/ionization, nanoelectrospray, and LC/MS sample pretreatment in proteomics. *Analytical Chemistry* **75**, 663-670.

- Reddy MR, Overgaard HJ, Abaga S, Reddy VP, Caccone A, Kiszewski AE, Slotman MA, 2011. Outdoor host seeking behaviour of *Anopheles gambiae* mosquitoes following initiation of malaria vector control on Bioko Island, Equatorial Guinea. *Malaria Journal* **10**.
- Reed MB, Sallba KJ, Caruana SR, Kirk K, Cowman AF, 2000. Pgh1 modulates sensitivity and resistance to multiple antimalarials in *Plasmodium falciparum*. *Nature* **403**, 906-909.
- Reis PA, Estato V, Da Silva TI, D'avila JC, Siqueira LD, Assis EF, Bozza PT, Bozza FA, Tibiriça EV, Zimmerman GA, Castro-Faria-Neto HC, 2012. Statins Decrease Neuroinflammation and Prevent Cognitive Impairment after Cerebral Malaria. *PLoS Pathogens* **8**.
- Ribaut C, Berry A, Chevalley S, Reybier K, Morlais I, Parzy D, Nepveu F, Benoit-Vical F, Valentin A, 2008. Concentration and purification by magnetic separation of the erythrocytic stages of all human *Plasmodium* species. *Malaria Journal* **7**.
- Rohrbach P, Sanchez CP, Hayton K, Friedrich O, Patel J, Sidhu ABS, Ferdig MT, Fidock DA, Lanzer M, 2006. Genetic linkage of *pfmdr1* with food vacuolar solute import in *Plasmodium falciparum*. *The EMBO Journal* **25**, 3000-3011.
- Rosenfeld J, Capdevielle J, Guillemot JC, Ferrara P, 1992. In-gel digestion of proteins for internal sequence analysis after one- or two-dimensional gel electrophoresis. *Analytical Biochemistry* **203**, 173-179.
- Rubinstein LV, Shoemaker RH, Paull KD, Simon RM, Tosini S, Skehan P, Scudiero DA, Monks A, Boyd MR, 1990. Comparison of in vitro anticancer-drug-screening data generated with a tetrazolium assay versus a protein assay against a diverse panel of human tumor cell lines. *Journal of the National Cancer Institute* **82**, 1113-1118.
- Sa JM, Twu O, 2010. Protecting the malaria drug arsenal: Halting the rise and spread of amodiaquine resistance by monitoring the PfCRT SVMNT type. *Malaria Journal* **9**.
- Saliba KJ, Folb PI, Smith PJ, 1998. Role for the *Plasmodium falciparum* digestive vacuole in chloroquine resistance. *Biochemical Pharmacology* **56**, 313-320.
- Saliba KJ, Lehane AM, Kirk K, 2008. A polymorphic drug pump in the malaria parasite. *Molecular Microbiology* **70**, 775-779.
- Scheibel LW, Ashton SH, Trager W, 1979. *Plasmodium falciparum*: Microaerophilic requirements in human red blood cells. *Experimental Parasitology* **47**, 410-418.
- Schepetkin IA, Khlebnikov AI, Ah SY, Woo SB, Jeong CS, Klubachuk ON, Kwon BS, 2003. Characterization and biological activities of humic substances from mumie. *Journal of Agricultural and Food Chemistry* **51**, 5245-5254.
- Schick BP, Schick PK, 1985. Cholesterol exchange in platelets, erythrocytes and megakaryocytes. *Biochimica et Biophysica Acta (BBA)/Lipids and Lipid Metabolism* **833**, 281-290.
- Schuster FL, 2002. Cultivation of plasmodium spp. *Clinical Microbiology Reviews* **15**, 355-364.
- Seder RA, Chang LJ, Enama ME, Zephir KL, Sarwar UN, Gordon IJ, Holman LA, James ER, Billingsley PF, Gunasekera A, Richman A, Chakravarty S, Manoj A, Velmurugan S, Li M, Ruben AJ, Li T, Eappen AG, Stafford RE, Plummer SH, Hendel CS, Novik L, Costner PJM, Mendoza FH, Saunders JG, Nason MC, Richardson JH, Murphy J, Davidson SA, Richie TL, Sedegah M, Sutamihardja A, Fahle GA, Lyke KE, Laurens MB, Roederer M, Tewari K, Epstein JE, Sim BKL, Ledgerwood JE, Graham BS, Hoffman SL, 2013. Protection against malaria by intravenous immunization with a nonreplicating sporozoite vaccine. *Science* **341**, 1359-1365.
- Sharma A, Radha Kishan KV, 2011. Serine protease inhibitor mediated peptide bond re-synthesis in diverse protein molecules. *FEBS Letters* **585**, 3465-3470.
- Sherry L, Jose A, Murray C, Williams C, Jones B, Millington O, Bagg J, Ramage G, 2012. Carbohydrate derived fulvic acid: An in vitro investigation of a novel membrane active antiseptic agent against *Candida albicans* biofilms. *Frontiers in Microbiology* **3**.
- Singh B, Daneshvar C, 2013. Human infections and detection of *Plasmodium knowlesi*. *Clinical Microbiology Reviews* **26**, 165-184.
- Singh G, Sehgal R, 2010. Transfusion-transmitted parasitic infections. *Asian Journal of Transfusion Science* **4**, 73-77.

- Singh Sidhu AB, Verdier-Pinard D, Fidock DA, 2002. Chloroquine resistance in *Plasmodium falciparum* malaria parasites conferred by *pfcr*t mutations. *Science* **298**, 210-213.
- Smilkstein M, Sriwilaijaroen N, Kelly JX, Wilairat P, Riscoe M, 2004. Simple and Inexpensive Fluorescence-Based Technique for High-Throughput Antimalarial Drug Screening. *Antimicrobial Agents and Chemotherapy* **48**, 1803-1806.
- Smith PK, Krohn RI, Hermanson GT, Mallia AK, Gartner FH, Provenzano MD, Fujimoto EK, Goeke NM, Olson BJ, Klenk DC, 1985. Measurement of protein using bicinchoninic acid. *Analytical Biochemistry* **150**, 76-85.
- Smith PW, Diagana TT, Yeung BKS, 2014. Progressing the global antimalarial portfolio: Finding drugs which target multiple *Plasmodium* life stages. *Parasitology* **141**, 66-76.
- Spengler B, Kirsch D, Kaufmann R, Karas M, Hillenkamp F, Giessmann U, 1990. The Detection of Large Molecules in Matrix-Assisted UV-Laser Desorption. *Rapid Communications in Mass Spectrometry*, 301-305.
- Sullivan Jr DJ, Gluzman IY, Russell DG, Goldberg DE, 1996. On the molecular mechanism of chloroquine's antimalarial action. *Proceedings of the National Academy of Sciences of the United States of America* **93**, 11865-11870.
- Taoufiq Z, Pino P, N'dilimabaka N, Arrouss I, Assi S, Soubrier F, Rebollo A, Mazier D, 2011. Atorvastatin prevents *Plasmodium falciparum* cytoadherence and endothelial damage. *Malaria Journal* **10**.
- Tokumasu F, Crivat G, Ackerman H, Hwang J, Wellems TE, 2014. Inward cholesterol gradient of the membrane system in *P. falciparum*-infected erythrocytes involves a dilution effect from parasite-produced lipids. *Biology Open* **3**, 529-541.
- Trager W, Jensen JB, 1976. Human malaria parasites in continuous culture. *Journal of Parasitology* **91**, 484-486.
- Tuteja R, 2007. Malaria - An overview. *FEBS Journal* **274**, 4670-4679.
- Valderramos SG, Fidock DA, 2006. Transporters involved in resistance to antimalarial drugs. *Trends in Pharmacological Sciences* **27**, 594-601.
- Van Rensburg CEJ, Jooné G, Anderson R, 1998. α -Tocopherol antagonizes the multidrug-resistance-reversal activity of cyclosporin A, verapamil, GF120918, clofazimine and B669. *Cancer Letters* **127**, 107-112.
- Van Schalkwyk DA, Priebe W, Saliba KJ, 2008. The inhibitory effect of 2-halo derivatives of D-glucose on glycolysis and on the proliferation of the human malaria parasite *Plasmodium falciparum*. *Journal of Pharmacology and Experimental Therapeutics* **327**, 511-517.
- Van Schalkwyk DA, Walden JC, Smith PJ, 2001. Reversal of chloroquine resistance in *Plasmodium falciparum* using combinations of chemosensitizers. *Antimicrobial Agents and Chemotherapy* **45**, 3171-3174.
- Vaudel M, Barsnes H, Berven FS, Sickmann A, Martens L, 2011. SearchGUI: An open-source graphical user interface for simultaneous OMSSA and X!Tandem searches. *Proteomics* **11**, 996-999.
- Vaudel M, Burkhart JM, Zahedi RP, Oveland E, Berven FS, Sickmann A, Martens L, Barsnes H, 2015. PeptideShaker enables reanalysis of MS-derived proteomics data sets: To the editor. *Nature Biotechnology* **33**, 22-24.
- Veiga MI, Ferreira PE, Jörnham L, Malmberg M, Kone A, Schmidt BA, Petzold M, Björkman A, Nosten F, Gil JP, 2011. Novel polymorphisms in *Plasmodium falciparum* ABC transporter genes are associated with major ACT Antimalarial drug resistance. *PLoS ONE* **6**.
- Veiga MI, Ferreira PE, Schmidt BA, Ribacke U, Björkman A, Tichopad A, Gil JP, 2010. Antimalarial exposure delays *Plasmodium falciparum* intra-erythrocytic cycle and drives drug transporter genes expression. *PLoS ONE* **5**, e12408.
- Verlinden BK, Niemand J, Snyman J, Sharma SK, Beattie RJ, Woster PM, Birkholtz LM, 2011. Discovery of novel alkylated (bis)urea and (bis)thiourea polyamine analogues with potent antimalarial activities. *Journal of Medicinal Chemistry* **54**, 6624-6633.

- Visser BJ, Van Vugt M, Grobusch MP, 2014. Malaria: An update on current chemotherapy. *Expert Opinion on Pharmacotherapy* **15**, 2219-2254.
- Wang P, Nirmalan N, Wang Q, Sims PFG, Hyde JE, 2004. Genetic and metabolic analysis of folate salvage in the human malaria parasite *Plasmodium falciparum*. *Molecular and Biochemical Parasitology* **135**, 77-87.
- Wang P, Read M, Sims PFG, Hyde JE, 1997. Sulfadoxine resistance in the human malaria parasite *Plasmodium falciparum* is determined by mutations in dihydropteroate synthetase and an additional factor associated with folate utilization. *Molecular Microbiology* **23**, 979-986.
- Wells TNC, Van Huijsduijnen RH, Van Voorhis WC, 2015. Malaria medicines: A glass half full? *Nature Reviews Drug Discovery* **14**, 424-442.
- Wickware P, 2002. Resurrecting the resurrection drug. *Nat Med* **8**, 908-909.
- Wilby KJ, Lau TTY, Gilchrist SE, Ensom MHH, 2012. Mosquirix (RTS,S): A novel vaccine for the prevention of *Plasmodium falciparum* malaria. *Annals of Pharmacotherapy* **46**, 384-393.
- Wilson DW, Langer C, Goodman CD, Mcfadden GI, Beeson JG, 2013. Defining the timing of action of antimalarial drugs against *Plasmodium falciparum*. *Antimicrobial Agents and Chemotherapy* **57**, 1455-1467.
- World Health Organisation, 2015. Malaria Vaccine Rainbow Tables. In.: Health Organisation World
- World Health Organization, 2013. World malaria report 2013. In: Organization WH, ed. Geneva, Switzerland: World Health Organization.
- Yadav IC, Devi NL, Syed JH, Cheng Z, Li J, Zhang G, Jones KC, 2015. Current status of persistent organic pesticides residues in air, water, and soil, and their possible effect on neighboring countries: A comprehensive review of India. *Science of the Total Environment* **511**, 123-137.
- Yaeger RG, 1996. Protozoa: Structure, Classification, Growth, and Development In: Baron S, ed. *Medical Microbiology*. University of Texas Medical Branch: Galveston (TX).
- Yaro A, 2009. Mechanisms of sulfadoxine pyrimethamine resistance and health implication in *Plasmodium falciparum* malaria: A mini review. *Annals of Tropical Medicine and Public Health* **2**, 20-23.
- Yasui K, Uegaki M, Shiraki K, Ishimizu T, 2010. Enhanced solubilization of membrane proteins by alkylamines and polyamines. *Protein Science : A Publication of the Protein Society* **19**, 486-493.
- Yeagle PL, 1985. Cholesterol and the cell membrane. *BBA - Reviews on Biomembranes* **822**, 267-287.
- Zardeneta G, Horowitz PM, 1994. Protein refolding at high concentrations using detergent/phospholipid mixtures. *Analytical Biochemistry* **218**, 392-398.
- Zimmerman J, Selhub J, Rosenberg IH, 1987. Competitive inhibition of folate absorption by dihydrofolate reductase inhibitors, trimethoprim and pyrimethamine. *American Journal of Clinical Nutrition* **46**, 518-522.
- Zipper H, Brunner H, Bernhagen J, Vitzthum F, 2004. Investigations on DNA intercalation and surface binding by SYBR Green I, its structure determination and methodological implications. *Nucleic Acids Research* **32**, e103-e103.

Appendix A: Glossary of terms

A

adjunct

A pharmaceutical entity administered in conjunction with a standard therapy to improve the efficacy of the latter drug, by modifying its effect.

affinity

The degree to which a given drug compound (ligand) will be attracted to its target receptor.

antimalarial

A pharmaceutical entity administered to halt the growth of or kill malaria parasites (*Plasmodium* species), synonyms used in text include antiplasmodial and antiprotozoal.

B

blank

The composition of a blank varies depending on the assay in which it is used, however the purpose remains to account for background “signal”. In most analytical procedure the blank served as a negative control. This background signal could be residual fluorescence (in the Malaria SYBR Green-1® assisted assays and IC₅₀ shift assays) or absorbance (of cellular debris in the Sulforhodamine B assay, or in the Bicinchoninic acid method for protein quantification).

C

chemoprophylactic

A chemical entity (generally a drug compound) used clinically to prevent the occurrence of an illness or infection.

chemotherapeutic

A chemical entity (generally a drug compound) used clinically to treat an illness or infection.

co-administration

The simultaneous administration of two independent chemical substances (generally drug compounds as prescribed or recommended doses) by a single individual or patient.

co-infection

When an individual or patient plays host to more than one infectious microorganism, for example in the instance of an Acquired Immunodeficiency Syndrome (AIDS) sufferer simultaneously being infected by a *Mycobacterium tuberculosis* bacterium.

combination therapies

Variations of this exist. Fixed-dose combination therapies are one tablet or capsule or dosage modality that contains two or more separate chemical compounds to treat a specific illness of infection. Combination therapy can also refer to multiple pharmaceutical entities in different dosage forms being administered together. The purpose of this practise is to enhance patient compliance, in some instances to decrease dose required and/or to decrease the likelihood of target micro-organisms’ development of resistance.

comparative proteomics

This field of study of protein expression focuses on comparing the abundance of select proteins between two conditions, typically control and test samples. There are a number of variations to this field of proteomics, including labelled and label-free techniques. Methods employed in this research project are label-free, relying on the relative abundance of peptides per protein identified.

complete culture medium

This refers to RPMI-1640 cell culture media with Albumax II, glucose and hypoxanthine used to culture malaria parasites. See “incomplete culture medium”.

contaminant

In terms of proteomics databases, the Max Planck Institute of Biochemistry Martinsried (MPI) common protein contaminants database was used to enlarge the *Plasmodium falciparum* proteome obtained from UniProt to decrease the likelihood of obtaining false-positive protein hits, and to enlarge the confidence of protein identification.

Variant: “**contaminated**” was used in text to refer to samples containing cellular components not expected to be present after the purification techniques employed.

E

edge effects

These effects are often observed on 96 well culture plates in the wells along the outer edges of a microplate where analytical values obtained with plate reading appear abnormal. This is due to evaporation of liquid from these wells when incubated over time. These effects were overcome in the Sulforhodamine B assay by placing microplates in an aseptic container with wetted paper towelling and in the Malaria SYBR Green-1® based fluorescence (MSF) assay by filling the edge wells with 200 µL distilled water instead of cultured cells.

efficacy

The ability of a given drug compound to elicit a defined pharmacological response. This is distinct from potency, see “potency”.

expression

This term refers to the transcription of genes and translation of gene products by ribosomes in order to generate active proteins.

F

false discovery rate

An FDR or false discovery rate of proteins in proteomic software programs is where a protein is identified as being present after comparing to a scrambled or reverse sequence database and is a built-in validation feature. A decoy database is an artificial database designed in proteomics software (by reversing the protein sequences in proteome database files screened) in order to enable the identification of false protein hits. The confidence threshold for protein hit was set at 98% confidence.

fixed

In terms of “fixed” samples, these are *Plasmodium falciparum* infected erythrocytes that are suspended in glutaraldehyde (0.025% v/v) to permanently preserve the morphological features of the cells for flow cytometry analysis. Blood smears were also “fixed” to microscope slides by exposure to pure methanol after brief drying in order to prevent to dissociation of the cells from the microscope slides when placed in staining fluid.

food vacuole

Also known as a digestive vacuole, is an intra-protozoal, membrane-enclosed vacuole distinct from the parasitophorous vacuole in which the parasite lives within the erythrocyte. The food vacuole serves a digestive function inside the parasite, and is also the site of haemozoin crystal formation and storage. The food vacuole is also the site of action of the quinoline and artesunate compounds.

fractionation

The eluent obtained by separation of peptides with nano-Liquid Chromatography (Thermo Scientific EASY-nLC II) was spotted into distinct fractions with a Proteiner fc II protein spotter (3 μ L spots). This process was performed to decrease the complexity of peptide sample obtained.

G

gating

This is the electronic filtering process of confining cells detected in flow cytometry and showing a particular characteristic to certain cell “populations” (e.g. uninfected erythrocytes versus infected erythrocytes) based on their size, shape, fluorescent character or nuclear complexity during flow cytometry analysis. Controls were incorporated to decrease the subjectivity of this process.

H

haematocrit

The percentage of erythrocytes in a whole blood sample. It can also refer to the percentage of erythrocytes in the final volume of culture medium to be placed in a flask or in a microplate well.

haeme

Refers to the protoporphyrin ring (nitrogen and carbon based), containing a central iron molecule to aid in the transport of oxygen molecules in blood. The haeme component adhered to globin chains to form a functional protein known as haemoglobin, the most abundant protein in erythrocytes.

haemozoin

Intra-erythrocytic *Plasmodium* parasites produce this dark-brown crystal of stacked haeme groups as a by-product of haemoglobin metabolism.

haplotype

Genomic variations in alleles or single nucleotides, also known as genetic polymorphisms.

harvest

After parasites were allowed to proliferate and reach a high parasitaemia in culture (>8%), the parasites were “harvested” by magnetic enrichment and purification to decrease the uninfected erythrocytes (95% purity).

heterogeneity

The presence and expression of different combination of genes in strains of the same species of organism, associated with genetic diversity and consequently distinct phenotypes (e.g. in terms of drug susceptibility).

high confidence

See “false positives”, this refers to the likelihood of being correct in identifying a protein based on the number of peptides matching the protein sequence and the unique sequences detected during database screening (as identified by Peptideshaker).

I

intra-erythrocytic

The localization of a molecule or parasite within an erythrocyte.

incomplete culture medium

This medium is RPMI-1640 without addition of Albumax II, and was used experimentally in wash steps (of magnetic columns) to prevent wastage of expensive reagents.

indication

The clinical use of a given pharmaceutical compound as approved by and registered with national authoritative bodies.

infection

The presence of invading organisms (such as *Plasmodium falciparum* parasites) in an otherwise healthy individual (human host) or cell (such as an erythrocyte) that has a detrimental effect on the functioning of the host organism or cell.

L

label-free (quantification)

This method of mass spectrometry determines the relative amount of proteins in two or more samples. Methods include comparison of precursor signal intensity or spectral counting of proteins.

life-cycle progression

The normal life-cycle of a *Plasmodium falciparum* parasite is from a ring stage (<2 Nuclear content or N), to a trophozoite (2N), to a schizonts undergoing numerous nuclear replications (>2N) to form merozoites. Progression refers to the development into the next life-cycle stages.

M

magnetic separation

Haemozoin crystals within parasite food vacuoles are paramagnetic, and can be induced by an external magnet (VarioMACS from Miltenyi Biotech). This induction, allows the trophozoites to remain trapped within a specially designed column whilst non-magnetic material is eluted. Upon the removal of the external magnetic source, the trophozoites are no longer trapped.

multi-drug resistance

This is the property of an organism or cell to have decreased susceptibility to a number of mechanistically unique pharmaceutical entities. This can be achieved by altering the transport into or out of the target organism of cell by transmembrane transporter proteins.

N

negative control

No growth is expected in the negative control in viability assays. Generally the negative control is interchangeable with the blank. See "blank".

P

parasitaemia

Also referred to as the parasite load or the percentage parasitaemia. This is the percentage erythrocytes infected by parasites. It is determined in monolayer blood smears by counting at least 500 erythrocytes in total.

parasitophorous vacuole

This vacuole forms around the parasite inside the host erythrocyte upon invasion of a merozoites, it provides the ideal protective niche for development of the parasite.

peptide mass fingerprinting

This technique, abbreviated as PMF, allows for the identification of unknown proteins from all the predicted and measured peptide masses through the measurement of absolute peptide masses on a mass spectrometer.

peptide sequencing

Peptides of a select mass are further fragmented to a series of product ions by low energy collisionally induced dissociation in a tandem mass spectrometer. The combination of the randomly fragmented peptide backbone gives charged ion-products with masses separated by amino acid masses and are then used to establish the sequence of the peptide.

percentage inhibition

This is the overall percentage by which a drug compound was able to inhibit the growth of a particular *Plasmodium* strain or hepatic cell. It is calculated experimentally by subtracting the mean blank readings from the mean sample readings (of duplicate wells) (%) mean samples followed by division by the mean positive control (no drug added, therefore uninhibited growth is seen) and multiplication by 100.

phenotype

The physical appearance or characteristics of an organism based on the expression of its genome. In terms of the *Plasmodium falciparum* strains, this refers to their trait of susceptibility to certain drug classes.

positive control

In the malaria culture setting this refers to samples where no drug compounds are added to these wells, and cells are nourished with equivalent amounts of culture medium as in other controls and test wells. Therefore the readings obtained from these wells (minus blanks) can be interpreted as 100% growth. Slight variations exist if the assay is for mammalian culture or for protozoal culture. See methods for more details.

potency

The amount of a drug compound required to produce a measured significant pharmacological response in target tissues.

prodrug

This drug compound is inactive in its non-metabolised state, but is activated to form an active drug compound through a metabolic activity such as in the case of artemisinin that requires conversion into dihydroartemisinin for appropriate absorption into target cells.

proteomics

This field of study looks at the total protein load of a defined source (the product of gene expression), including their identity, structure, function, location, concentration and abundance (relative or absolute) and modifications of these proteins can also be determined.

purification

This term is used interchangeably with “harvesting”, and refers to the removal of any cellular components that are not of interest, be it through centrifugation, supernatant aspiration, elution, magnetic separation, or other technique. This was performed specifically for trophozoite and then for food vacuole isolation. See these methods for more detail.

R

relapse

In malaria this is the return of dormant stages (usually residing in the liver of a human host) of *Plasmodium* parasites (commonly *P. vivax* and *P. ovale*) into circulation to infect erythrocytes.

replicate

In terms of the number of repeated samples or experiments performed for each assay, this allows for increased reliability of results when readings with low variability is obtained.

resistant (drug)

An organism (such as *Plasmodium falciparum* strains) are deemed drug resistant or less susceptible to drug action when a higher than normal concentration of a pharmaceutical substance is required to kill or inhibit growth of the parasite. This is also known as treatment failure or drug tolerance.

S

selectivity index

A selectivity index (SI) value indicated that selective toxicity of a drug compound and was calculated by the following formula:

selective toxicity (selectivity)

The ability of a drug compound to produce a therapeutic effect (toxicity: ability to kill or inhibit growth) in a particular cells species over another. For example, artemisinin is said to be selectively toxic, because it is at least 3000 times more likely to harm an *in vitro* strain of *P. falciparum* than a human hepatocyte (see Results: Table 5.2.3).

sensitisation

For the purpose of this study, sensitisation refers to the ability of a drug compound to enhance the the sensitivity or susceptibility profile of a parasite to a drug to which it was previously more tolerant (see “tolerance”).

sensitiser

This refers to a chemical or drug entity that is capable to increasing the susceptibility of an organism or target cell to the actions of another substance (pharmaceutical). In this study, clofazimine was tested for its ability to potentiate the accumulation of chloroquine in a chloroquine resistance strain of *P. falciparum*.

sensitive (drug sensitivity)

Can also be referred to as drug intolerance of an organism (*P. falciparum*). A lower threshold than normal drug efficacy is required to harm the organism.

sequencing (genome and proteome)

This is the process of determining the order of nucleotides in a stretch of DNA and chromosomes (genome), or the order of amino acids in one or more peptides (proteome).

sequestration (sequester)

The process of sequestration is to accumulate a specific chemical compound. This can refer to the chelation or inactivation of active residual groups of a compound to form a stable compound, or the actual isolation of the compound by stored in cellular organelles (food vacuole), causing it to no longer be available for chemical reactions.

spectral counting

This is the total number of actual spectra positively identified for a protein, and can be used as a tool of “label-free” semi-quantitative measure of a protein’s relative abundance in proteomic studies.

strains

A strain is a genetic variant or subtype of a micro-organism (protozoan). The resistance of a strain often depends on the region where it was contracted, suggesting that strains develop genetic variance based on host population, environmental and drug exposure factors.

susceptibility

This term is interchangeable in text with sensitivity. The degree to which an infective organism can be harmed by a pharmaceutical agent at therapeutic doses.

synchronise

Cultures were exposed to D-sorbitol when parasites were in the ring stage of their development, in order to lyse the weakened erythrocyte membranes of parasites that have progressed past this life-cycle stage. This process resulted in cultures that were synchronised to >95% in the early ring stage of their life-cycle.

T

tolerance

Drug tolerance is the *Plasmodium* parasite's decreased response to a drug, due to the ability of the organism to resist the effects of the drug (see "resistant").

Precursor tolerance: this is an adjustable parameter of a mass spectrometer search engine (e.g. Mascot) to indicate the ion masses above which results should be retained for evaluation (value is enterable as Daltons, millimass units, percentage or parts per million, Daltons were used here).

Fragment tolerance: identical to precursor tolerance only difference is that it pertains to the precursor's fragment ions.

toxicity

The degree to which a pharmaceutical or chemical substance can cause damage to a micro-organism, or mammalian cells.

triplicate

The majority of experiments were performed in triplicate, meaning three repeats, with triplicates of wells and or samples (unless specified otherwise). This enabled the reporting of values as means \pm standard deviations or standard error of means.

trypsinisation

The addition of the proteolytic enzyme, trypsin (obtained from porcine pancreas), for the cleavage or "cutting" of proteins at the C-terminal (carboxyl) end of lysine and arginine amino acids. This process aids in mass to charge identification of unknown proteins with further mass spectrometric analysis.

U

uninfected erythrocytes

These are healthy erythrocytes, 6-8 μm in diameter and biconcave in shape, that contain haemoglobin proteins that stain pink-red (eosinophilic) with Romanovsky dyes (such as Giemsa).

untreated

This refers to either infected or uninfected erythrocytes, that are cultured in complete culture medium according to protocols to obtain optimum growth, without the addition of a drug compound. These erythrocyte samples usually served as positive controls for growth.